

UC San Diego

UC San Diego Electronic Theses and Dissertations

Title

Cancer Being Extra: Extrachromosomal DNA Promotes Heterogeneity and Resistance in Cancer

Permalink

<https://escholarship.org/uc/item/4pj6h0x9>

Author

Lange, Joshua

Publication Date

2022

Peer reviewed|Thesis/dissertation

UNIVERSITY OF CALIFORNIA SAN DIEGO

Cancer Being Extra: Extrachromosomal DNA Promotes Heterogeneity and Resistance in
Cancer

A dissertation submitted in partial satisfaction of the
requirements for the degree Doctor of Philosophy

in

Biomedical Sciences

by

Joshua T. Lange

Committee in charge:

Professor Arshad Desai, Chair
Professor Paul S. Mischel, Co-Chair
Professor Vineet Bafna
Professor Don W. Cleveland
Professor Karen Oegema

2022

Copyright

Joshua T. Lange, 2022

All rights reserved.

The dissertation of Joshua T. Lange is approved, and it is acceptable in quality and form for publication on microfilm and electronically.

University of California San Diego

2022

iii

DEDICATION

To those who conduct science with the aim of improving human health and understanding.

And to those whose cells and tumors we study with the hope of improving the future for others.

EPIGRAPH

“Nothing in life is to be feared, it is only to be understood. Now is the time to understand more, so that we may fear less.”

-Marie Curie

“Remember to look up at the stars and not down at your feet.”

-Stephen Hawking

“Let us think the unthinkable, let us do the undoable, let us prepare to grapple with the ineffable itself, and see if we may not eff it after all.”

-Douglas Adams

TABLE OF CONTENTS

| | |
|--|-----|
| DISSERTATION APPROVAL PAGE | iii |
| DEDICATION..... | iv |
| EPIGRAPH..... | v |
| TABLE OF CONTENTS..... | vi |
| LIST OF FIGURES | vii |
| ACKNOWLEDGEMENTS..... | ix |
| VITA..... | xi |
| ABSTRACT OF THE DISSERTATION..... | xiv |
| CHAPTER I: INTRODUCTION..... | 1 |
| A. Oncogene amplification in cancer | 2 |
| B. Extrachromosomal DNA (ecDNA)..... | 2 |
| C. Intratumor heterogeneity, evolution and resistance | 7 |
| D. Key outstanding questions | 8 |
| CHAPTER II: RANDOM INHERITANCE OF ECDNA DRIVES HETEROGENEITY AND RESISTANCE IN HUMAN CANCER..... | 11 |
| A. Introduction..... | 12 |
| B. Results | 14 |
| C. Discussion | 27 |
| D. Methods and Materials..... | 43 |
| E. Acknowledgements | 49 |
| CHAPTER III: IDENTIFYING GENETIC TARGETS TO DISRUPT ECDNA SEGREGATION AND PROLIFERATION | 51 |
| A. Introduction..... | 52 |
| B. Results | 55 |
| D. Materials and Methods..... | 81 |
| E. Acknowledgements | 87 |
| CHAPTER IV: CONCLUSIONS AND FUTURE DIRECTIONS..... | 88 |
| A. Summary of findings..... | 89 |
| REFERENCES | 95 |

LIST OF FIGURES

| | |
|---|----|
| Figure 1.1 Schematic of ecDNA formation. | 10 |
| Figure 2.1 Panel of cell lines with ecDNA. | 29 |
| Figure 2.2 ecDNA is randomly inherited by daughter cells. | 30 |
| Figure 2.3 Live-cell imaging of ecDNA behavior through mitosis. | 31 |
| Figure 2.4 Random inheritance of ecDNA causes significant and modellable heterogeneity in cell lines and patient tumors. | 33 |
| Figure 2.5 Isogenic ecDNA +/- GBM cell lines. | 34 |
| Figure 2.6 ecDNA promotes resistance and adaptation to environmental and therapeutic challenges. | 35 |
| Figure 2.7 ecDNA enables GBM and NB tumors to shift copy number in response to therapy and changing environment. | 36 |
| Figure 2.8 SNU16 ecDNA change ecDNA copy number in a species-specific manner. | 37 |
| Figure 2.9 Segregation of distinct ecDNA species in the same cell line is random but non-independent. | 38 |
| Figure 2.10 Non-independent segregation of ecDNA species is not due to fused molecules. | 39 |
| Figure 2.11 Frequency and prognosis for tumors with multiple ecDNA species in TCGA. | 40 |
| Figure 2.12 Similarity of cohesion dynamics between chromosomes and ecDNA throughout mitosis. | 41 |
| Figure 3.1 Analysis of expression data from TCGA tumor samples. | 67 |
| Figure 3.2 Gene set enrichment analysis of ecDNA+ and ecDNA- tumors. | 68 |
| Figure 3.3 Gene ontology analysis of the top 1,000 enriched genes in ecDNA+ tumors. | 69 |
| Figure 3.4 ecDNA are more prone to incorporation into micronuclei. | 70 |
| Figure 3.5 Differential sensitivity of isogenic ecDNA cell lines to mitotic disruption. | 71 |
| Figure 3.6 ecDNA cell lines have fewer cells in G2/M phase and a concentration of cells in G1. | 72 |
| Figure 3.7 Chromokinesins show increased expression levels in ecDNA+ tumors. | 73 |

Figure 3.8 | Chromokinesins localize to ecDNA along with chromosome arms in metaphase.74

Figure 3.9 | Genetic knockdown of KIF4A and KIF22 increase rates of ecDNA+ micronuclei across multiple cell line models.75

Figure 3.10 | Chromokinesins aid in proper segregation of ecDNA.....77

Figure 3.11 | Chromokinesin knockdown reduces proliferation rates in ecDNA+ cell lines. ..78

Figure 3.12 | Chromokinesin knockdown reduces proliferation in GBM39-EC relative to GBM39-HSR.80

ACKNOWLEDGEMENTS

I would like to acknowledge Professor Paul S. Mischel for his support as my primary mentor and advisor. His fostering of my scientific curiosity and exploration has proven invaluable. I would also like to acknowledge Professor Arshad Desai and Professor Karen Oegema for their support during the final year of my dissertation research. Their generosity was essential in the completion of this work. I thank all past and current members of the Mischel lab with whom I have had the pleasure of interacting. You all contributed to making my dissertation experience enjoyable and scientifically fulfilling. Thank you also to all members of the Oegema/Desai lab for taking me in for the final months of my dissertation.

I would like to acknowledge my wife, Alexandra Lange, for her unending encouragement of my career and my passions. The findings presented in this dissertation, as well as the lack of comma, splices, are significantly due to her support. Thank you also to our dog, Maia, for her unending encouragement of my walking and my lack of sleep.

Chapter II contains multiple figures from the following manuscript, which has been submitted for publication. The dissertation author was the primary investigator and author of this paper. Joshua T. Lange[#], John C. Rose[#], Celine Y. Chen[#], Yuriy Pichugin[#], Liangqi Xie, Jun Tang, King L. Hung, Kathryn E. Yost, Quanming Shi, Marcella L. Erb, Utkrisht Rajkumar, Sihan Wu, Sabine Taschner-Mandl, Marie Bernkopf, Charles Swanton, Zhe Liu, Weini Huang*, Howard Y. Chang*, Vineet Bafna*, Anton G. Henssen*, Benjamin Werner*, Paul S. Mischel*. “The evolutionary dynamics of extrachromosomal DNA (ecDNA) in human cancers”.

Chapter III contains co-authored/unpublished material of which the dissertation author was the primary investigator and author. Joshua T. Lange, Jens Luebeck, Vineet Bafna, Paul S.

Mischel. Chapter III, Identifying genetic targets to disrupt ecDNA segregation and proliferation.

VITA

- 2017 Bachelor of Arts, Dartmouth College
- 2021 Graduate Instructional Apprentice, Department of Biological Sciences,
University of California San Diego
- 2022 Doctor of Philosophy, University of California San Diego

PUBLICATIONS

“Principles of ecDNA random inheritance drive rapid genome change and therapy resistance in human cancers.” J.T. Lange, J.H. Rose, C.Y. Chen, Y. Pichugin, L. Xie, J. Tang, K.L. Hung, K.E. Yost, Q. Shi, M.L. Erb, U. Rajkumar, S. Wu, S. Taschner-Mandl, M. Bernkopf, C. Swanton, Z. Liu, W. Huang, H.Y. Chang, V. Bafna, A.G. Henssen, B. Werner, P.S. Mischel. *Under Submission*. 2022.

“The landscape of extrachromosomal circular DNA in medulloblastoma.” O.S. Chapman, J. Luebeck, S. Wani, A. Tiwari, M. Pagadala, S. Wang, J.D. Larson, J.T. Lange, I.T-L. Wong, S.R. Dehkordi, S. Chandran, M. Adam, Y. Lin, E. Juarez, J.T. Robinson, S. Sridhar, D.M. Malicki, N. Coufal, M. Levy, J.R. Crawford, S.L. Pomeroy, J. Rich, R.H. Scheuermann, H. Carter, J. Dixon, P.S. Mischel, E. Fraenkel, R.J. Wechsler-Reya, V. Bafna, J.P. Mesirov, L. Chavez. *Under Review*. 2022.

“Peptides from lncRNA PVT1 reciprocally co-ordinate MYC in human cancer.” A. Tiwari, K. Tashiro, U. Paithane, O. Saulnier, K.B. Guerra, A. Vishvanathan, Q. Trinh, T. Nakashima, T. Mohammad, J.T. Lange, S. Wu, M.B. Masihi, J. Friedlein, O. Chapman, B. Hall, A. Shukla,

L. Denis, L. Hendrikse, S. Saha, J. Luebeck, B. Konety, S. Dehm, Y. Marahrens, L. Stein, L. Chavez, V. Bafna, P.S. Mischel, H. Suzuki, M.I. Hassan, R.J. Wechsler-Reya, A. Deshpande, M.D. Taylor, A. Bagchi. *Under Submission*. 2022.

“ecDNA hubs drive cooperative intermolecular oncogene expression.” K.L. Hung, K.E. Yost, L. Xie, Q. Shi, K. Helmsauer, J. Luebeck, R. Schopflin, J.T. Lange, R.C. Gonzalez, N.E. Weiser, C. Chen, M.E. Valieva, I.T-L. Wong, S. Wu, S.R. Dehkordi, C.V. Duffy, K. Kraft, J. Tang, J.A. Belk, J.C. Rose, M.R. Corces, J.M. Granja, R. Li, U. Rajkumar, J. Friedlein, A. Bagchi, A.T. Satpathy, R. Tjian, S. Mundlos, V. Bafna, A.G. Henssen, P.S. Mischel, Z. Liu, H.Y. Chang. *Nature* 600, 731-736. 2021.

“AmpliconReconstructor integrates NGS and optical mapping to resolve the complex structures of focal amplifications.” J. Luebeck, C. Coruh, S.R. Dehkordi, J.T. Lange, K.M. Turner, V. Deshpande, D.A. Pai, C. Zhang, U. Rajkumar, J.A. Law, P.S. Mischel, V. Bafna. *Nature Communications* 11, 4374. 2020.

“Genomic characterization of patient-derived xenograft models established from fine needle aspirate biopsies of a primary pancreatic ductal adenocarcinoma and from patient-matched metastatic sites.” R.J. Allaway, D.A. Fischer, F.B. de Abreu, T.B. Gardner, S.R. Gordon, R.J. Barth, T.A. Colacchio, M. Wood, B.Z. Kacsoh, S.J. Bouley, J. Cui, J. Hamilton, J.A. Choi, J.T. Lange, J.D. Peterson, V. Padmanabhan, C.R. Tomlinson, G.J. Tsongalis, A.A. Suriawinata, C.S. Greene, Y. Sanchez, K.D. Smith. *Oncotarget* 7, 17087. 2016.

FIELDS OF STUDY

Major Field: Biomedical Sciences (Cancer Biology)

ABSTRACT OF THE DISSERTATION

Cancer Being Extra: Extrachromosomal DNA Promotes Heterogeneity and
Resistance in Cancer

by

Joshua T. Lange

Doctor of Philosophy in Biomedical Sciences

University of California San Diego, 2022

Professor Arshad Desai, Chair

Professor Paul S. Mischel, Co-Chair

In cancer, oncogenes are frequently amplified on extrachromosomal DNA (ecDNA), circular acentric DNA fragments ranging from hundreds of kilobases to multiple megabases. Oncogene amplification on ecDNA is associated with extremely high copy number and poor prognosis in patients. However, the specific mechanisms through which ecDNA alter cell behavior and tumor evolution are poorly understood. Here, I report that ecDNA are inherited randomly by daughter cells during mitosis. This breakdown of canonical mendelian inheritance patterns results in significant increases in population and tumor heterogeneity. I further demonstrate that cell lines with ecDNA are able to rapidly alter their distribution of ecDNA copy number to adapt and gain resistance to both environmental and therapeutic challenges. Interestingly, investigations into the behavior of multiple species of ecDNA within individual cells demonstrate that while ecDNA is inherited randomly by daughter cells, different ecDNA species are not inherited independently of each other. Further, I show that ecDNA demonstrates an increased frequency of missegregation into micronuclei during mitosis.

Finally, I investigate proteins that may be essential for the maintenance and inheritance of ecDNA. Analysis of gene expression data from The Cancer Genome Atlas identifies several proteins involved in chromosomal segregation and DNA repair and metabolism. I specifically analyze the chromokinesins KIF4A and KIF22 and demonstrate that they may play a significant role in ensuring proper segregation of ecDNA into daughter cells.

Taken together, the data presented here clearly demonstrate how the random inheritance of ecDNA at each cell division generates a dynamic and heterogeneous distribution of amplified oncogenes. This enables cancer cells to adapt to and resist environmental and therapeutic pressures more readily. I also describe the behavior of ecDNA during mitosis and identify

specific proteins that may be able to be targeted to specifically disrupt the proliferation of ecDNA⁺ cell lines and tumors.

CHAPTER I: INTRODUCTION

A. Oncogene amplification in cancer

Oncogene amplification is a common driving event in many solid human tumors and can increase the copy number of both wild-type and mutant oncogenes¹⁻³. The primary mechanisms through which regions of the genome increase in copy number include: 1) missegregation of whole chromosomes or chromosome arms⁴; 2) breakage-fusion-bridge (BFB) cycles caused by telomere dysfunction⁵; 3) abnormally repaired DNA damage especially near chromosomal fragile sites (CFS)⁶; 4) circular extrachromosomal DNA (ecDNA) elements caused by aberrant repair of double-strand breaks (DSB)^{7,8}.

Focal amplifications, in which a discrete region of the genome increases in copy number relative to the cell's karyotype, are the most common copy number alterations found in cancer^{1,2}. While it is difficult to attribute specific DNA damage mechanisms to specific amplifications, studies have shown that amplification via extrachromosomal DNA (ecDNA) is commonly observed in cancer cell lines and tumor samples^{8,9}.

B. Extrachromosomal DNA (ecDNA)

ecDNA was first described in metaphase spreads of medulloblastoma and neuroblastoma tumors^{10,11}. Early work referred to these chromatin bodies as double minutes (DMs) as they frequently, though not always, appeared as paired circles in metaphase¹². ecDNA are circular fragments of genomic DNA, typically ranging in size from hundreds of kilobases to a few megabases¹³. ecDNA are distinguished from other forms of genomic rearrangement, such as neochromosomes¹⁴, by their lack of centromere⁸.

ecDNA were first studied in the context of acquired drug resistance, especially to the chemotherapy methotrexate⁷. Researchers found that long-term methotrexate treatment of various cell lines from multiple species resulted in amplification of methotrexate's target, dihydrofolate reductase (DHFR)^{7,15,16}. This amplification was frequently observed to occur via ecDNA. Early work also demonstrated the dynamic nature of ecDNA amplification – with ecDNA being lost from cell populations after removal of the methotrexate pressure and ecDNA potentially being converted into chromosomal amplifications in the form of homogeneously staining regions (HSRs)^{17,18}. Studies into the manner and mechanism of ecDNA segregation followed, including work suggesting that ecDNA may rely on 'tethering' or 'hitchhiking' to mitotic chromosomes, similar to viral episomes, to segregate into daughter cells¹⁹.

Previously, the only method to verify the presence of ecDNA in a tumor or a cell population was to prepare metaphase spreads and view them microscopically. This creates challenges for understanding how widespread ecDNA are in large samples and datasets, such as The Cancer Genome Atlas (TCGA). To solve this problem, researchers have developed algorithmic methods to predict the presence and structure of ecDNA from ubiquitous whole exome and whole genome sequences^{5,20}. This has enabled insights into the prevalence of ecDNA in human cancer patients and the impact of ecDNA on prognosis and other outcomes. Thus far, this work has suggested ecDNA has a prevalence of around 20% across all cancers, with some sub-types such as glioblastoma (GBM) among the highest with a prevalence of more than 50%⁹. Research has also suggested that ecDNA correlates with significantly worse prognosis, controlling for tumor-type and other

demographic variables⁹. Measures of the frequency of ecDNA in cancer cell lines, patient-derived xenograft (PDX) models, and immortalized cell lines have shown a clear trend that ecDNA is essentially never found in healthy, normal tissue⁸. ecDNA appears, for now, to be a phenomenon distinct to cancer as a mechanism to drive unregulated proliferation. One interesting finding of both cell line studies visualizing ecDNA in metaphase spreads and analyses of tumor sequencing data is that ecDNA is consistently found at a high frequency in brain tumors, including pediatric medulloblastoma^{8,9,21}. Correlational data suggests that aggressive cancer types that rely primarily on copy number changes, as opposed to mutations, are likely to use ecDNA as a mechanism to drive high copy number amplification and expression.

Recent work has also studied the structure and gene expression of ecDNA. The circularity of ecDNA has been demonstrated both microscopically and through the use of long-read sequencing and optical mapping¹³. This circular rearrangement of the genome results in significant alterations to the gene expression environment of the locus. In one example, an ecDNA carrying EGFR and its neighboring regions resulted in increased expression of genes previously distal to the EGFR promoter as they were brought into closer proximity due to the physical rearrangement. This altered morphology can result in the altered behavior of enhancer and insulator elements^{13,22}. ecDNA represents some of the most highly transcribed genes in the genome of cancer cell lines. It has also been suggested that ecDNA-housed enhancer elements may promote increased transcription of chromosomal genes due to their dynamic nature and their ability to effectively license super-enhancers to distal regions of the genome²³. Perhaps not surprisingly, the regulatory

non-coding regions that circularized oncogenes relied on for transcriptional activation when they were housed on the chromosome are preferentially included on ecDNA in order to continue transcriptional activation²².

In addition to dysregulation of the normal genetic and epigenetic machinery regulating gene expression in ecDNA regions, it has been suggested that ecDNA are prone to forming clusters around transcriptional hubs, which may contribute further to the increased expression of ecDNA amplified genes²⁴. These hubs are regulated by the epigenetic regulator BRD4 and can be dissolved with the BRD4 inhibitor JQ1. Together, these findings suggest that the unique properties of ecDNA cause unique behavior related to gene expression and localization within the nucleus.

ecDNA has also been suggested to behave differently than chromosomes during mitosis, where the lack of centromere results in different behaviors. Mitotic ecDNA has been reported to cluster amongst other ecDNA and ‘tether’ or ‘hitchhike’ on mitotic chromosomes, through an unknown mechanism—though similar in principle to viral episomes¹⁹. Since attachments between kinetochores at centromeres and the mitotic spindle are mechanism cells use to count chromosomes and ensure equal distribution of chromatids to daughter cells, ecDNA have been proposed and demonstrated to be distributed unevenly to daughter cells^{25,26}. While this does occur at some frequency for mitotic chromosomes, the rate is significantly lower and is generally dependent on the disruption of one or more mitotic regulators²⁷. Missegregation of ecDNA is likely to be random and abnormal in cells that retain the capability to segregate mitotic chromosomes with fidelity.

Understanding how ecDNA initially arise in cancers has been a challenge for the field. Formation must minimally require two double strand breaks (DSB) in the DNA, at a distance close enough—in nuclear proximity rather than genomic distance—to promote errant repair of the breaks together forming a circle rather than repair back into the chromosome, and at a distance far enough apart to include selectable elements including genes and regulatory regions (Figure 1.1). Note that this niche in size distinguishes ecDNA from smaller more ubiquitous circular DNA (eccDNA) which is too small to contain genes, and larger circularized chromosomes which may arise as an intermediary step in breakage-fusion-bridge cycles first characterized by Dr. Barbara McClintock²⁸. Given this minimal requirement, many mechanisms which induce DNA damage have been suggested to cause ecDNA formation. Replication stress, DNA damage caused by depletion of nucleotides or replication enzymes, was the first mechanism described to generate ecDNA as inhibition of the nucleotide metabolism enzyme DHFR by methotrexate caused formation of DHFR containing ecDNA as a mechanism of resistance⁷. Chromothripsis, or the shattering and rearranging of an entire chromosome or discrete genomic region, has also been demonstrated to generate ecDNA^{26,29}. These studies also suggested that the non-homologous end joining (NHEJ) DNA repair process may be a primary mechanism for joining broken DNA ends into circles after chromothripsis²⁹. The formation of ecDNA by artificial cutting of two neighboring regions of a chromosome by a CRISPR-Cas9 approach (CRISPR-C) further demonstrates that ecDNA formation is unlikely to be attributable to a single mechanism of genomic insult³⁰. Rather, all DNA damaging events are likely to cause ecDNA formation at varying frequencies.

C. Intratumor heterogeneity, evolution and resistance

Cancer is a broad term for an incredibly heterogeneous disease. There are many levels of cancer heterogeneity that contribute to difficulties in treatment, especially using pharmacologic and biologic therapeutics designed to target specific alterations—personalized medicine³¹. To begin with, there are significant differences in the growth rate, metabolic characteristics, metastatic potential, genetic abnormalities, immunogenicity, and prognosis for different tumor-types—breast cancer compared to brain cancer for example. Within a given sub-type such as breast cancer, we also find significant diversity in these characteristics, leading us to cluster patients in categories such as HR+ ER-, or triple-negative (TNBC). However, recent work has made it increasingly clear that the presence of intratumor heterogeneity, or heterogeneity between different cells and regions of a single tumor, may represent the most significant challenge to successful long-term treatment of cancer³².

Advances in sequencing technologies and our understanding of tumor behavior and evolution have enabled a much clearer picture of how tumors evolve, especially when faced with environmental and therapeutic challenges, such as treatment of a lung tumor with a targeted epidermal growth factor receptor (EGFR) inhibitor³³⁻³⁵. At the highest level for an individual tumor, many tumors are made up of somewhat distinct populations of cancer cells, referred to as clones³⁶. This clonal heterogeneity can be detected by sampling and sequencing distinct regions of a tumor after resection³⁷⁻³⁹. Clones are generally distinguished by their molecular alterations, with all clones sharing alterations that

occurred early in the tumor's evolution and containing distinct alterations that caused those clones to outcompete. These distinct clones compete against each other with the balance of competition influenced by the presence or absence of various drugs or environmental factors.

ecDNA may represent an additional level of heterogeneity that has not been sufficiently appreciated in this field. Given ecDNA is suggested to be distributed unequally to daughter cells, tumors with ecDNA may have significant phenotypic differences between two neighboring cells. This additional level of complexity and diversity may help to further explain the failure of many drugs to elicit meaningful responses. Given the prevalence of ecDNA in cancer, this represents an important gap in our understanding of tumor behavior and evolution.

D. Key outstanding questions

While ecDNA was first described more than 50 years ago, research into ecDNA has only recently begun to gain significant attention from scientists and funding agencies. The primary objective of my studies was to further our understanding of ecDNA behavior and to connect these findings to clinical outcomes for tumors with ecDNA. Specifically, I focused on how ecDNA behaves during mitosis, a stage which for chromosomes is significantly defined by interactions between centromeric DNA, kinetochores, and canonical mitotic checkpoint proteins.

In Chapter II, I both qualitatively and quantitatively describe and measure the distribution of ecDNA to daughter cells in dividing cancer cell lines. I then aim to

understand how this distribution influences the heterogeneity of cell line populations and patient tumor samples. Finally, I sought to connect these findings of ecDNA distribution and heterogeneity to the ability of cancers with ecDNA to adapt and evolve to environmental and therapeutic challenges. I will present findings that demonstrate the immense complexity that ecDNA can introduce into a tumor by looking into cell lines and tumors that contain more than one primary ‘species’ of ecDNA.

The field of ecDNA biology still lacks understanding of the mechanisms and consequences of how ecDNA segregates to daughter cells without centromeric DNA to attach to the mitotic spindle. In Chapter III, I ask questions regarding the ability of ecDNA to segregate successfully and the consequences of missegregation of ecDNA.

Finally, given the importance of ecDNA to our understanding of cancer and our ability to improve therapeutic outcomes, I seek to identify novel genes and processes that may be required to maintain ecDNA within a tumor in Chapter IV. I will present data on a subset of these genes, chromokinesins, which may play an important role in the successful segregation and maintenance of ecDNA.

Improving our understanding of ecDNA and how it influences tumor evolution and resistance is essential to improving outcomes for an estimated 20% of all cancer patients. Identifying novel therapeutics that either target ecDNA directly or preferentially disrupt the proliferation of ecDNA containing cancer cells would be a huge advance in cancer therapy. In Chapter V, I will discuss the broader impact of my findings and highlight key future directions for investigation.

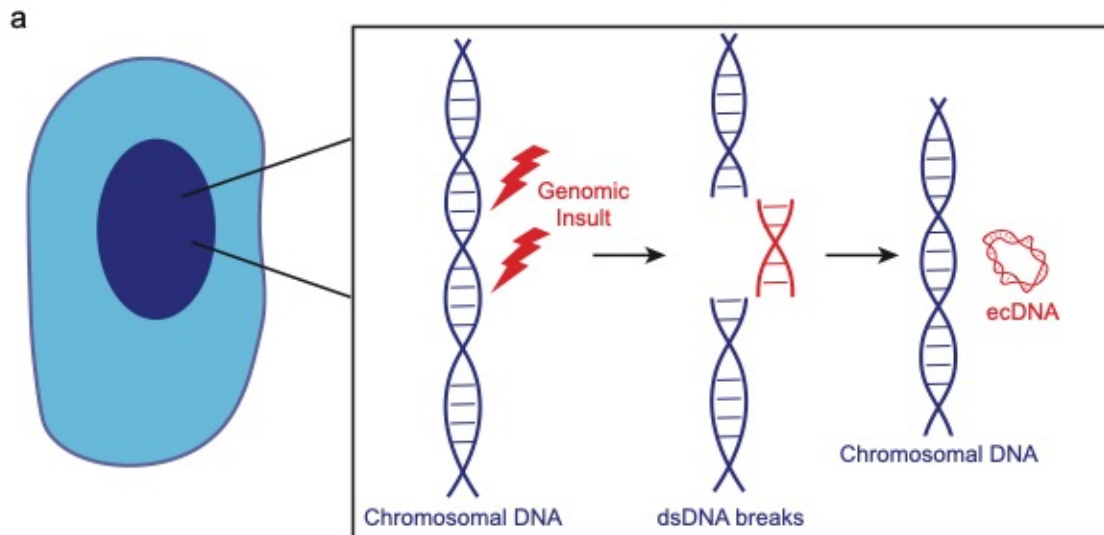


Figure 1.1 | Schematic of ecDNA formation.

a, Schematic representation of the general mechanism that is accepted for ecDNA formation. Genomic insults that can generate double-stranded DNA (dsDNA) breaks are likely capable of ecDNA generation. If two dsDNA breaks are localized close enough, aberrant DNA repair mechanisms may errantly repair the breaks by rejoining the chromosomal ends and ligating the fragment ends together, resulting in ecDNA formation and a deletion at the chromosomal locus.

CHAPTER II: RANDOM INHERITANCE OF ECDNA DRIVES HETEROGENEITY
AND RESISTANCE IN HUMAN CANCER

A. Introduction

ecDNA are frequently found in human tumors^{8,9,21}. Lack of centromeric DNA sequences on ecDNA suggests that they may behave quite differently from chromosomes during mitosis, during which centromeres play an essential role in checkpoint signaling and physical partitioning of equal complements of genetic material to daughter cells⁴⁰. Initial qualitative descriptions of ecDNA segregation at mitosis suggested behavior significantly different from that of chromosomes, with apparent clustering and tethering of ecDNA⁴¹. More recent research has quantitatively suggested ecDNA segregates randomly to daughter cells^{25,26}. However, our understanding of the consequences of this random segregation for heterogeneity within populations of cancer cells and tumors remains theoretical.

Intratumoral heterogeneity represents one of the greatest challenges for achieving long-term responses to cancer treatments, including targeted small molecules and immunotherapy^{31,36}. Recent evidence has suggested that tumors are extremely heterogeneous, often being made up of multiple genetically distinct but related clones that have evolved from an initial cancer cell³⁹. These clones have differential relative fitness that changes in relation to the changing environment of the tumor. Environmental changes due to the growth of the tumor or due to the introduction of various treatments alter this selection profile causing some clones to outcompete others⁴². The presence of *a priori* genetic (and epigenetic) diversity within a tumor increases the chances that a subset of cells within the tumor are less sensitive or resistant to a therapeutic⁴³⁻⁴⁵. Thus, it is believed that tumors with higher levels of intratumoral heterogeneity are more likely to rapidly progress

after challenged with a treatment. Given ecDNA's random segregation, it is thus likely that ecDNA within a tumor increases this intratumoral heterogeneity and thus its ability to form resistance⁸. Importantly, the scale at which ecDNA may influence tumor heterogeneity is different than the clonal behavior described previously. ecDNA is likely to introduce a higher than normal level of genetic diversity between neighboring cells within a clonal region. This increases the level of complexity within a tumor past the level we currently understand and use to model responses to treatments.

While tumors are recognized as heterogeneous collections of cancer cells, research has shown that cancer cells are constantly mutating and reorganizing their genome, referred to as genomic instability (GI)^{46,47} and chromosomal instability (CIN)⁴⁸⁻⁵⁰ respectively. ecDNA may play a role in increasing CIN as previous research has suggested that ecDNA are more prone to genomic rearrangement with other ecDNA and other parts of the chromosomal compartment of the genome. Thus, ecDNA may also increase the rate at which cancers are continuously evolving.

While research into the segregation of ecDNA at mitosis has been consistent, further qualitative and quantitative data regarding ecDNA inheritance is needed given the potential importance of ecDNA to many different areas of tumor behavior. Further, the connection between ecDNA inheritance and its influence on broader questions of intratumoral heterogeneity and resistance have yet to be understood. Here, I present my collaborative work to try to understand these processes further. First, I present qualitative and quantitative data regarding ecDNA inheritance in multiple cancer cell lines. Then, I demonstrate how this inheritance increases levels of heterogeneity and resistance in both

cancer cell lines and patient samples. Finally, I will discuss data which suggests the genetic complexity of a tumor can expand beyond a single heterogeneous pool of ecDNA.

B. Results

Quantitative and qualitative analysis of ecDNA inheritance patterns

To further understand the dynamics of ecDNA at mitosis and through segregation to daughter cells, I first designed a method for quantitative analysis of ecDNA segregation in fixed cells. I first identified a panel of cancer cell lines with varying levels of ecDNA amplification (Figure 2.1A). This panel included 5 cancer types – glioblastoma (GBM), colorectal, prostate, stomach, neuroblastoma (NB) – and 5 different oncogenes amplified on ecDNA – MYC, MYCN, CDK4, EGFR, FGFR2. To identify late-mitotic cells (anaphase or later) I detected Aurora B, which localizes from centromeres to the mitotic midbody at anaphase, by immunofluorescence (IF). I combined this with detection of the ecDNA elements by fluorescence *in situ* hybridization (FISH). These IF-FISH experiments allowed quantification of both individual ecDNA by automated foci identification software (ImageJ) and total ecDNA signal by pixel intensity (ImageJ). I imaged approximately 100 of these mitoses (~200 daughter cells) on a confocal microscope. Qualitatively, these images clearly demonstrated unequal inheritance of ecDNA (Figure 2.2A).

I quantified the fraction of total ecDNA that each daughter cell inherited from the mother cell. For each cell line and each oncogene, this quantification clearly showed a wide distribution of ecDNA inheritance that was centered around 0.5 (Figure 2.2B). We wanted to understand whether these distributions are what would occur under completely random

inheritance. For each cell line, we ran stochastic simulations of ecDNA segregation, treating each division as a Binomial trial, such that $B(n, p)$, where n represents the number of ecDNA in the mother cell and p represents the probability of each ecDNA to be inherited by one of the daughter cells. Thus, $p=0.5$ represents a completely random inheritance process. We ran these simulations 10^7 iterations and plotted the distribution of ecDNA inheritance fractions overlaid with the empirical cell line data (Figure 2.2B dashed curves). We performed Kolmogorov-Smirnov (KS) tests to statistically test the similarity of the empirical and simulated distributions. KS test p values > 0.05 suggest the distributions are not statistically different. This held true for each cell line and oncogene analyzed. These data provide clear quantitative evidence that ecDNA is segregated randomly to daughter cells.

To further understand the dynamics of ecDNA during mitosis, we engineered a system which enabled live-cell imaging of ecDNA in the PC3 prostate cancer cell line with MYC ecDNA amplification. To accomplish this, we designed a DNA cassette of 96 TetO repeats, as previously described. We then designed sgRNAs to direct the Cas9 enzyme to a region of the ecDNA between the MYC and PVT1 loci (Figure 2.3A). The donor cassette was designed to have homology to the sgRNA regions to promote homologous recombination of our donor segment into the cut site. We confirmed the successful integration of the TetO array into this site by FISH, PCR, and sequencing (Figure 2.3B-D). With this cassette inserted, we expressed a TetR-GFP fusion protein which would bind the TetO loci.

We then performed live-cell confocal imaging of these cells, with the DNA visualized with H2B-JF₆₆₉ by expression of H2B-SNAP. This enabled us to observe ecDNA dynamics prior to and throughout mitosis and the next cell cycle (Figure 2.3E). We again observed a clear example of unequal segregation of ecDNA between two daughter cells, further corroborating the quantitative experiments described previously. Further, this experiment also demonstrated some novel behavior of ecDNA. Upon mitotic onset, ecDNA appeared to conglomerate from a multitude of small foci into a few larger foci. This behavior has not been described previously and more work will need to be done to establish whether this is a universal behavior of ecDNA at mitosis to perhaps aid in non-centromeric segregation.

Random inheritance of ecDNA promotes genetic heterogeneity in cancer cell lines and patient tumors

I next wanted to understand the impact of the observed random inheritance of ecDNA on the heterogeneity of cancer cell lines and patient tumors with ecDNA. To accomplish this I quantified the distribution of ecDNA copy number in the cell lines described previously by FISH (Figure 2.4A). Quantification ecDNA foci in interphase nuclei demonstrated that there is extreme variability and heterogeneity in the ecDNA copy number of these cells.

Next, we wanted to determine whether the extent of the heterogeneity was attributable to the random inheritance of ecDNA as previously described. To test this, we ran stochastic simulations in which our initial conditions were a single cell with k ecDNA,

where k is the mean ecDNA number in a given cell line. We then simulated growth of this cell until we reached a population size of 10^6 (Figure 2.4A). The only assumption in these simulations was that inheritance of the ecDNA was exactly random, as we previously demonstrated. We then analyzed the distribution of ecDNA throughout the population and compared it to the distribution of ecDNA in the cell lines we analyzed (Figure 2.4B). The distributions were largely similar and, accounting for multiple hypotheses, statistically not significantly different. These data suggested that the random inheritance of ecDNA was sufficient to generate a level of genetic heterogeneity that we observed in our ecDNA cell lines.

I then wanted to determine whether this level of heterogeneity was also observable in patient tumors. To test this I analyzed FISH for oncogenes suspected of being on ecDNA (based on copy number profiles and amplicon distributions) in patient tumor tissue samples. I analyzed samples from 6 GBM patients and 4 NB patients. The ecDNA distributions were extremely similar to those in the cell lines, though with a smaller average copy number. Again we wanted to establish whether random segregation of ecDNA was sufficient to establish the level of intratumoral heterogeneity we observed in these patient samples. We again ran stochastic simulations in which our initial condition was a single cell with a single ecDNA – these simulations were designed to more closely mimic the development of a tumor from a single transformed cell (Figure 2.4C). We continued these simulations until the simulated tumors reached a size of 10^{11} cells, a size reasonable to prompt detection and resection in a patient. We then compared the distribution of ecDNA in these simulated tumors to the patient samples; we found the distributions matched

extremely well, suggesting again that random inheritance of ecDNA is sufficient to establish a significant degree of intratumoral heterogeneity in patient tumors (Figure 2.4E-F). Interestingly, when analyzing the distributions at extremely high copy numbers, we found that the simulated distributions very closely approximated a power-law process with an exponential cutoff (Figure 2.4D). This is similar to other biological processes in nature, suggesting ecDNA behavior results in a mathematically governed process.

ecDNA promote rapid adaptation and resistance to environmental challenges

Having demonstrated the impact of ecDNA random inheritance on intratumoral heterogeneity, I then wanted to determine whether these abnormal inheritance patterns affected the ability of cancer cells and tumors to adapt and gain resistance to environmental and therapeutic challenges. I made use of an isogenic cell line model of ecDNA in glioblastoma – GBM39-EC and GBM39-HSR. The GBM39-EC cell line harbors high copy number amplification of the EGFRvIII variant almost exclusively on ecDNA (Figure 2.5A). GBM39-HSR similarly has a near identical level of EGFRvIII amplification; however, these amplicons are almost exclusively maintained on a few chromosomal regions referred to as homogeneously staining regions (HSRs). GBM39-HSR was derived from a single cell isolate of the GBM39-EC; thus, these cell lines are nearly identical in terms of their bulk genetic and gene expression identity. This enabled me to experimentally test the effect of ecDNA on how these cell lines adapt to environmental changes.

First, I verified the increased heterogeneity in GBM39-EC relative to GBM39-HSR, as would be predicted based on our understanding of how ecDNA promotes

heterogeneity from our prior analyses. I quantified the number of ecDNA per metaphase spread in GBM39-EC and the number of HSRs per metaphase spread in GBM39-HSR and calculated the Shannon Diversity Index for both cell lines (Figure 2.5B). GBM39-EC had a significantly higher level of diversity of EGFR copy number. I also verified that this relationship held at the protein level as well. I performed flow cytometry analysis of the two cell lines. Using an EGFRvIII specific antibody, I found that similar to the copy number analysis, GBM39-HSR had a narrow distribution of high EGFR protein expressing cells while GBM39-EC had a wide distribution from almost no EGFR to high EGFR protein expression (Figure 2.5C).

We then wanted to explore how these two cell lines would respond to environmental challenges. We hypothesized that the diversity of phenotypes induced by the random inheritance would make GBM39-EC less sensitive to challenges. We first tested the ability of these cells to continue to proliferate in a low glucose environment (20% of normal cell culture levels). We chose glucose deprivation because prior work from our group had shown that these cells are highly glycolytic. When we grew cells in these conditions for 1 week, we found that the growth rate of GBM39-HSR fell to about 50% compared to control while the growth rate of GBM39-EC maintained the same rate as control (Figure 2.6A). To understand the mechanism underlying this differential response, we quantified the distribution of ecDNA and HSRs in the two cell lines at multiple time points through 15 days of glucose deprivation. We expected that the distribution of ecDNA could adapt to the glucose deprivation, while the HSRs, since they are ‘locked’ onto chromosomes, would not be able to adjust their distribution in response to deprivation.

Indeed, we saw the distribution of HSRs in GBM39-HSR stay remarkably constant while GBM39-EC showed a significant and rapid decrease in the distribution of ecDNA copy number (Figure 2.6B). The vastly differential behavior of these two cell lines strongly suggests ecDNA can play a significant role in shaping how cells respond to environmental challenges.

I next wanted to determine whether this was also the case in a more clinically relevant experiment. I treated these cell lines with the EGFR tyrosine kinase inhibitor (TKI) erlotinib, which is a frequent therapeutic option for patients with EGFR mutated tumors. I treated both cell lines with 5 μ M erlotinib for 17 days. I found that GBM39-EC was initially less sensitive to the treatment than GBM39-HSR (Figure 2.6C). I also found that GBM39-EC was able to eventually overcome the growth defect of erlotinib and establish resistance, while GBM39-HSR continued to decrease in cell number (Figure 2.6C). Again I analyzed the distribution of ecDNA and HSR before and after erlotinib therapy and found a similar trend to the glucose withdrawal. After 7 days of treatment, GBM39-EC had significantly decreased its distribution of EGFRvIII ecDNA while GBM39-HSR's distribution of EGFRvIII amplification remained remarkably constant (Figure 2.6D). I then withdrew treatment for 7 days and GBM39-EC's distribution partially recovered to pre-treatment levels, while GBM39-HSR again remained constant (Figure 2.6D). Taken together these data demonstrate the remarkable affect ecDNA can have on the heterogeneity and resistance of a given population of cancer cells.

Given these results, I next wanted to determine whether we could see evidence of this process we observed in our cell lines taking place in patients' tumors. To study this I

analyzed EGFR FISH done on GBM patient tumor tissue as part of a clinical trial in which patients had their primary tumor resected and compared to a relapse that was pre-treated with lapatinib (another EGFR TKI) for 7-10 days before resection. I quantified the distribution of EGFR copy number in these patients' tumor tissue and compared the distribution of the primary (naïve) tumor to the distribution of the lapatinib-treated relapse. Both patients showed a significant decline in the distribution of EGFR copy number (Figure 2.7A).

I sought to expand these findings into another tumor type to ensure that these effects were not isolated to GBM. We analyzed tumor tissue of two NB patients who were part of a clinical trial. We compared the distribution of their highly amplified MYCN oncogene in a biopsy taken prior to treatment to the resected tumor after approximately 4-5 months of an intensive treatment regimen, which included vincristine, a drug that we had evidence decreased MYCN ecDNA in cell lines (Figure 2.7B). We quantified the distribution of MYCN amplification in these patient samples and compared each patient's copy number distribution in the initial biopsy (naïve) and the treated resected primary. We found both patients showed a significant decrease in MYCN copy number distribution after therapy (Figure 2.7B). Taken together these patient data strongly suggest that the dynamics we observed and tested experimentally *in vitro* may be taking place similarly in patients' tumors, both prior to treatment in establishing high levels of intratumoral heterogeneity and after treatment in rapidly altering the genomic makeup of the tumor to generate resistance.

Next, I wanted to further understand how universal this adaptability is within cell lines derived from different cancer types and ecDNA with different oncogenes and targeted therapies. I planned to utilize the stomach cancer cell line SNU16, since it has amplification of FGFR2, a tyrosine kinase similar to EGFR, though distinct in its specific ligand and targeted therapeutics that block its function. Interestingly, this cell line also has significant amplification of MYC on separate ecDNA molecules. Given the very different nature of MYC and FGFR2 amplifications in terms of mechanisms, this provided me with an excellent model to test the sensitivity of ecDNA populations within cells to targeted therapeutics.

To test this, I treated SNU16 cells with 1 μ M of ponatinib, a broad tyrosine kinase inhibitor with significant activity toward FGFR2 amplified cancer models⁵¹. After one week of treatment, I prepared metaphase spreads and did FISH for both ecDNA amplified oncogenes (Figure 2.8A). Similar to previous examples, I found that FGFR2 copy number distributions declined rapidly and significantly compared to DMSO treated samples (Figure 2.8B). Surprisingly, however, MYC ecDNA showed no significant change in copy number distribution over this period (Figure 2.8B). This experiment suggests that ecDNA can specifically respond and adapt to targeted therapies while ecDNA not targeted can maintain a constant distribution throughout the population. This adds an incredibly level of complexity in terms of thinking about and modeling tumor response to therapy and the development of resistance in the context of tumors with multiple species of ecDNA. Given this interesting result, I wanted to understand more about how cell lines and tumors with multiple species of ecDNA behave.

Non-independent inheritance of multiple ecDNA species

Recent research into the behavior of ecDNA during interphase has suggested that ecDNA form ‘hubs’ which are sites of increased transcriptional activity and intermolecular transcriptional enhancement²⁴. This was found to be the case in instances where a single cell contains multiple ‘species’ of ecDNA (i.e. 20 copies of MYC ecDNA and 40 copies of FGFR2 ecDNA). I was interested in determining whether this interphase behavior may influence how ecDNA behave through mitosis.

To test this I repeated the experimental design presented in Figure 2.2 in which I used IF-FISH to identify late mitoses and quantify the ecDNA distribution in daughter cells. Here, I used cell lines which were known to have at least 2 species of ecDNA: 1) SNU16 (FGFR2 and MYC), 2) GBM39-EC (EGFR and MYC), 3) TR14 (CDK4 and MYCN). I imaged these IF-dualFISH samples and quantified the inheritance of both ecDNAs in the same pairs of daughter cells. This yielded very interesting results. While inheritance of each individual ecDNA was random, as previously described, inheritance of the two species was not independent of each other (Figure 2.9A-B); that is, the daughter cell that inherits more than 50% of one ecDNA is likely to inherit more than 50% of the other ecDNA. I verified that this was not due to rearranging of the two oncogenes onto the same ecDNA by using a variant of the SNU16 cell line which was selected for distinct ecDNA molecules of FGFR2 and MYC (SNU16-m1, Figure 2.10A-B). I also quantified the frequency of colocalization of FGFR2 and MYC pixels in metaphase FISH done in this cell line and found this value to be less than 10% – even so, this is likely to be an

overestimate due to some steric overlap that does not represent fusing of the two molecules (Figure 2.10C). These data add a fascinating level of complexity to our prior understanding of ecDNA and its random inheritance. In fact, it is possible that this suggests that cancer cells will have diminishing returns in terms of their ability to promote heterogeneity when there are multiple ecDNA species. That is, because of the behavior of ecDNA – perhaps influenced by failure to dissolve interphase hubs – these cancer cells are not optimizing their level of diversity, which would be accomplished by both ecDNA segregating randomly and *independently*.

These data may help to explain the results presented previously in which SNU16 cells decreased FGFR2 ecDNA copy number specifically in response to ponatinib treatment while MYC ecDNA copy number dropped only slightly (Figure 2.8). One question that this experiment brought up was, why did the MYC ecDNA copy number respond at all to a TKI treatment? Given these segregation data, it is distinctly possible that due to the non-independent inheritance of ecDNA species, MYC ecDNA are decreased to a lesser extent due to ‘collateral’ damage. As cells with fewer FGFR2 ecDNA are more likely to survive, given these cells were more likely to receive fewer MYC ecDNA, cells with fewer MYC ecDNA are more likely to survive, without the need for a mechanistic link to the drug treatment.

To understand the potential clinical impact of this finding, we next looked to TCGA data to determine how frequently tumors develop multiple distinct ecDNA species. We used AmpliconClassifier to determine the presence of ecDNA, but instead of a binary ecDNA +/-, we determined whether there were distinct ecDNA species. We found that

while the majority of tumors with ecDNA have a single species, a surprisingly high proportion have multiple ecDNA species (30%, Figure 2.11A-B).

Next, I was interested in determining whether multiple species of ecDNA correlated with worse prognosis in patients, given the resultant increase in diversity that was likely to go along. Analysis of survival outcomes of these patients, stratified into 1 or 2+ ecDNA species showed no statistical difference between the two groups (Figure 2.11C). Given the relatively small sample sizes we were unable to control for tumor type and other variables; a larger analysis of this type would be informative for understanding whether increased tumor complexity correlates with poorer survival.

Doublet structures of ecDNA in metaphase are tethered sister ‘chromatids’

Initial discoveries and research into ecDNA referred to these structures seen in metaphase spreads as double minutes (DMs)⁵². This was because they appeared often, though certainly not always, as paired circular structures, significantly smaller than even the smallest chromosomes. Understanding the nature of these structures is important both for understanding the dynamics of ecDNA throughout mitosis, but also to inform quantification methods which could yield significantly different results depending on whether doublet ecDNA are counted as one or two ecDNA.

In order to better understand this biology, I imaged several metaphase spreads from two ecDNA cell lines, GBM39-EC and COLO320DM. I was most interested in determining whether ecDNA doublet structures correlated with the stage of mitosis we were viewing. While metaphase spread procedures are intended to enrich for cells in

metaphase, cells anywhere from prophase to metaphase are observed. The specific stage for a given spread can be inferred based on the morphology and presentation of the chromosomes. For example, in prophase, chromosomes are incompletely condensed, often appearing as long slender structures and completely attached along their length to their sister chromatid due to the continued presence of cohesin⁵³. Spreads that have been stalled in metaphase for long periods of time due to the microtubule poison show the classic ‘X’ shaped chromosomes with sister chromatids only attached at the centromeres, with cohesin having been removed from the chromosome arms by WAPL⁵⁴.

I developed a simple scoring method in which I quantified the fraction of chromosomes still cohered along their entire length and correlated this with the fraction of ecDNA that were present in doublet structure compared to singlets. I plotted these data and observed a clear correlation between the cohesion of chromosomes and the frequency of doublet ecDNA structures (Figure 2.12A). This strongly suggested that doublet structures represented the ecDNA equivalent of sister chromatids, with the lack of centromere resulting in complete loss of cohesion when cohesin was removed from chromosome arms.

Given these data, I pursued a strategy to conclusively determine whether ecDNA doublets are sister chromatids. I developed an assay to test this, utilizing the semi-conservative nature of DNA replication to incorporate BrdU, a nucleotide analog, over the course of two S-phases resulting in differential levels of BrdU incorporation between sister chromatids (Figure 2.12B). At the conclusion of BrdU incorporation over two S-phases, one sister chromatid will have both DNA strands labeled with BrdU while the other has a single labeled strand and a single unlabeled strand (Figure 2.12B). With differential BrdU

labeling, I then added Hoechst 33342, a fluorescent DNA dye that is partially quenched when binding to BrdU incorporated DNA⁵⁵. Finally, exposure of these samples to UV light to improve the differential fluorescence of the Hoechst on BrdU incorporated and normal DNA⁵⁶. When I imaged these metaphase spreads, the results were immediately striking. Chromosomes showed clear differential fluorescence of the sister chromatids, confirming the success of the assay (Figure 2.12C). Interestingly, the ecDNA doublet structures showed the exact same pattern of light-dark staining, providing conclusive evidence that ecDNA doublet structures viewed at metaphase are ecDNA bodies that are still cohered to their sister chromatid (Figure 2.12C). This data both confirms my hypothesis that ecDNA doublets (DMs) are instances of ecDNA with cohered sister chromatids and provides important insight into the dynamics of ecDNA during mitosis. Given these data (Figure 2.12A), we can infer that ecDNA likely have cohesin cleaved at a similar stage as chromosome arms and separate completely prior to anaphase due to the lack of centromere region which maintains cohesin until anaphase.

C. Discussion

The results presented here in Chapter II represent a thorough analysis of the mathematical rules that inheritance of ecDNA follows and the downstream consequences in terms of tumor heterogeneity and resistance. We quantitatively and qualitatively analyzed the inheritance of ecDNA and demonstrated that the process can be well represented as a random binomial test for each ecDNA molecule. This was shown to be true across cancer types and across oncogenes.

We further demonstrated that this pattern of random inheritance plays a significant role in increasing the genetic diversity in patients' tumors. We showed that this, in turn, increased the ability of tumors to adapt and develop resistance to therapeutics. Finally, we demonstrated that in cancers with more than 1 ecDNA species, segregation does not occur independently which may help to suggest why patients with multiple species do not have a worse prognosis than those with a single species.

This is the first study to our knowledge that clearly and quantitatively connects the random inheritance of ecDNA and the clinical impact that has on heterogeneity and resistance. It has been suggested that patients with ecDNA tumors have a worse prognosis than those without ecDNA, controlling for tumor type and demographic variables. However, our understanding of the mechanisms underlying this discrepancy in outcomes is severely lacking. Here we propose that one of the fundamental properties of ecDNA may be playing a significant role in increasing the aggressiveness and ability to achieve resistance in tumors.

More research into this area must be done to validate and further these findings. Our grasp of the clinical implications of random ecDNA inheritance could be furthered by tissue level analysis done on larger cohorts of patients. Similarly, identification of patients in trials in which a naïve biopsy is obtainable followed by a treated primary resection will enable us to further understand the ability of ecDNA to adapt and alter the genome of tumors in response to treatment.

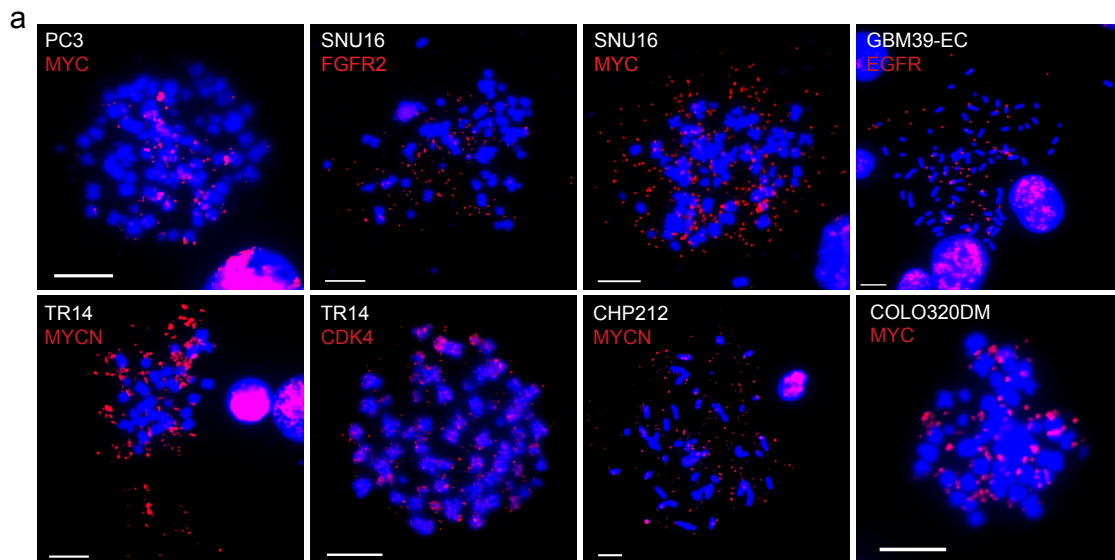


Figure 2.1 | Panel of cell lines with ecDNA.

a, Representative images of metaphase FISH for all ecDNA-containing cell lines to be included in the experiments in this dissertation. It contains a breadth of cancer types (PC3-prostate; SNU16-stomach; GBM39-EC-glioblastoma, TR14-neuroblastoma; CHP212-neuroblastoma; COLO320DM-colorectal) and ecDNA-amplified oncogenes. Scale bars 10 μ m.

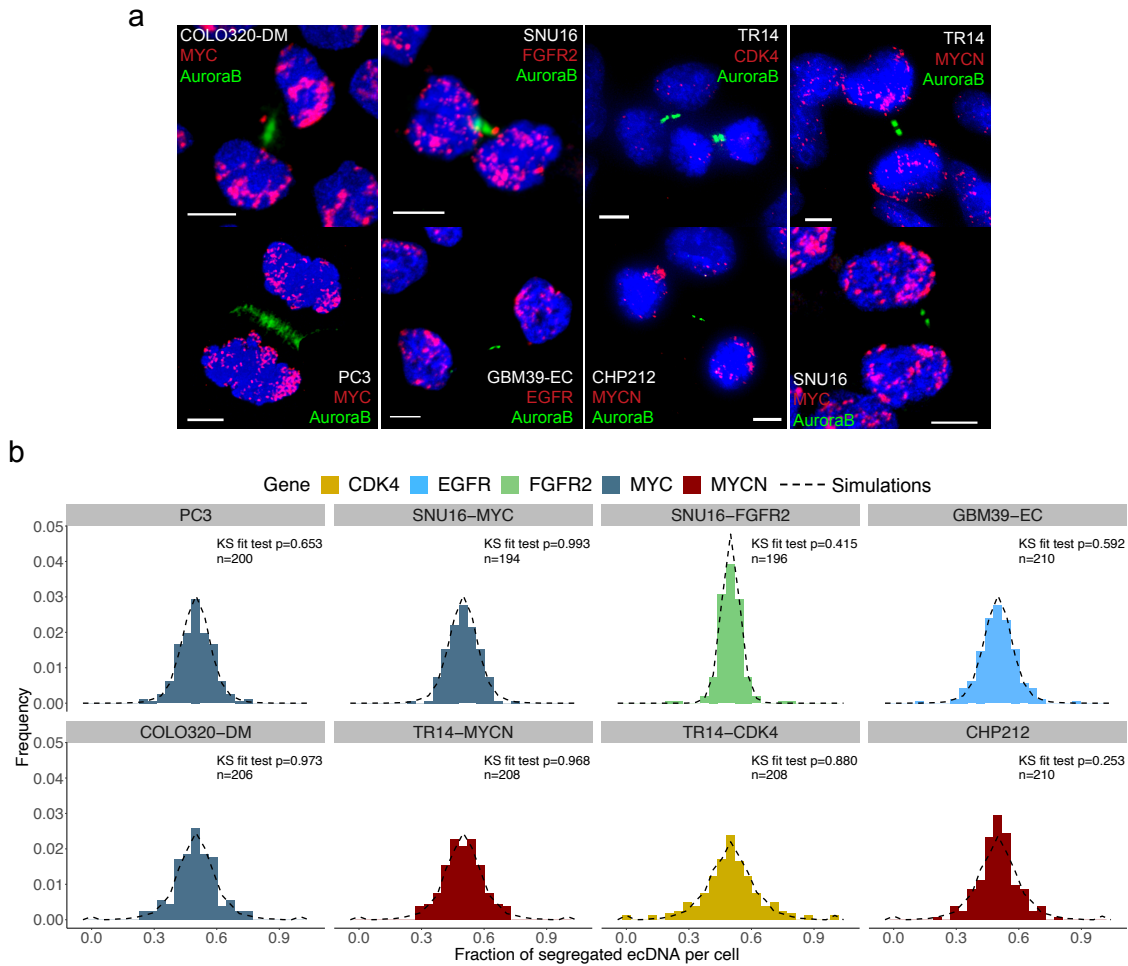
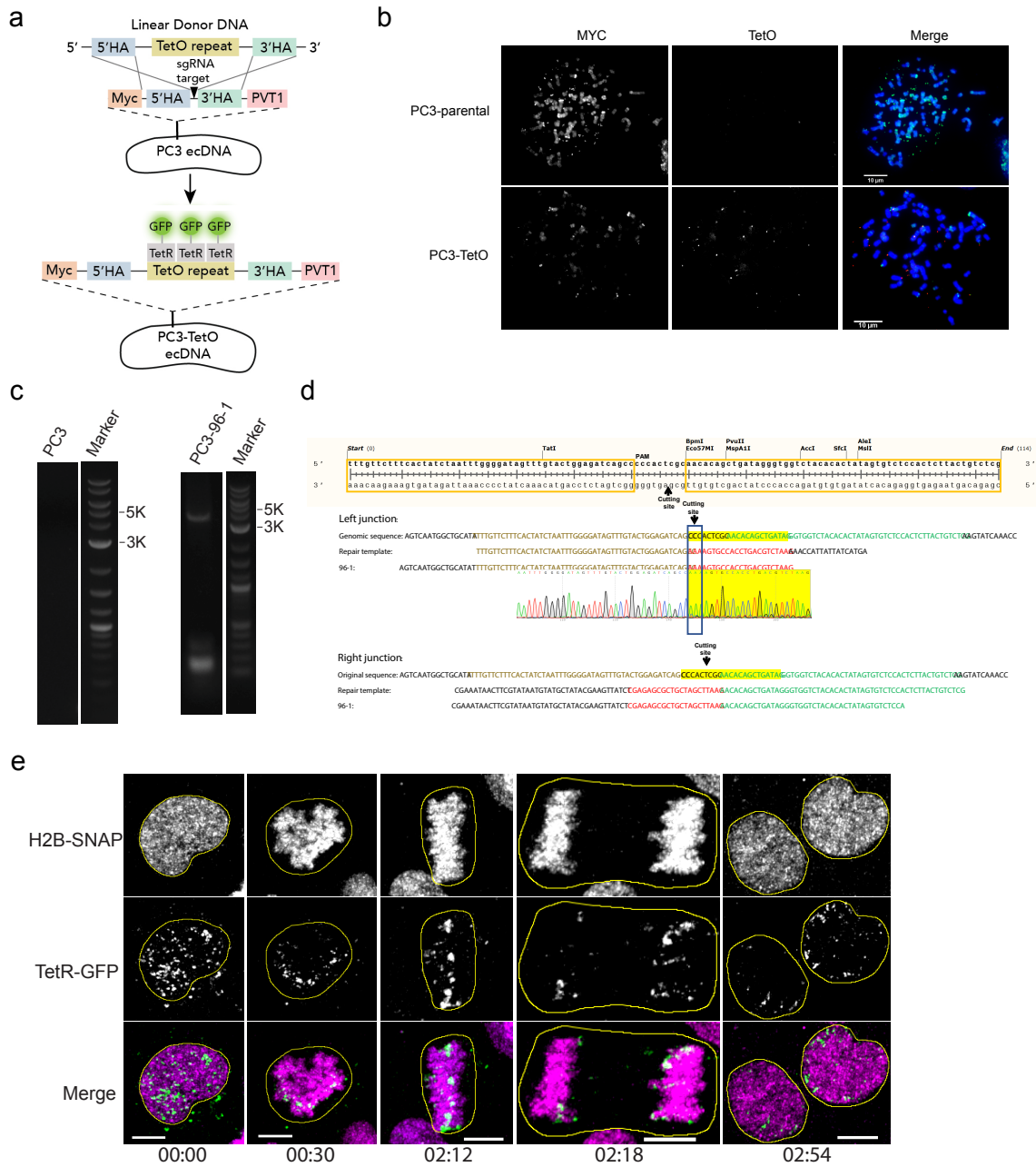


Figure 2.2 | ecDNA is randomly inherited by daughter cells.

a, Representative images of cell line panel used to measure ecDNA segregation dynamics. IF-FISH images with Aurora B detected by IF shown in green at the midbody of late mitotic cells, and ecDNA-based oncogenes detected by FISH shown in red. Scale bars 5 μ m. **b**, Quantification of ecDNA segregation for each cell line presented as the fraction of mother cell ecDNA inherited by each daughter cell. Colored histograms represent quantification of experiment shown in **a**. Dashed outline of distribution represents expected distribution for each cell line for perfectly random inheritance of ecDNA. KS test values > 0.05 suggest no significant difference between observed data and perfectly random segregation.

Figure 2.3 | Live-cell imaging of ecDNA behavior through mitosis.

a, Schematic depiction of strategy used to engineer a fluorescent tracker of ecDNA in PC3 cells. Briefly, a 96-mer TetO repeat cassette was inserted between MYC and PVT1 on the PC3 ecDNA via CRISPR/Cas9 mediated cutting. Homology arms (HA) were designed to promote repair of the Cas9 cut with the TetO cassette via homologous recombination (HR). Subsequent expression of TetR-GFP enabled live-cell fluorescent tracking of ecDNA. **b**, FISH for MYC and TetO sequences in PC3 and PC3-TetO cell lines showing integration of TetO sequences in MYC ecDNA. **c**, PCR amplification of TetO cassette region in DNA extracted from PC3 and PC3-TetO cells showing integration of cassette. **d**, Sequencing of left and right junctions of PCR amplified TetO cassette from PC3-TetO cell line showing repair of cut region with the TetO repair template. **e**, Images of a cell division in PC3-TetO cells showing unequal segregation of ecDNA at mitosis and clustering of ecDNA in early-mid mitosis.



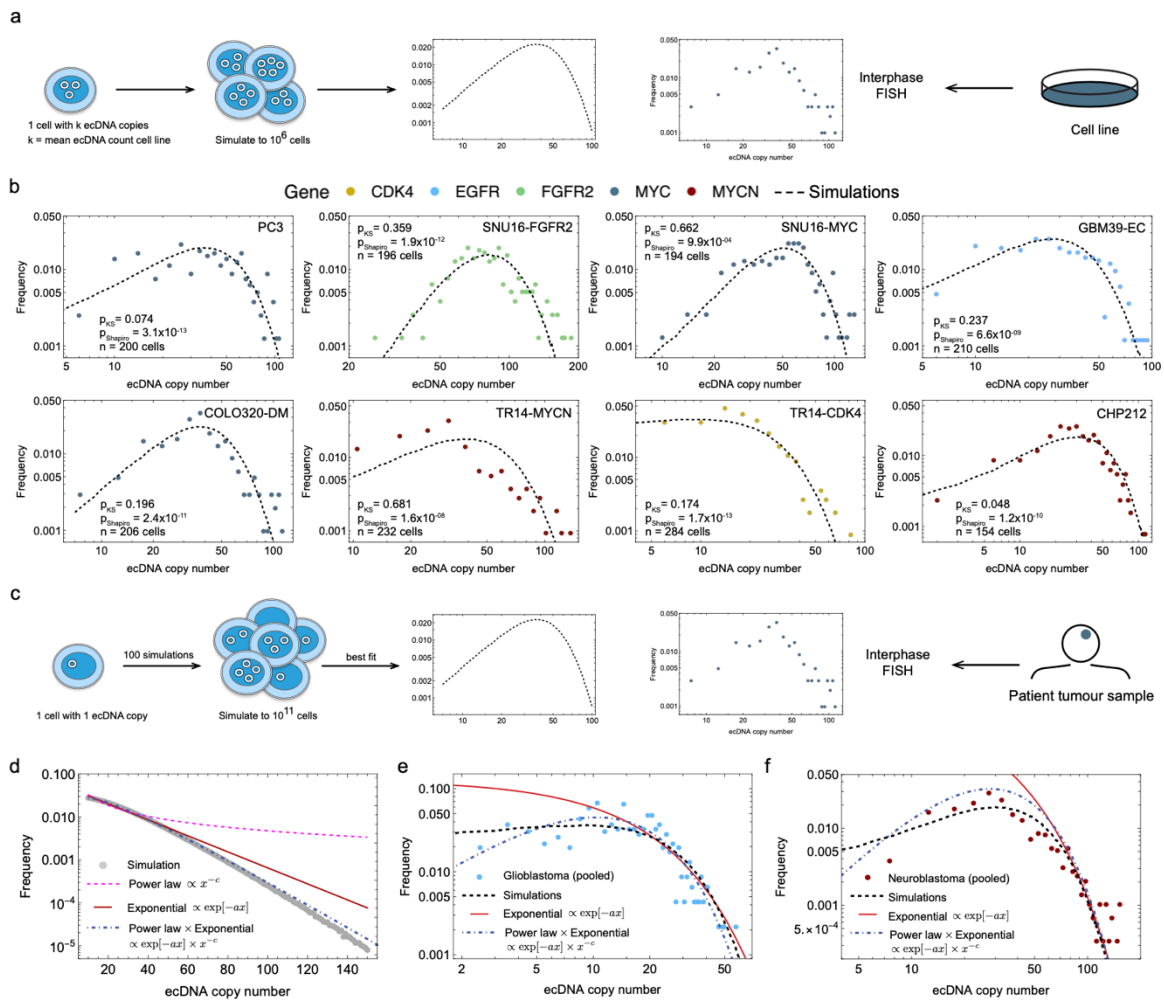


Figure 2.4 | Random inheritance of ecDNA causes significant and modellable heterogeneity in cell lines and patient tumors.

a, Schema demonstrating the acquisition of ecDNA copy number heterogeneity data from simulations and cell line samples. **b**, Comparisons of the heterogeneity seen in cell line samples (colored points) and in simulations (dotted curves) showing the high level of heterogeneity and strong agreement of empirical and modeled data (KS tests > 0.05). **c**, Schema demonstrating the acquisition of ecDNA copy number heterogeneity data from simulations of tumor development and FISH on patient tumor tissue. **d**, Scaling of ecDNA copy number distribution from simulated data at low frequency and high copy number suggest a distribution which scales in a manner most resembling a power law process with an exponential cutoff. **e-f**, Comparison of high level of intratumoral heterogeneity in GBM and NB patient tissue (colored points) with simulated ecDNA heterogeneity in simulated tumor progression (dashed curves) – also showing agreement with scaling as an exponential and power law with exponential cutoff process.

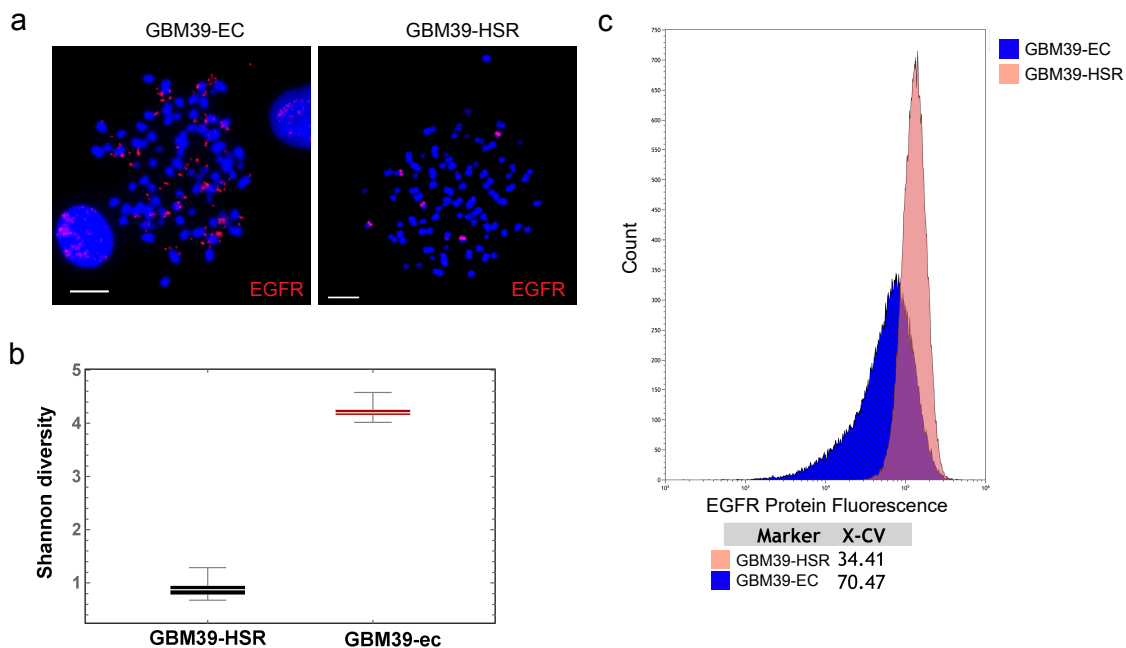


Figure 2.5 | Isogenic ecDNA +/- GBM cell lines.

a, Representative images of metaphase spread FISH from GBM39-EC and GBM39-HSR showing amplification of EGFRvIII on ecDNA in the former and amplification of EGFRvIII on HSRs in the latter. Scale bars 10 μ m. **b**, Shannon diversity index calculated based on the number of distinct amplicons identified on metaphase spreads from GBM39-EC and GBM39-HSR. **c**, Heterogeneity of EGFRvIII protein levels between the two cell lines assessed by flow cytometry showing a narrow band of high EGFRvIII expression in GBM39-HSR and a broad range of EGFRvIII expression levels in GBM39-EC.

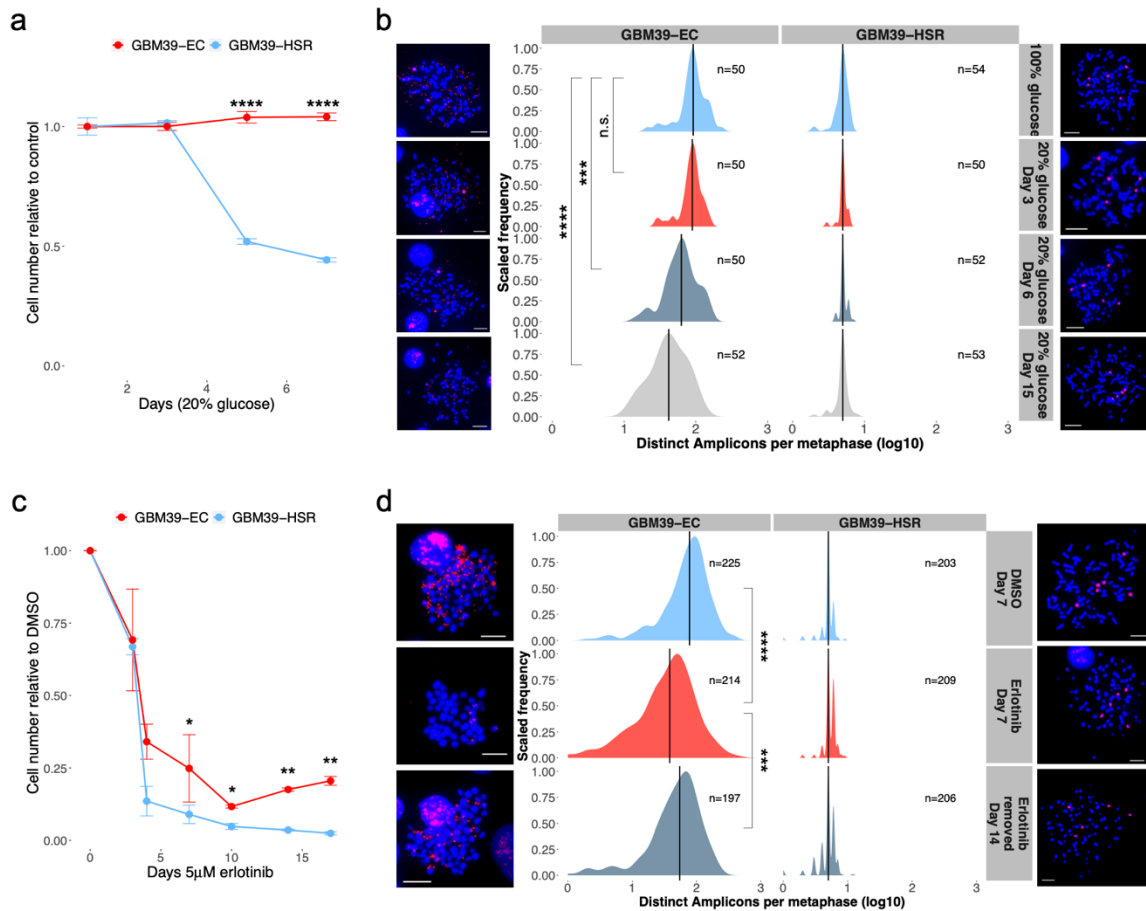


Figure 2.6 | ecDNA promotes resistance and adaptation to environmental and therapeutic challenges.

a, GBM39-EC shows no change in cell number after 7 days of glucose deprivation (20% of normal levels) while GBM39-HSR shows significant growth defect under these conditions. **b**, Quantification of EGFRvIII ecDNA copy number distributions in the two cell lines over time for 15 days of glucose deprivation showing adaptation of GBM39-EC copy number and no change of the distribution for GBM39-HSR. **c**, GBM39-EC shows less sensitivity and formation of resistance to 5 μ M erlotinib treatment while GBM39-HSR shows significant sensitivity. **d**, Quantification of EGFRvIII ecDNA copy number distributions in the two cell lines after 7 days of 5 μ M erlotinib treatment and 7 days of drug removal. GBM39-EC shows left-shift in distribution after treatment which recovers when drug is removed; GBM39-HSR shows constant distribution irrespective of treatment condition.

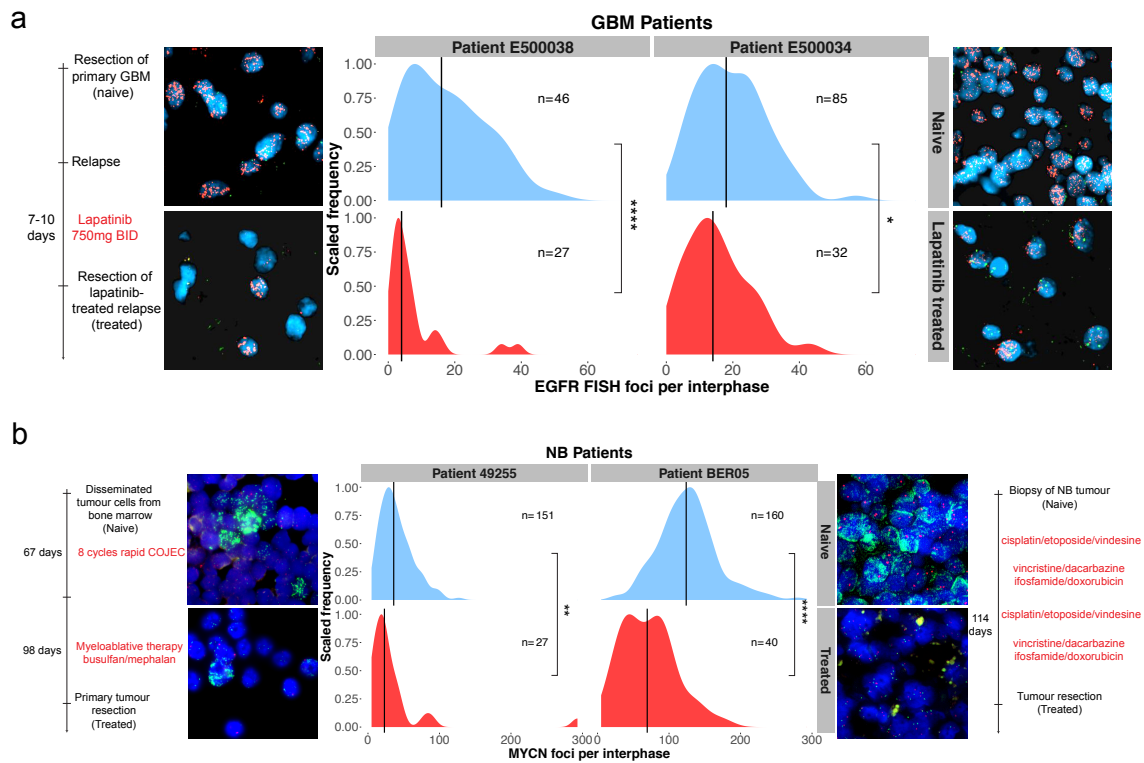


Figure 2.7 | ecDNA enables GBM and NB tumors to shift copy number in response to therapy and changing environment.

a, Representative images of tissue FISH for EGFR for two GBM patient who followed an approximate time course as presented on the left timeline. Quantification of ecDNA copy number distributions in the center show intratumoral heterogeneity and high EGFR copy number amplification under treatment naïve conditions. The recurrence which was treated briefly with Lapatinib prior to resection shows a significant decrease in EGFR copy number distribution, similar to the behavior of ecDNA seen in controlled cell lines. **b**, Representative images of tissue FISH for two NB patients treated under the protocols outlined on either side of the panel. Quantification of the distributions of MYCN amplification shows high levels of amplification and heterogeneity for both patients under treatment naïve conditions. After rounds of therapy including vincristine, both patients' tumors show a significant left-shift in their MYCN copy number distribution similar to the behavior of ecDNA seen in cell line experiments.

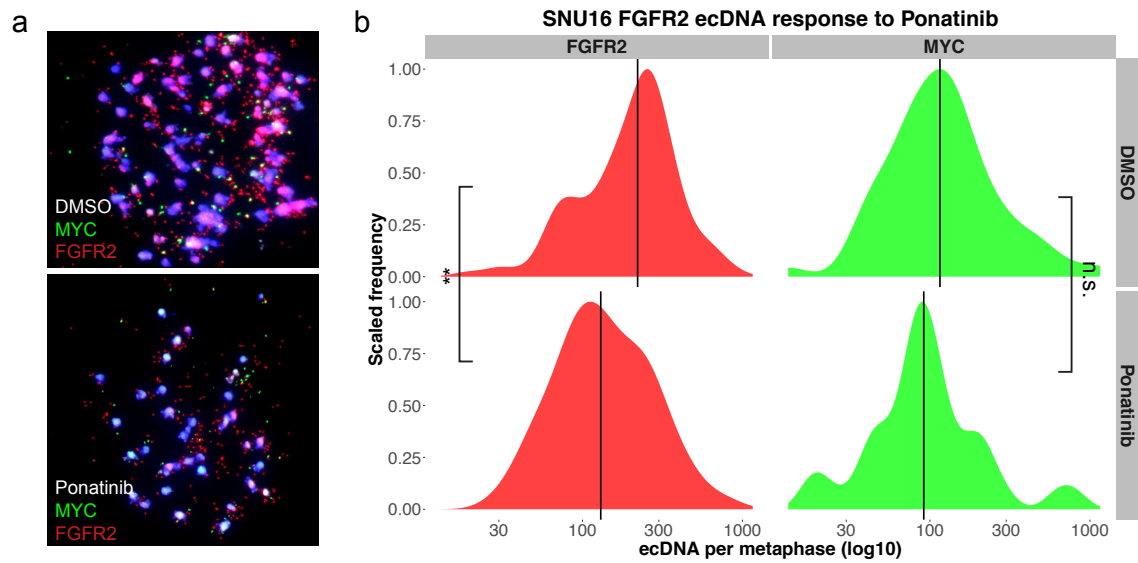


Figure 2.8 | SNU16 ecDNA change ecDNA copy number in a species-specific manner.

a, Representative images of SNU16 metaphase FISH with MYC visualized in green and FGFR2 visualized in red. The top image corresponds to 1 week of DMSO control treatment. The lower image corresponds to 1 week of 1 μ M Ponatinib treatment. **b**, Quantification of the experiment described in **a**. SNU16 cells significantly decrease the distribution of FGFR2 ecDNA in response to an FGFR2 inhibitor, while MYC ecDNA stayed relatively constant.

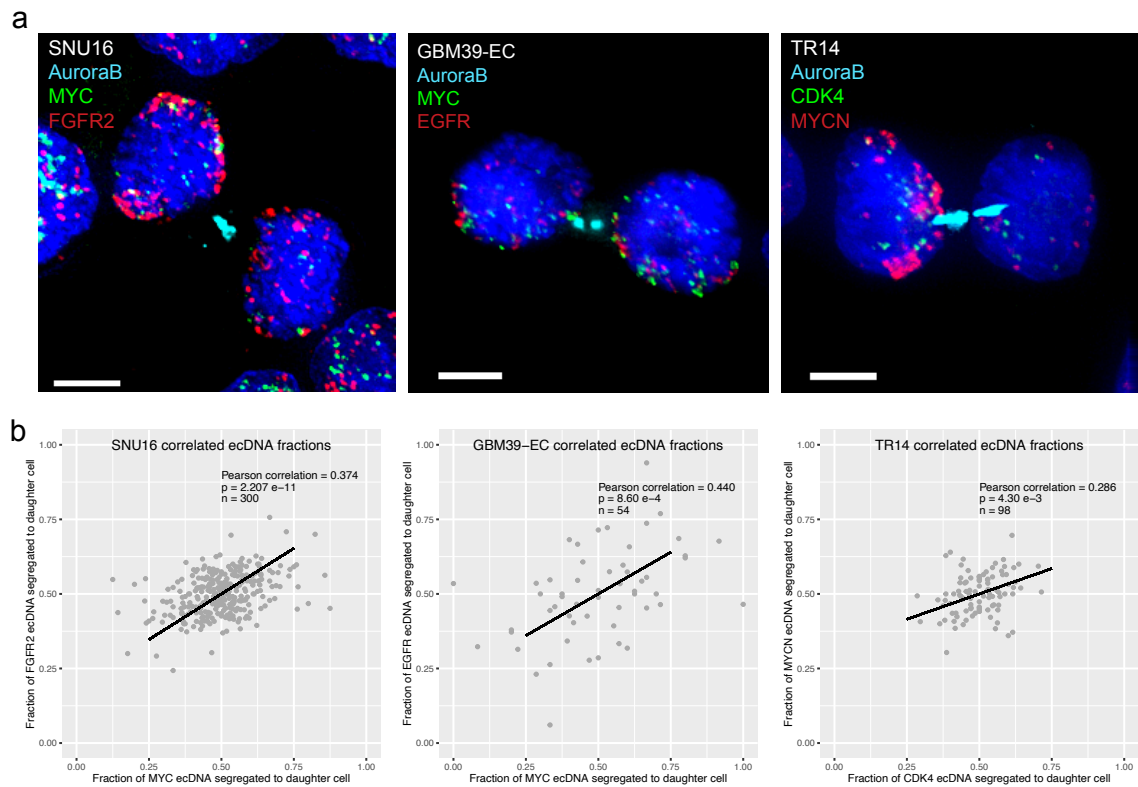


Figure 2.9 | Segregation of distinct ecDNA species in the same cell line is random but non-independent.

a, Representative IF-dualFISH images for 3 cell lines with 2 ecDNA species each. Aurora B detected by IF at late-mitotic midbody structures is shown in aqua and ecDNA is shown with green and red FISH foci. Scale bars 5 μ m. **b**, Quantification of ecDNA segregation fractions for the cell lines shown in **a**. Each point represents a single daughter cell and is plotted as a representation of the fraction of segregation of one ecDNA species on the x-axis and the fraction of segregation of the other ecDNA species on the y-axis. Pearson correlations are shown for each cell line with all cell lines showing significant correlation in the segregation fraction of both ecDNA species.

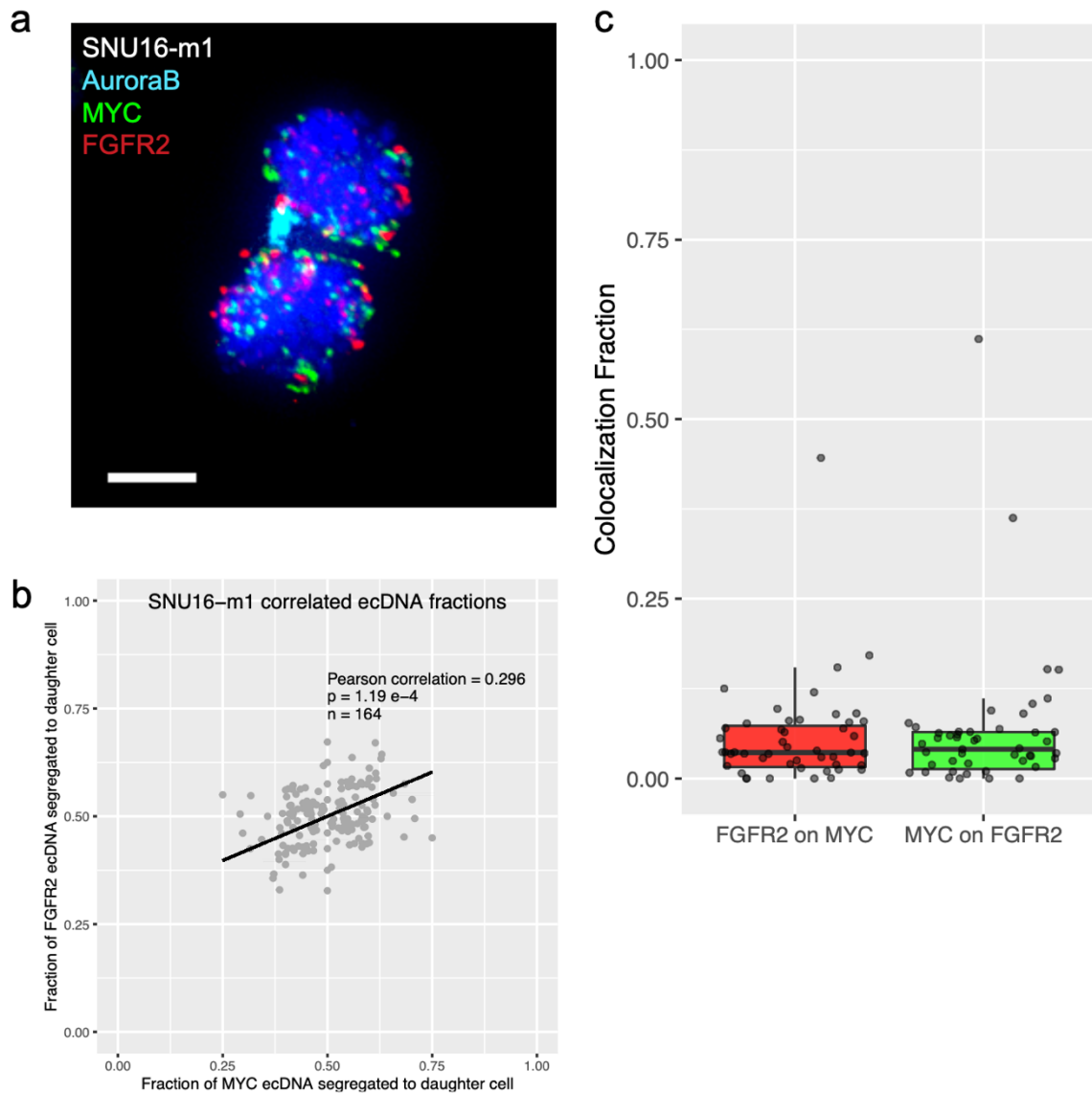


Figure 2.10 | Non-independent segregation of ecDNA species is not due to fused molecules.

a, Representative image of a dividing SNU16-m1 cell, which was selected to avoid instances of fused MYC and FGFR2 ecDNA. Scale bar 5 μm . **b**, Segregation correlation of the MYC and FGFR2 ecDNA in SNU16-m1 showing positive and significant Pearson correlation. **c**, Quantification of colocalization fractions for MYC and FGFR2 ecDNA from metaphase spread FISH of SNU16-m1 cells showing minimal colocalization on metaphase spreads indicating correlated segregation is not likely due to fused ecDNA species.

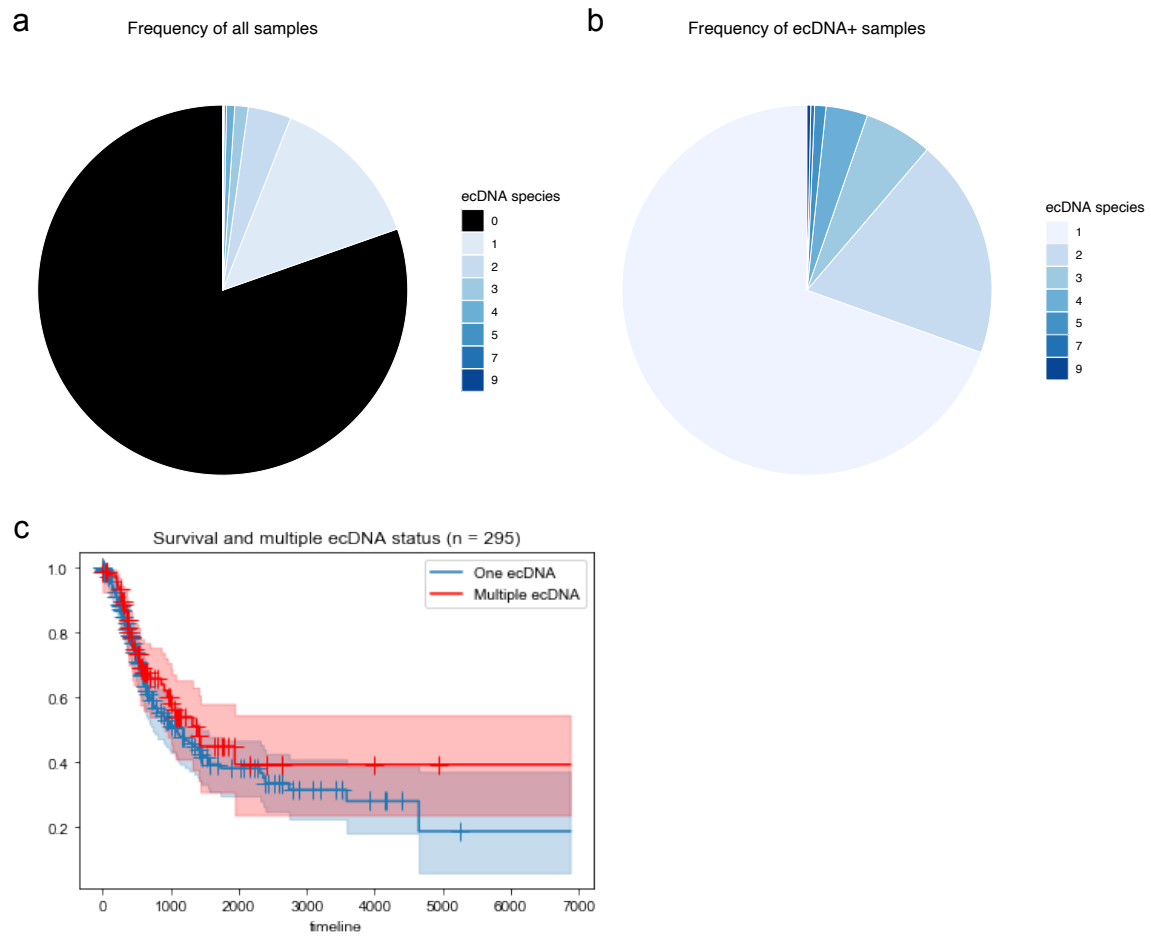
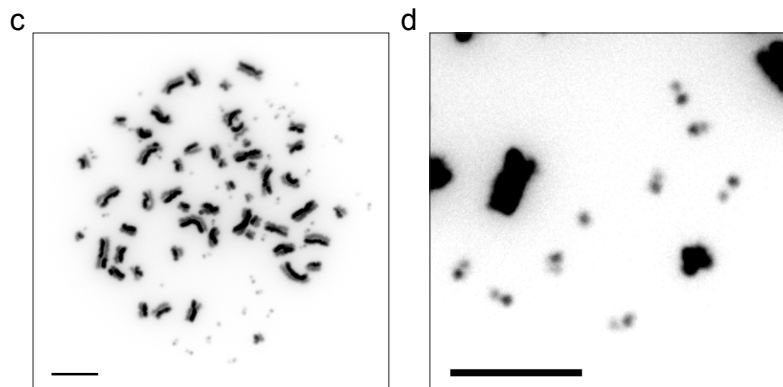
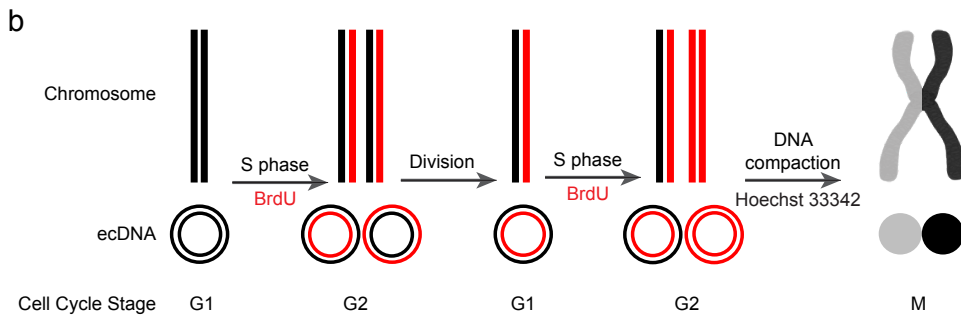
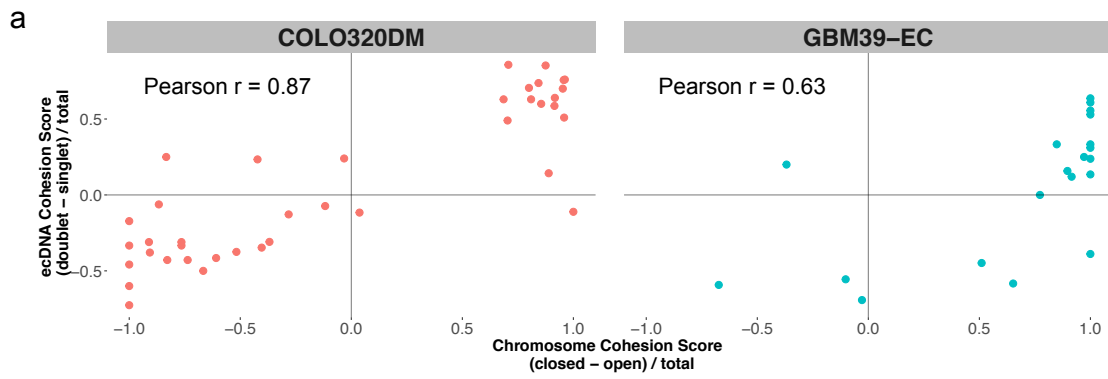


Figure 2.11 | Frequency and prognosis for tumors with multiple ecDNA species in TCGA.

a, Pie chart depicting the frequency of all TCGA samples analyzed containing various numbers of distinct ecDNA species. **b**, Pie chart depicting the frequency of all ecDNA+ TCGA samples analyzed containing various numbers of distinct ecDNA species. **c**, Kaplan-Meier curves for overall survival of patients with either one ecDNA species or multiple ecDNA species ($p = 0.34$). Analyses of TCGA data done by Dr. Jens Luebeck using AmpliconClassifier.

Figure 2.12 | Similarity of cohesion dynamics between chromosomes and ecDNA throughout mitosis.

a, Correlation of chromosome and ecDNA cohesion dynamics quantified from metaphase spreads. X-axis quantifies the frequency of chromosomes that have arms still cohered (positive) and the frequency of chromosomes that have sister chromatid arms separated (negative). Y-axis quantifies the frequency of ecDNA appearing as doublet structures (positive) and the frequency of ecDNA appearing as singlet structures (negative). Significant Pearson correlations are shown. **b**, Schema depicting assay to cause differential fluorescence of sister chromatids. Briefly, incorporation of BrdU over 2 successive S-phases results in one sister chromatid with both strands labeled and one sister chromatid with 1 strand labeled. Hoechst staining differentially fluoresces based on BrdU concentration resulting in differential fluorescence. **c**, Representative inverted image of COLO320DM cells after the assay described in **b**. Note the differential light/dark staining of sister chromatids. **d**, Increased magnification and exposure of a section of the image presented in **c** enabling visualization of light/dark pattern on ecDNA doublet structures.



D. Methods and Materials

Cell Culture

Cell lines were purchased from ATCC or DSMZ-German Collection of Microorganisms and Cell Cultures (Leibniz Institute) or were a kind gift from J.H. Schulte. GBM39-HSR and GBM39-EC were derived from a GBM patient as previously described.

PC3 cells were cultured in DMEM with 10% fetal bovine serum (FBS). COLO320-HSR and COLO320-DM were cultured in DMEM/F12 50%:50% with 10% FBS. SNU16 were grown in RPMI-1640 with 10% FBS. GBM39-HSR and GBM39-EC neurospheres were grown in DMEM/F12 with B27, Glutamax, heparin (5 µg/ml), EGF (20 ng/ml) and FGF (20 ng/ml). TR14-cells were grown in RPMI-1640 with 20% FBS. Cell numbers were counted with a TC20 automated cell counter (Bio-Rad). For drug treatments, drug was replaced every 3-4 days.

Metaphase chromosome spreads

Cells were concentrated in metaphase by treatment with KaryoMAX colcemid (Gibco) at 100 ng/ml for between 3 hours and overnight (based on proliferation rate). Cells were washed once with PBS and a single cell suspension was incubated in 75 mM KCl for 15 min. at 37°C. Cells were then fixed with Carnoy's fixative (3:1 methanol : glacial acetic acid) and spun down. Cells were washed with fixative 3 additional times. Cells were then dropped onto humidified glass slides and aged overnight.

Fluorescence *in situ* hybridization (FISH)

Fixed samples on coverslips or slides were equilibrated in 2x SSC. They were dehydrated in ascending ethanol series of 70%, 85% and 100% for approximately 2 min. each. FISH probes were diluted in hybridization buffer (Empire Genomics) and added to the sample with the addition of a coverslip or slide. Samples were denatured at 72°C for 2 minutes and then hybridized at 37°C overnight in a humid and dark chamber. Samples were then washed with 0.4x SSC followed by 2x SSC 0.1% Tween-20 and 2x SSC (2 min. each). DAPI (100 ng/ml) was applied to the samples for 10 minutes. Samples were washed again with 2x SSC Tween and 2x SSC. Samples were briefly washed in water and mounted with Prolong Gold and sealed with nail polish. EGFR, MYC, FGFR2, CDK4, and MYCN FISH probes were purchased from Empire Genomics and diluted to manufacturer's recommendations. CDK4/Cen12 and MYCN/2q11 FISH probes used on NB tissue samples were purchased from ZytoVision (ZytoLight SPEC) and used according to manufacturer's recommendations.

Immunofluorescence – fluorescence *in situ* hybridization (IF_FISH)

Asynchronous cells were grown on poly-l-lysine coated coverslips (mouse laminin for GBM39-EC). Cells were washed once with PBS and fixed with cold 4% paraformaldehyde (PFA) at room temperature for 10-15 minutes. Samples were permeabilized with 0.5% Triton-X in PBS for 10 minutes at room temperature and then washed with PBS. Samples were blocked with 3% BSA in PBS-0.05% Triton-X (PBS-T) for 30 minutes at room temperature. Samples were incubated in primary antibody, diluted

in blocking buffer, for either 1 hour at room temperature or overnight at 4°C. Samples were washed thrice in PBS-T. Samples were incubated in secondary antibody, diluted in blocking buffer, for 1 hour at room temperature and then washed thrice in PBS-T. Cells were washed once with PBS and re-fixed with cold 4% PFA for 20 minutes at room temperature. Cells were washed once with PBS then once with 2x SSC. FISH proceeded as described above, with denaturation conditions altered to 80°C for 20 minutes. Aurora B polyclonal antibody (A300-431A) was purchased from ThermoFisher and diluted to 1:100-1:200 for detection.

Microscopy

Conventional fluorescence microscopy was performed using an Olympus BX43 microscope; images were acquired with a QI-Click cooled camera. Conventional fluorescence microscopy when z-stacks were acquired and for IF-dualFISH experiments was performed using a DeltaVision Elite imaging system (Applied Precision) and microscope (model IX-71; Olympus) controlled by SoftWoRx software (Applied Precision) with a CoolSNAP HQ2 camera (Photometrics). Confocal microscopy was performed using a Leica SP8 microscope with lightning deconvolution (UCSD School of Medicine Microscopy Core).

Flow cytometry

Single cell suspensions were made and passed through a cell filter to ensure single cells. Cells were suspended in flow cytometry buffer (HBSS buffer without calcium and

magnesium, 1x Glutamax, 0.5% FBS, 10 mM HEPES). EGFRvIII mab 806 was added at 1 μg per million cells and incubated on ice for one hour. Cells were washed in flow cytometry buffer and resuspended in buffer with anti-mouse alexa-488 antibody (1:1000) for 45 minutes on ice in the dark. Cells were washed again with flow cytometry buffer and resuspended in flow cytometry buffer at approximately 4 million cells per milliliter. Cells were sorted using a Sony SH800 FACS sorter and was calibrated and gating was informed using a secondary only negative control.

Simulations of ecDNA inheritance patterns

Stochastic simulations were implemented in C++ by Dr. Benjamin Werner. A single cell is initiated with a random number of ecDNA copies, n , chosen from a uniform distribution $U(20,200)$ based on our observations of copy numbers found in our cell lines. ecDNA is then replicated each cell cycle to $2n$. Segregation of the $2n$ ecDNA copies are determined using a binomial trial $B(2n, 0.5)$. Where 0.5 represents the 50% chance each ecDNA has of being segregated into a given daughter under perfectly random segregation. This process is iterated 10^7 times and the distribution of segregation patterns is then calculated.

Simulations of ecDNA population dynamics

Stochastic simulations were implemented in C++ by Dr. Benjamin Werner. Simulations to mimic cell line equilibrium were initiated with a single cell with n_0 copies of ecDNA. During modeled proliferation, ecDNA are doubled and randomly segregated as

in the segregation simulations described above. For cell line models, simulations were initiated with a single cell with n copies of ecDNA equal to the mean ecDNA number in that cell line and iterated until a population size of 10^6 was reached. For tumor progression models, simulations were initiated with a single cell with a single ecDNA. Simulations were run until a tumor size of 10^{11} cells was reached.

PC3-TetO cell line engineering

pSP2-96-merTetO-EFS-BlaR and F9-TetR-EGFR-IRES-PuroR plasmids were kind gifts from Dr. Huimin Zhao. DNA sequences for the region between MYC and PVT1 amplified on ecDNA in PC3 cells was retrieved from UCSC Genome Browser. Guide sequences were designed by CRISPRdirect web tool, and amplification of these sequences on the ecDNA was confirmed using WGS data. Guide sequences were inserted into pSpCas9(BB)-2A-Puro (PX459) – a kind gift from Dr. Feng Zhang (Addgene plasmid #62988; <http://n2t.net/addgene:62988>; RRID: Addgene_62988). The DNA cassette was obtained by PCR amplifying the pSP2-96-merTetO-EFS_BlaR plasmid with primers containing the 50 nucleotide homology arms upstream and downstream of the predicted cutting site.

| Primer Name | Sequence |
|---------------------------------------|---|
| crispr-MYC-P-4-F | CACCGCTATCAGCTGTGTTGCGAGT |
| crispr-MYC-P-4-R | AAACACTCGCAACACAGCTGATAGC |
| donor-4-for | T*T*TGTTCTTTCACCTATCTAATTTGG GGATAGTTTGTACTGGAGATCAGCCA AAAGTGCCACCTGACGTCTAAG |
| donor-4-rev | C*A*GTAAGAGTGGAGACACTATAGT GTGTAGACCACCCTATCAGCTGTGTT CTTAAGCTAGCAGCGCTCTCG |
| genotyping In-Forward | CACGAGGCCCTTTCGTCTTC |
| genotyping 4-rev | CGAGACAGTAAGAGTGGAGACAC |
| 1 st primer for tetO-pBEST | CACAGGAAACAGCTATGACCatgcat DDDDDDDDDDTCCCTATCAGTGAT AGAGADDDDDDDDDTCCCTATCA GTGATAGA |
| 2 nd primer for tetO-pBEST | GADDDDDDDDDTCCCTATCAGTG ATAGAGADDDDDDDDDctgcagTAG GATGAAGctgcagGTTGTAAAACGACG GCCAGT |

Transfection of CRISPR/Cas9 plasmid and donor cassette was achieved with XtremeGENE HP according to manufacturer's instructions. Blasticidin was added on day 3 for 3 days (timing determined by blasticidin killing of negative control cells). Surviving clones were genotyped using primers flanking the donor cassette and sanger sequencing. Visualization of the donor cassette in cells was achieved by infection of these cells with F9-TetR-EGFP-IRES-PuroR containing lentivirus and selected by puromycin.

Live cell imaging of PC3-TetO cell line

Optimization of imaging conditions was performed using the Leica SP8 with White Light Laser and Lightning Deconvolution at the UCSD School of Medicine Microscopy Core. Imaging included in this dissertation was performed by Dr. Liangqi Xi at the Janelia Research Campus.

PC3-TetO cell line was transfected with PiggyBac vector expressing H2B-SNAPf and the super PiggyBac transposase (2:1) as previously described⁵⁷. Stable transfectants were selected using 500 µg/ml G418 and sorted by fluorescence-activated cell sorting (FACS). Cells were adhered to 10 µg/ml human fibronectin coated 8-well chamber cover glass (Lab-Tek). Cells were stained with 25 nM SNAP tag ligand JF₆₆₉⁵⁸ at 37°C for 30 minutes followed by 3 washes with normal medium for 30 minutes total.

Cells were then transferred to imaging buffer with 20% serum in 1x Opti-Klear at 37°C. Cells were imaged using a Zeiss LSM880 microscope. The sample was illuminated with 1.5% 488nm laser and 0.75% 633nm laser with the EC Plan-Neofluar 40x/1.30 oil objective, beam splitter MBS 488/561/633 and filter BP 495-550 + LP 570. Z-stacks were acquired with 0.3 µm step size in 4-minute intervals for a total of 16 hours.

E. Acknowledgements

I acknowledge the following funding grants that made this work possible: The National Brain Tumour Society, NIH R01-CA238349, NIH R35-CA209919, HHMI, MGU045, NINDS NS047101, U24CA264379, R01-GM114362.

Chapter II contains multiple figures from the following manuscript, which has been submitted for publication. The dissertation author was the primary investigator and author of this paper. Joshua T. Lange[#], John C. Rose[#], Celine Y. Chen[#], Yuriy Pichugin[#], Liangqi Xie, Jun Tang, King L. Hung, Kathryn E. Yost, Quanming Shi, Marcella L. Erb, Utkrisht Rajkumar, Sihan Wu, Sabine Taschner-Mandl, Marie Bernkopf, Charles Swanton, Zhe Liu, Weini Huang*, Howard Y. Chang*, Vineet Bafna*, Anton G. Henssen*, Benjamin Werner*, Paul S. Mischel*. “The evolutionary dynamics of extrachromosomal DNA (ecDNA) in human cancers”.

CHAPTER III: IDENTIFYING GENETIC TARGETS TO DISRUPT ECDNA
SEGREGATION AND PROLIFERATION

A. Introduction

Extrachromosomal DNA (ecDNA) are a primary mechanism for cancer cells to amplify focal regions of their genome containing oncogenes and important regulatory elements^{8,13,22}. As described in the previous chapter, ecDNA behave quite differently than oncogene mutations or amplifications that reside on chromosomes, primarily due to their circular topology and lack of centromeric DNA⁸. Critically, recent research has found that patients with ecDNA amplification face poorer survival odds than those with other forms of genome rearrangement and amplification⁹. However, the specific mechanisms behind this differential survival are unknown.

With approximately 20% of cancers fostering ecDNA and the concomitant worse prognosis, it is essential that we rapidly identify biological mechanisms that ecDNA rely on preferentially in order to design therapeutic strategies specifically targeted to disrupt cancer cells with ecDNA. Recent research has found novelties in ecDNA behavior in a wide range of areas, from local gene expression to intermolecular enhancer connections^{13,24}. However, ecDNA behavior at mitosis is consistently suggested to be significantly different from that of chromosomes, and evidence for this was first shown qualitatively more than 20 years ago^{19,41}. The lack of centromeric DNA on ecDNA has led to frequent speculation and observation that ecDNA behavior throughout mitosis is abnormal. However, we do not have a strong mechanistic understanding of how ecDNA are segregated to daughter cells without centromeres, and thus have not identified specific targets that could be disrupted to specifically disrupt ecDNA containing cells.

Initial observations of ecDNA in mitosis using both fixed and live-cell imaging demonstrated that ecDNA frequently clustered and appeared to ‘tether’ to mitotic chromosomes to facilitate segregation⁴¹. However, a sufficient mechanistic description of this behavior has yet to be proposed or tested.

The mitotic stage of the cell cycle has long been a primary aim for both general and targeted therapeutics in the oncology space⁵⁹⁻⁶¹. Drugs targeting either specific mitotic kinases, such as Polo Like Kinase 1 (PLK1), or functions essential to mitosis, such as Taxol disruption of mitotic spindle formation, have shown minimal utility in the clinic, primarily due to a narrow or absent therapeutic window in which the drugs will disrupt tumor cell proliferation without causing significant on-target side-effects from disruption of rapidly proliferating healthy cells, such as those in the gut and bone-marrow⁶²⁻⁶⁴. One key failure of these drugs is in their inability to specifically disrupt tumor cell mitoses without disrupting health mitoses. Given ecDNA are predicted to behave quite differently from mitotic chromosomes, and given ecDNA are essentially absent from healthy tissue, identifying proteins or functions that are necessary for ecDNA segregation but dispensable for normal mitosis is an attractive goal for improving outcomes for patients with ecDNA positive tumors.

While very little research has been done on ecDNA in general, and regarding ecDNA mechanisms in mitosis more specifically, some research into the function of various mitotic proteins has focused on how cells handle acentric fragments of mitotic chromosomes during mitosis. These experiments seek to understand how cells handle a situation that is predicted to arise with significant frequency, as acentric fragments can be

generated by a number of errant processes such as chromothripsis. While not circular, acentric fragments are likely to be dealt with by the cell in similar terms to ecDNA, given their similar size and lack of centromere.

Most research in this area has focused in on the activity of a particular family of mitotic motor proteins referred to as chromokinesins. Chromokinesins are a specialized family of kinesins which retain the motor domains of canonical kinesins and contain DNA binding domains (or DNA-factor binding domains) on the n-terminus⁶⁵. Their primary functions in mitosis have been proposed to be the manipulation and spatial organization of mitotic chromosome arms, mostly functioning away from the heavily regulated and studied centromere-kinetochore region⁶⁶⁻⁷¹.

Studies in which acentric fragments are observed through mitosis have shown a role for the two primary chromokinesins, KIF4A and KIF22 (also referred to as KID and Kinesin-10), in promoting their eventual segregation into a daughter cell^{68,69,72-77}. Data in this area is shallow and sometimes contradictory. Evidence has been provided that attributes promotion of both DNA congression toward the metaphase plate and poleward DNA movement to both KIF4A and KIF22 in different studies. Clearly our understanding of the function of these proteins is lacking. One aspect that is shared across the literature is that these kinesins play a role in the movement and manipulation of acentric DNA during mitosis.

These proteins have also been implicated in a wide range of other cellular functions, including organization of the mitotic spindle and interphase organelle transport⁷⁸. Most research into chromokinesins to date has focused on their role in mitosis. As mitotic genes,

these proteins have also, unsurprisingly, been implicated in gene expression studies of tumor genomes which has suggested they may play a role in cancer progression^{72,79}. Especially given chromokinesins' potential link to acentric ecDNA segregation, significantly more research is warranted in this area.

B. Results

Identification of upregulated genes in ecDNA-containing tumors

In order to better understand the specific mechanisms cells use to continue to proliferate while maintaining high levels of ecDNA amplification, I wanted to study gene expression patterns in patient tumor samples. I chose to analyze gene expression in tumors in order to avoid the countless confounding and artificial factors that change when cells are explanted from a patient's tumor into cell culture or even xenograft conditions. To accomplish this, I focused on The Cancer Genome Atlas (TCGA), a commonly used public database of human cancers whose genomes and gene expression have been sequenced. I also relied on a previous study which used a novel algorithmic approach called AmpliconArchitect to determine whether ecDNA had been generated within a given tumor⁹. This study stratified hundreds of tumors from TCGA based on the presence or absence of various types of genomic rearrangements, such as ecDNA and BFBs.

Given this resource of tumors called for ecDNA or not-ecDNA status, I then downloaded the RNA-seq profiles for the tumors for which this data was available. This data was downloaded from the National Cancer Institute (NCI) Genomic Data Commons (GDC) repository (Figure 3.1A). I was able to successfully obtain the gene expression

profiles for approximately 300 ecDNA+ tumors and 1,300 ecDNA- tumors which together spanned 21 tumor sub-types (Figure 3.1B – panel showing representation of types by subgroup). I then generated normalized read counts for each gene for each patient using the Bioconductor package DESeq2 in R⁸⁰. I then ran Gene Set Enrichment Analysis (GSEA)⁸¹ to identify the gene sets that were most differentially expressed in the ecDNA+ and ecDNA- tumors. Finally, I used gene ontology (GO)^{82,83} analysis of the most significantly upregulated ecDNA+ genes to identify the primary cellular functions that were upregulated in ecDNA+ cancers.

After doing the GSEA analysis of ecDNA+ versus ecDNA- tumors, the resultant upregulated and downregulated pathways were striking and interesting. The most significantly overexpressed gene sets in ecDNA tumors were those focused around the G2 to M transition, proliferation and the mitotic spindle (Figure 3.2A). Other upregulated pathways that were of particular interest for their potential direct connection to ecDNA biology were DNA repair and epithelial to mesenchymal transition (Figure 3.2B). I also identified the gene sets which were most significantly enriched in the ecDNA- cancers. Here, there was a surprisingly consistent trend of various metabolic genes, such as those involved in adipogenesis, fatty acid metabolism and cholesterol (Figure 3.2C,D).

To further understand the specific cellular processes that saw overexpression in the ecDNA tumors, I performed a GO analysis of the top 1000 overexpressed genes from the GSEA analysis for ecDNA tumors. This analysis demonstrated the significant overrepresentation of genes involved in regulating mitosis and DNA metabolic processes (such as repair and replication) (Figure 3.3A).

Taking the GSEA and GO analyses together, these data demonstrate a significant upregulation of mitotic genes in ecDNA tumors, as compared to ecDNA- tumors. While these analyses were not normalized for tumor sub-type, the relatively similar distribution of samples across tumor types suggests this result is unlikely to be due to confounding biological differences due to ecDNA prevalence or underrepresentation in a particular type of tumor (Figure 3.1B). This apparent reliance on higher expression of mitotic genes is interesting in the context of the abnormal mitotic dynamics of ecDNA discussed in Chapter II. Given these dynamics, a plausible explanation for these results is that ecDNA present cancer cells with a significant challenge to overcome in completing mitosis without significant micronucleation or other defect which would be detrimental to proliferation.

ecDNA promote abnormal mitoses

In order to understand this result further, I next wanted to investigate the propensity of ecDNA containing cells to encounter problems in completing mitosis as compared to cells without ecDNA. To answer this question, I relied on two isogenic cell line systems that essentially only differ in the presence or absence of ecDNA. These two systems are the colorectal cell lines COLO320HSR and COLO320DM which both have high copy number amplification of MYC, with the amplification residing primarily on chromosomes in COLO320HSR and residing primarily on ecDNA in COLO320DM, and the GBM cell lines GBM39-HSR and GBM39-EC, which were described previously (Figure 2.4). For these cell lines, I performed FISH on fixed cell line samples and quantified the frequency of micronuclei within each population.

Micronuclei are secondary nuclear structures which are formed when a component of the mitotic DNA does not segregate along with the rest of the chromosomes⁸⁴. These structures have long been used to identify mitotic abnormalities and DNA damage. Micronuclei are not simply a result of erroneous segregation, they play additional detrimental roles in proliferation as they are frequent sites of DNA damage, including shattering of chromosomes called chromothripsis^{29,85,86}. In general, micronuclei represent evidence of errant mitosis and a worse proliferative outlook for a given cell⁸⁷.

I quantified the frequency of micronuclei in these isogenic cell lines and found conclusive evidence that ecDNA containing cells are more likely to generate micronuclei after mitosis (Figure 3.4A). More importantly, I also quantified the fraction of micronuclei that contained ecDNA, to better approximate the fraction of micronuclei that may be the direct result of problematic segregation of ecDNA. I found that the vast majority of micronuclei in ecDNA+ cell lines contained ecDNA (Figure 3.4B). As a control, I quantified the fraction of micronuclei in the HSR cell lines that contained the amplicons housed on chromosomes. As expected, I found these amplicons in a minority of micronuclei (Figure 3.4B). These data provide strong support for the hypothesis that ecDNA represents a mitotic challenge for cells, which may then have to upregulate mitotic genes to promote proper segregation and maintain proliferation. This is further supported by the fact that in each isogenic system, the cell line with ecDNA grows at a noticeably slower rate than the HSR line. Together, these data support the theory that ecDNA represent an advantage to cancers by providing genetic diversity and adaptability (Chapter

II); however, they are not without their costs, which may be focused on the difficulty in avoiding abnormal mitoses with ecDNA.

ecDNA cell lines are not more sensitive to mitotic dysregulators

Given these data, I hypothesized that ecDNA⁺ cancers may have a mitotic vulnerability that could be therapeutically targeted. If ecDNA presents a mitotic difficulty that prompts cancers to upregulate mitotic fidelity genes to overcome, it seemed likely that these cells would be more sensitive to mitotic disruption than cells without ecDNA. To test this, I wanted to identify the IC₅₀ (the point at which 50% of cell proliferation is inhibited) for mitotic drugs in these isogenic cell lines. I first tested nocodazole, a small molecule that antagonizes microtubule polymerization, a necessary step in mitosis. Interestingly, I found that while there was a slight difference in the IC₅₀ for GBM39-EC compared to GBM39-HSR, COLO320DM was significantly less sensitive to nocodazole compared to COLO320HSR (Figure 3.5A). This result was surprising and contrary to my hypothesis. I also tested the effect of Monastrol, a small molecule inhibitor of Eg5 (Kinesin-5) which prevents the formation of the bipolar spindle in mitosis. Similar to nocodazole treatment, I found a slight sensitivity in GBM39-EC compared to GBM39-HSR and a significantly more resistant phenotype in the COLO320DM compared to the COLO320HSR cells (Figure 3.5B). I was again surprised by these data.

One potential explanation for these results is that ecDNA containing cell lines face a very different set of challenges *in vivo* as compared with these *in vitro* conditions. Given growth promoting conditions in cell culture, it is possible that ecDNA⁺ cell lines do not

experience a significant growth defect due to increased missegregation and micronuclei rates that they may experience *in vivo*. It is further possible that the increased ability of ecDNA⁺ cell lines to adapt and gain resistance to therapy (Chapter II) may be counteracting a real sensitivity to mitotic disruption compared to ecDNA⁻ cells. These experiments should be repeated *in vivo* to understand whether these relationships hold in more challenging growth environments.

To further understand the influence of ecDNA on cell cycle dynamics, I next sought to compare the distribution of cells by cell cycle phase between our isogenic ecDNA cell lines. To test this, I performed cell cycle profiling experiments by fixing asynchronously growing cells and adding propidium iodide (PI), which fluorescently labeled the cells' DNA. I then analyzed the relative amounts of DNA within each cell by flow cytometry and plotted the resultant profiles. I manually gated for the different cell cycle phases. I found that in both of the isogenic ecDNA systems, the ecDNA containing cells lines showed a smaller fraction of cells in S and G2/M phases and a higher concentration of cells in G1 (Figure 3.6A,B).

Taken together, these data suggest that ecDNA do not promote a prolonged mitosis. This is not altogether surprising. Mitotic timing is primarily determined by the activation and degradation of key mitotic checkpoint proteins. These proteins are primarily sensing the accurate and proper attachment of the mitotic spindle at the kinetochore. Given ecDNA are unlikely to disrupt these attachments or be sensed as unattached chromosomes, ecDNA are likely to be more or less ignored by the primary machinery that determines mitotic duration and timing. However, the apparent accumulation of G1 cells in ecDNA cell lines

could be the result of aberrant mitoses causing a G1 delay in order to address increased levels of micronuclei and DNA damage in these cells.

Role of chromokinesins in promoting ecDNA segregation in mitosis

The data presented thus far in Chapter III suggest that ecDNA do behave differently in mitosis and may require increased expression of mitotic proteins to facilitate their proper segregation. I was thus interested in identifying mitotic proteins that may be preferentially important for ecDNA segregation compared with chromosomal segregation. I identified potential proteins to research further based on their activity in mitosis away from the centromere and kinetochore. I identified a class of mitotic protein referred to as ‘chromokinesins’ to investigate further. This family of kinesins binds DNA as its cargo and uses its kinesin motor domain to manipulate and move the DNA, especially in mitosis. Importantly, this activity occurs along the length of chromosome arms, not specific to centromeric DNA. KIF4A and KIF22 are thought to be the primary members of this family of kinesins active in humans.

I first wanted to identify the expression levels of these two proteins to determine whether there was evidence that ecDNA containing tumors may preferentially rely on these proteins to facilitate ecDNA segregation. I first compared the level of KIF4A and KIF22 mRNA expression in tumor versus normal tissue. Using the same general approach and source of sequenced samples as previously described (Figure 3.1A), I found that both chromokinesins were significantly overexpressed in tumor samples compared to normal tissue (Figure 3.7A). I then compared their expression levels in ecDNA⁺ and ecDNA⁻

tumors, again using the classifications made in a previous study. Combining all tumor subtypes to obtain sufficient sample sizes, I found that both KIF4A and KIF22 were significantly overexpressed in ecDNA⁺ tumors compared with all other tumors (Figure 3.7B). Comparisons of this type within tumor subtypes were difficult, limited by insufficient resolution; however, many tumor types followed this overall trend, with GBM and lung adenocarcinoma showing higher levels of KIF4A and KIF22 expression in ecDNA⁺ subsets of these tumor types (Figure 3.7C-D). To further corroborate this trend, KIF4A and KIF22 were ranked at number 25 and number 773 respectively in terms of their overexpression in ecDNA⁺ tumors out of all genes. Taken together, these expression data strongly suggest that ecDNA⁺ tumors are more reliant on expression of chromokinesins and promote the hypothesis that they may be necessary to facilitate proper segregation of ecDNA.

Next, I wanted to test the role of chromokinesins in promoting ecDNA segregation experimental in our cell line models. To my knowledge, no small molecules have been identified that specifically inhibit these proteins. Therefore, I used a genetic approach to disrupt them and test the resultant effects on ecDNA segregation and proliferation of ecDNA cell lines. While significant evidence exists that chromokinesins localize along mitotic chromosome arms, I first wanted to establish whether they localize to ecDNA during mitosis. To test this I generated metaphase spreads of COLO320DM cells. Using a cytospin to spread non-fixed samples onto a slide, I was able to perform immunofluorescence on the metaphase spreads, with primary antibodies for KIF4A and KIF22. This experiment clearly demonstrated the presence of both proteins on ecDNA

during mitosis, in addition to localization on chromosome arms (Figure 3.8A). Further, these images corroborated prior findings that suggested KIF4A is primarily localized on the chromosomal cortex, with KIF4A staining appearing to be localized centrally along each chromatid arm (Figure 3.8A)^{69,88}.

Having verified the presence of chromokinesins on ecDNA, I next tested the effects of knocking down the levels of these proteins in the isogenic ecDNA cell lines. I was interested in determining whether knockdown of these proteins would increase the frequency of missegregation of ecDNA, more so than the frequency of missegregation of chromosomes. In COLO320DM cells, KIF22 knockdown by siRNA significantly increased the frequency of total and ecDNA-containing micronuclei, while knockdown of KIF4A and KIF4A/KIF22 combined showed minimal impact on segregation (Figure 3.9A,B). Using shRNA knockdown in the GBM39-EC cell line, I similarly found knockdown of KIF22 to significantly increase the frequency of total and ecDNA-containing micronuclei (Figure 3.9C,D). To expand these findings further, I tested siRNA knockdown of the chromokinesins in other ecDNA containing cell lines SNU16 and PC3. These experiments showed a broader effect, with knockdown of KIF4A and KIF22 both increasing micronuclei frequency (Figure 3.9E-H). Finally, to capture a more nuanced understanding of how chromokinesins knockdown affects ecDNA segregation, I fixed COLO320DM knockdown samples and performed FISH staining for the MYC ecDNA. I imaged anaphase and telophase cells and scored the frequency of ‘catastrophic’ ecDNA missegregation, which I defined as an anaphase or telophase cell with more than 3 ecDNA foci not connected to the chromosomal masses. I found knockdown of both KIF4A and

KIF22 showed significantly increased rates of ‘catastrophic’ ecDNA missegregation (Figure 3.10A,B). Together, these knockdown data strongly suggest that chromokinesins KIF4A and KIF22 play a significant role in segregating ecDNA to daughter cells. There is significant variability in which chromokinesins knockdown has more of an effect across cell lines, but the trend is clear that chromokinesin knockdown increases rates of ecDNA missegregation. Next, I wanted to understand whether this impact on ecDNA segregation would result in a proliferation defect for ecDNA+ cell lines.

I repeated the knockdown experiments using siRNA for COLO320HSR and COLO320DM cell lines. I quantified cell number at days 1, 3 and 6. The data clearly showed that COLO320DM cells were more sensitive to knockdown of KIF4A and KIF22 than COLO320HSR cells (Figure 3.11A). I repeated this experiment doubling the dose of siRNA to 40nM and found that the trend held firm with COLO320DM showing more sensitivity, even at a level of siRNA knockdown that resulted in a measurable growth defect in COLO320HSR (Figure 3.11A). I next performed a similar experiment in the GBM39 isogenic system. I also performed siRNA knockdown in PC3 cells and measured the effect on proliferation by Cell Titer Glo. I found again that knockdown of these chromokinesins resulted in significant defect in proliferation in an ecDNA cell line (Figure 3.11C). Using shRNA to knockdown both KIF4A and KIF22, I again saw increased sensitivity to this treatment by the GBM39-EC cells as compared to the GBM39-HSR cells (Figure 3.12A-C). Together, these data clearly demonstrate a preferential growth defect on knockdown of chromokinesins KIF4A and KIF22 in ecDNA+ cell lines. Considering the increased micronuclei frequency in ecDNA cell lines upon chromokinesin knockdown, these data

suggest a clear mechanism in which chromokinesins are required to promote the normal segregation of ecDNA. When the levels of these proteins are depleted, ecDNA are more likely to missegregate and be incorporated into micronuclei, which have been shown to be detrimental to cell proliferation rates.

C. Discussion

The results I have presented in Chapter III aim to improve our understanding of the specific mechanisms governing the segregation of ecDNA. In this pursuit, I have analyzed mRNA expression data from hundreds of ecDNA⁺ and ecDNA⁻ tumors and have found a significant enrichment of mitotic genes upregulated in ecDNA⁺ tumors. I have also demonstrated that ecDNA does not extend the duration of mitosis in an isogenic ecDNA system. However, ecDNA does appear to present a mitotic challenge for cells to overcome, as we see increased rates of micronuclei formation and an accumulation of cells in G1.

In order to study the specific proteins that may regulate ecDNA segregation, I focused on the chromokinesins KIF4A and KIF22 which in healthy cells manipulate the dynamics and positioning of chromosome arms in mitosis. I found that these proteins play a role in ecDNA segregation, showing depletion of their levels increases rates of missegregation and micronuclei specifically in ecDNA cell lines. I also demonstrated that there is a resultant penalty in proliferation rate when levels of KIF4A and KIF22 are depleted, again preferentially in ecDNA cells lines. Taken together, Chapter III suggests chromokinesins KIF4A and KIF22 may play a significant role in ecDNA dynamics in mitosis and targeting them therapeutically may represent a mechanism to specifically

inhibit growth of ecDNA tumors while avoiding the broad toxicity that has plagued more general mitotic disruptors in the clinic.

Significantly more research is warranted in this area, with the most immediate next steps to expand these experimental paradigms into *in vivo* models of ecDNA tumor growth. Given the initial data presented was founded on tumor sequencing data, the role of KIF4A and KIF22 in ecDNA maintenance and proliferation may be significantly underestimated in cell culture conditions. Additionally, research into identifying small molecules that specifically inhibit one or both of these chromokinesins is important. To date, there have yet to be any therapeutic options to specifically target ecDNA cancers. Most research into ecDNA has focused on the response of ecDNA to drugs targeting the specific amplified oncogene, lapatinib targeting EGFR ecDNA for example in Chapter II. However, identifying targets and drugs that can disrupt ecDNA biology agnostic of the specific oncogene amplified could drastically improve therapeutic outcomes for a significant proportion of cancer patients.

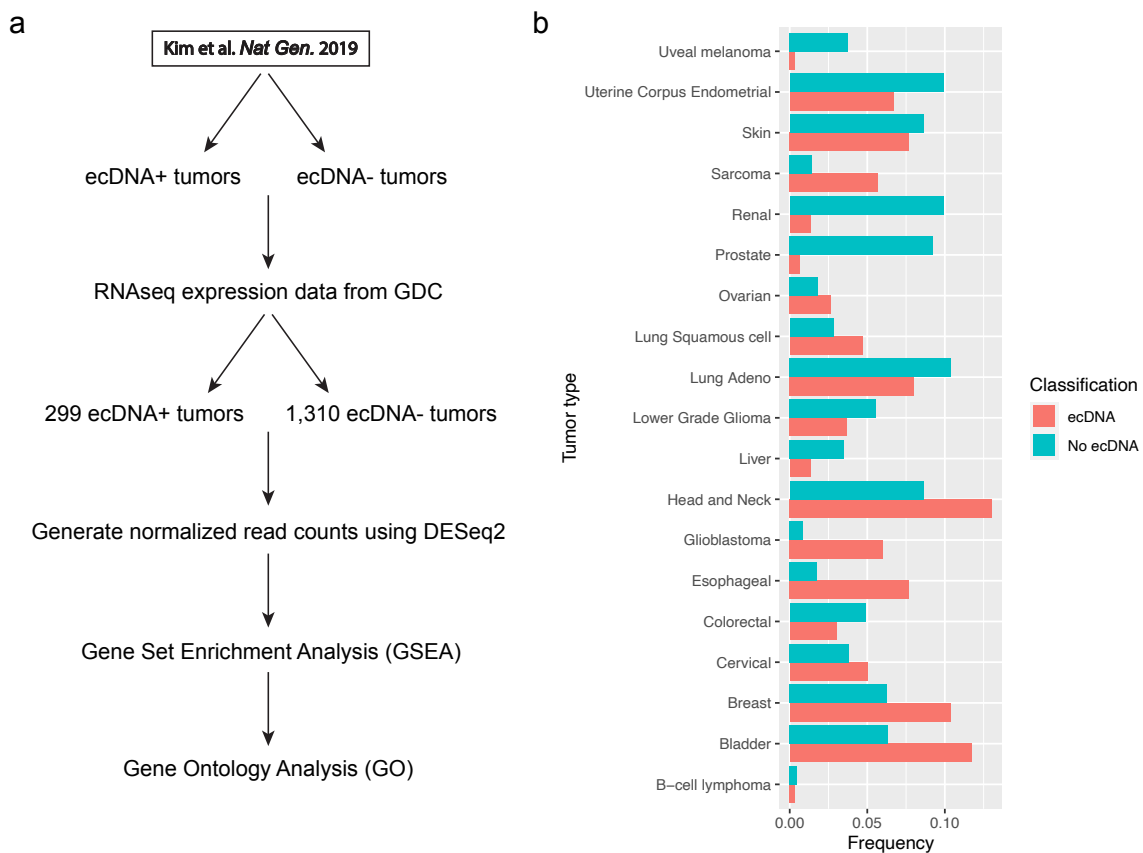


Figure 3.1 | Analysis of expression data from TCGA tumor samples.

a, Schema depicting the workflow to analyze TCGA expression data for ecDNA+ and ecDNA- tumors. **b**, Representation frequency of different tumor types in each sample.

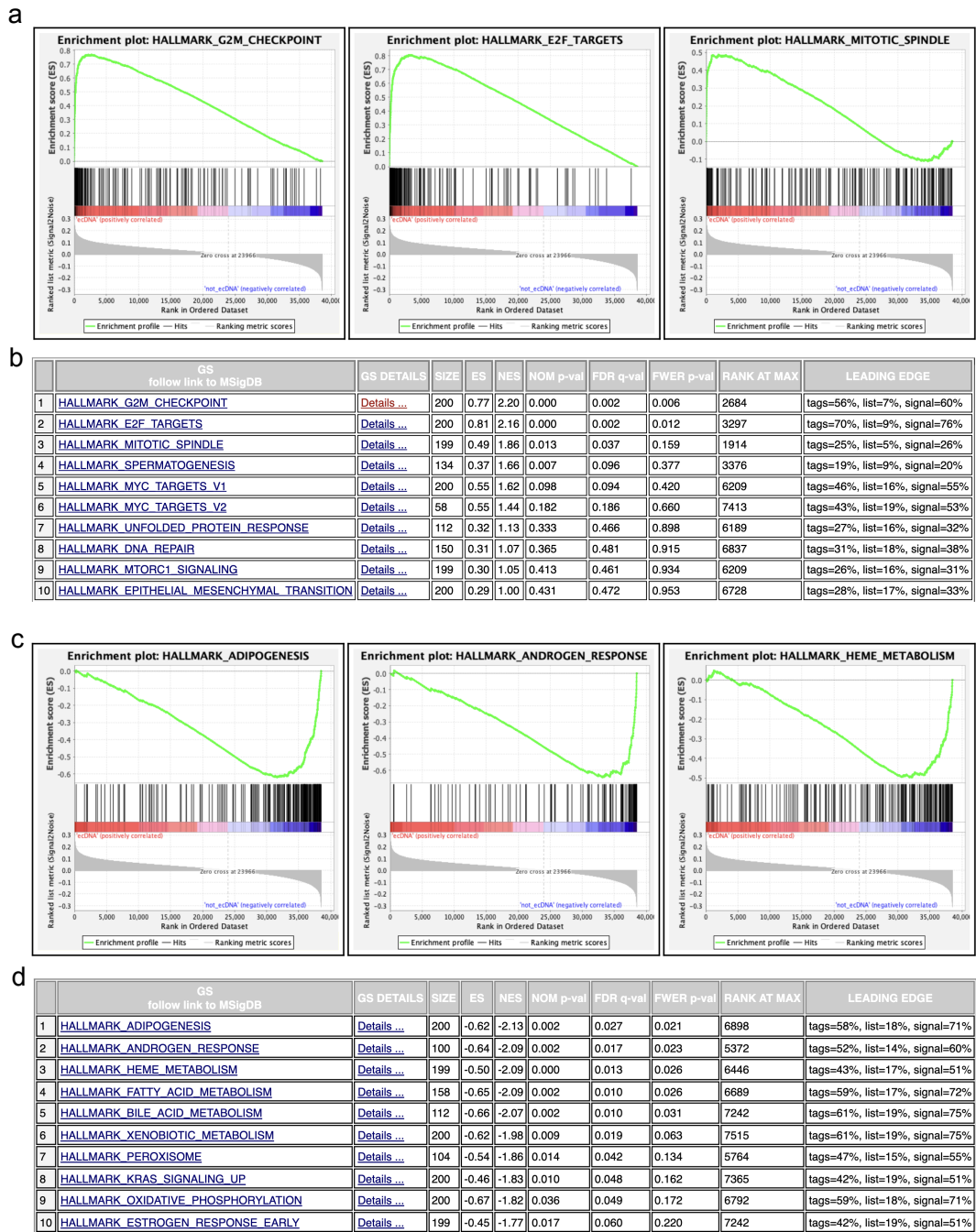


Figure 3.2 | Gene set enrichment analysis of ecDNA+ and ecDNA- tumors.

a, Depiction of enrichment profiles for the top 3 enriched gene sets in ecDNA+ tumors. **b**, Table of the top 10 enriched gene sets in ecDNA+ tumors. **c**, Depiction of enrichment profiles for the top 3 enriched gene sets in ecDNA- tumors. **d**, Table of the top 10 enriched gene sets in ecDNA- tumors.

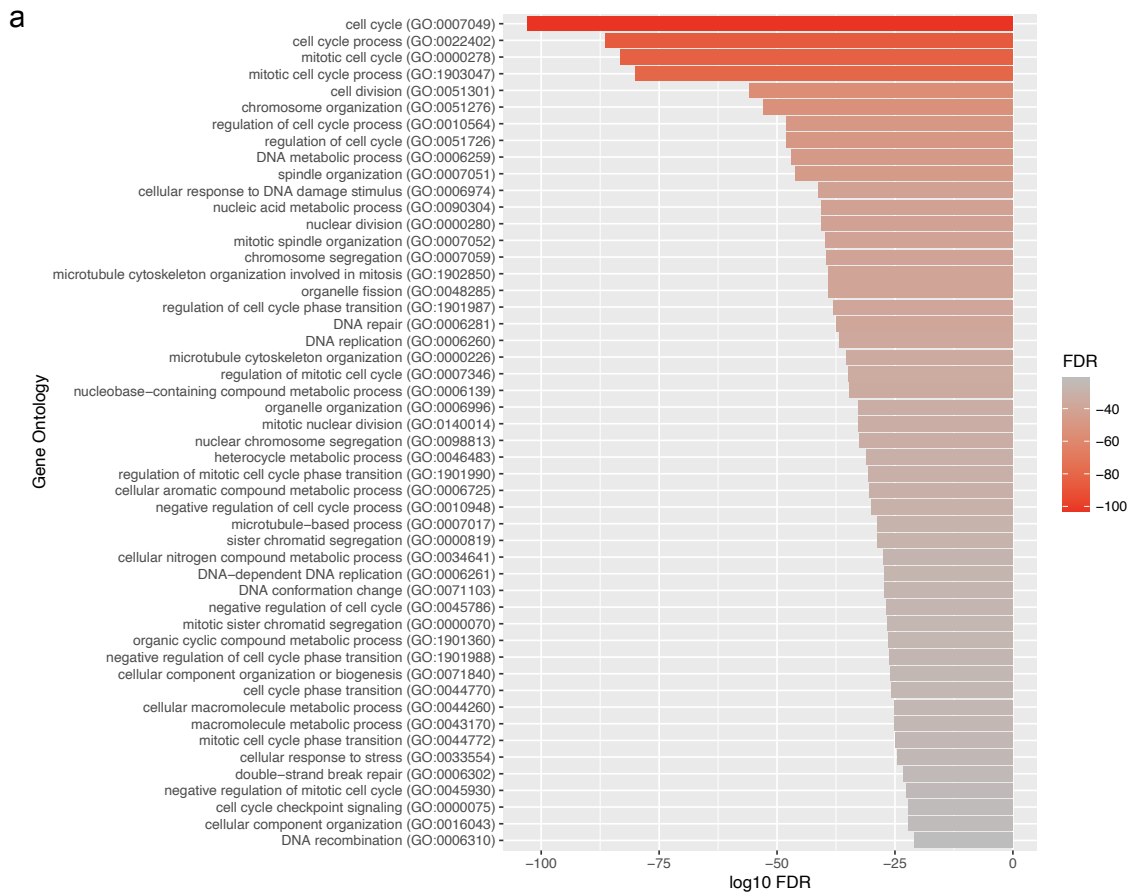


Figure 3.3 | Gene ontology analysis of the top 1,000 enriched genes in ecDNA+ tumors.

a, Ranked figure showing the top 51 GO biological processes enriched in the top 1,000 enriched genes in ecDNA+ tumors. Processes are ranked by their log₁₀ false discovery rate (FDR), most significant at the top.

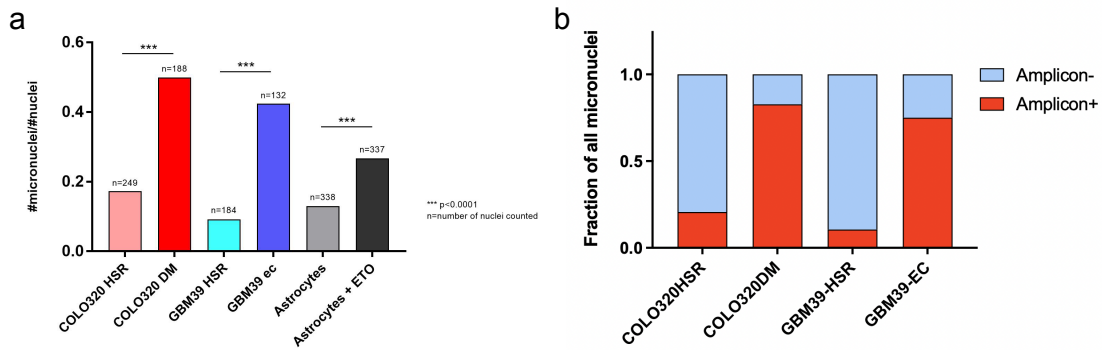


Figure 3.4 | ecDNA are more prone to incorporation into micronuclei.

a, Quantification of micronuclei frequency (total micronuclei / total cells) in isogenic ecDNA \pm cell lines. Astrocytes represent a control cell line with treatment with etoposide (ETO) used as a positive control to induce missegregation and micronuclei. **b**, In isogenic cell lines, quantification of the fraction of total micronuclei that contain the amplified oncogene as assessed by FISH.

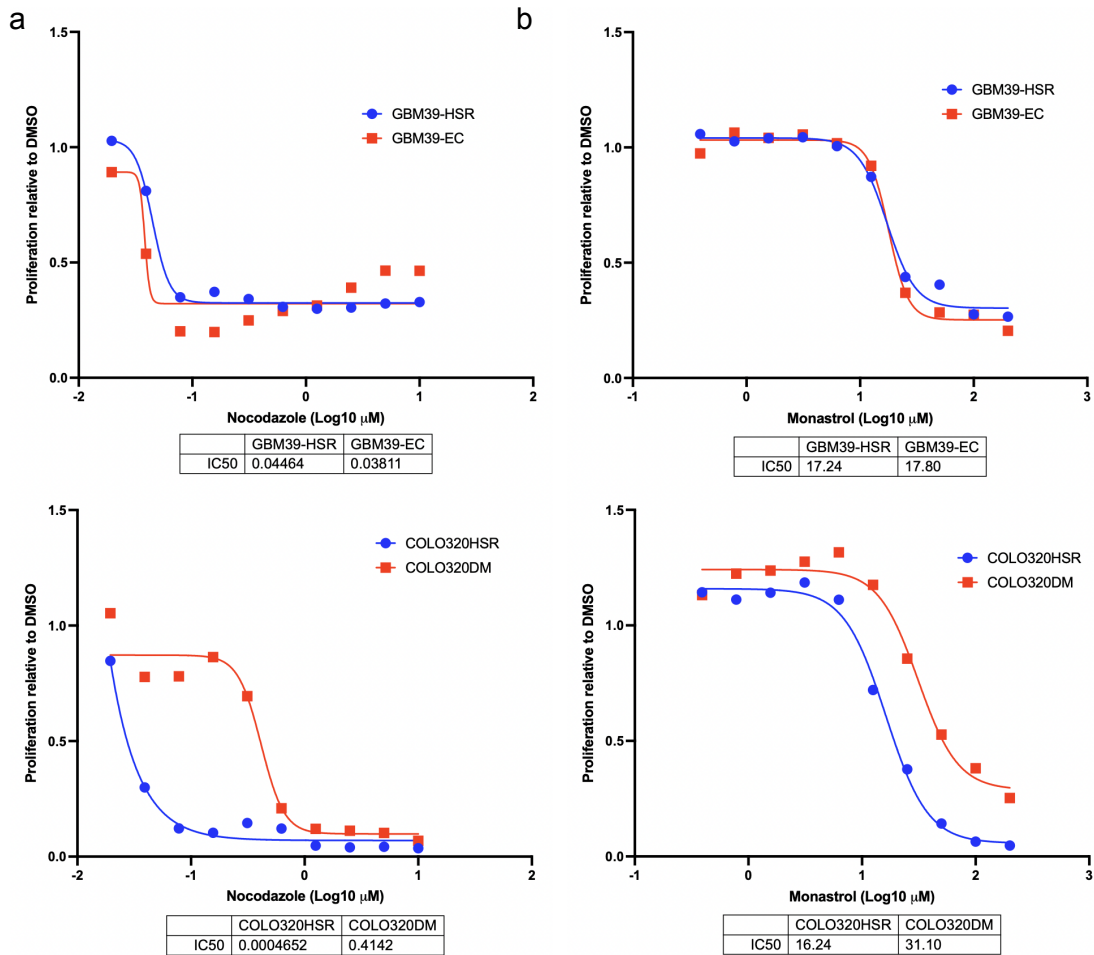


Figure 3.5 | Differential sensitivity of isogenic ecDNA cell lines to mitotic disruption.

a, 10-point dose response curves with indicated IC50 values in μM values for nocodazole treatment. **b**, 10-point dose response curves with indicated IC50 values in μM values for Monastrol treatment. Proliferation rates were measured relative to a DMSO control and readout was performed using Cell Titer Glo 2.0 which approximates ATP levels.

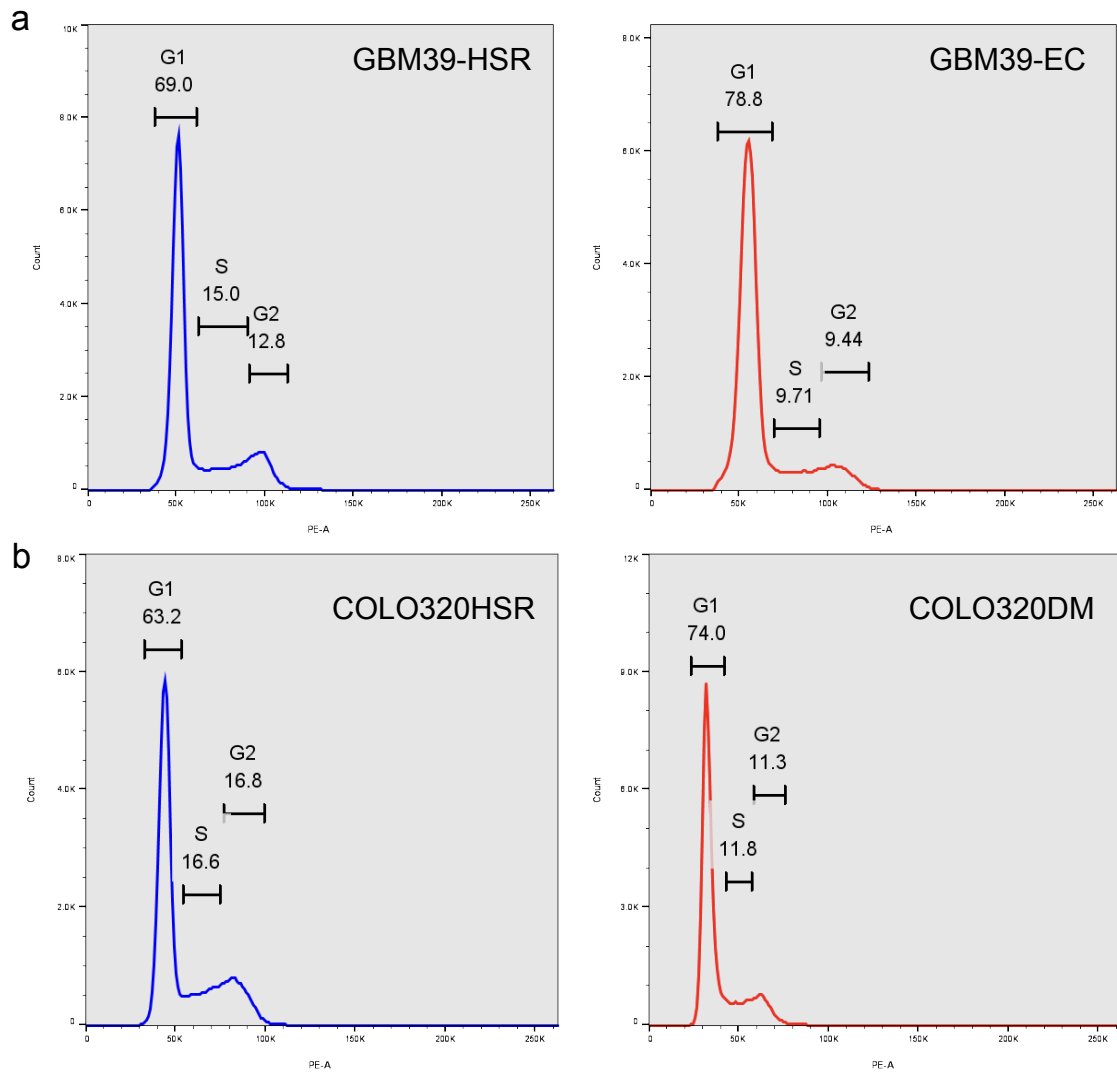


Figure 3.6 | ecDNA cell lines have fewer cells in G2/M phase and a concentration of cells in G1.

a, Cell cycle profiles of GBM39-HSR and GBM39-EC as measured by propidium iodide staining and flow cytometry. Gating was performed manually, and percentages are indicated along with gates. Note the increased G1 representation in GBM39-EC and decreased G2/M frequency. **b**, Cell cycle profiles of COLO320HSR and COLO320DM as measured by propidium iodide staining and flow cytometry. Gating was performed manually, and percentages are indicated along with gates. Y-axes indicate cell counts; x-axes indicate propidium iodide fluorescence.

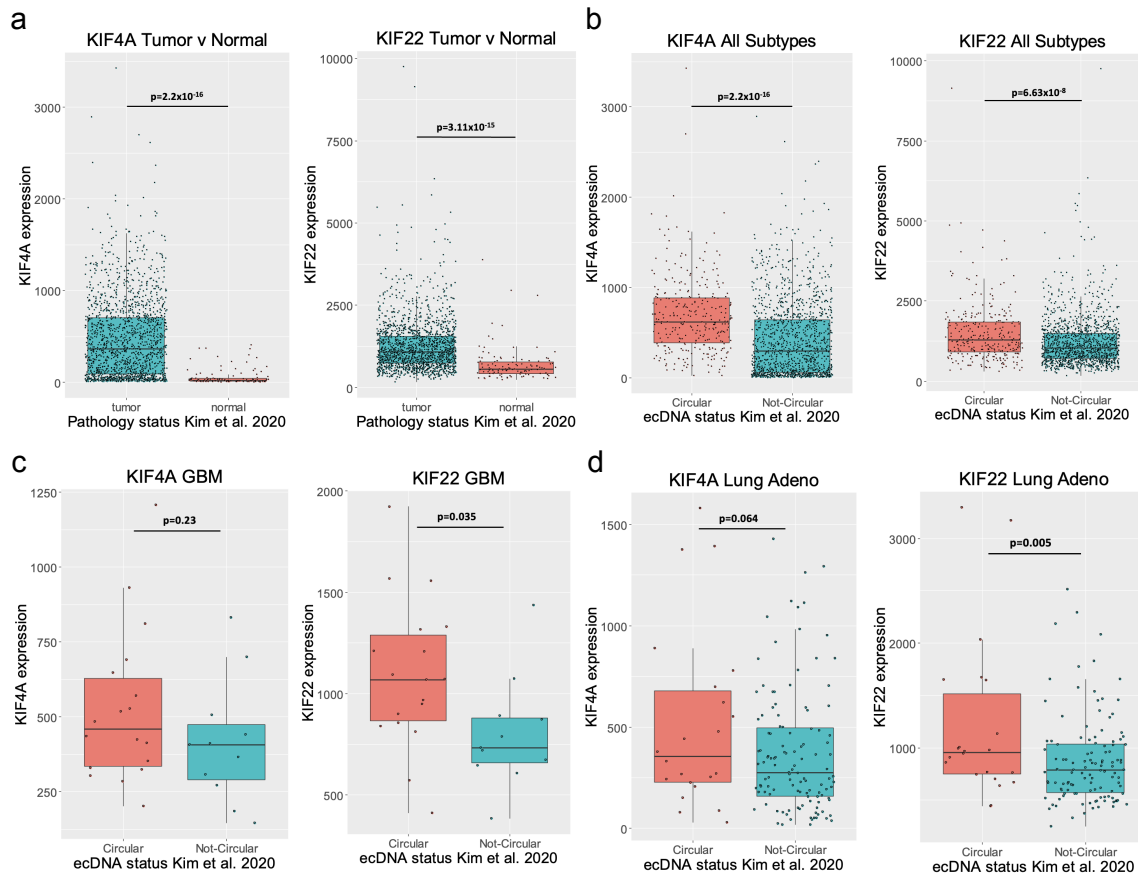


Figure 3.7 | Chromokinesins show increased expression levels in ecDNA+ tumors.

a, Quantification of KIF4A (left) and KIF22 (right) mRNA expression levels in tumor versus normal tissue. **b**, Quantification of KIF4A (left) and KIF22 (right) mRNA expression levels in tumors, classified as either having ecDNA (circular) or not having ecDNA (Not-Circular) based on a prior publication. **c**, Quantification of KIF4A (left) and KIF22 (right) mRNA expression levels in GBM tumors classified as either having ecDNA (circular) or not having ecDNA (Not-Circular). **d**, Quantification of KIF4A (left) and KIF22 (right) mRNA expression levels in Lung Adenocarcinoma tumors classified as either having ecDNA (circular) or not having ecDNA (Not-Circular).

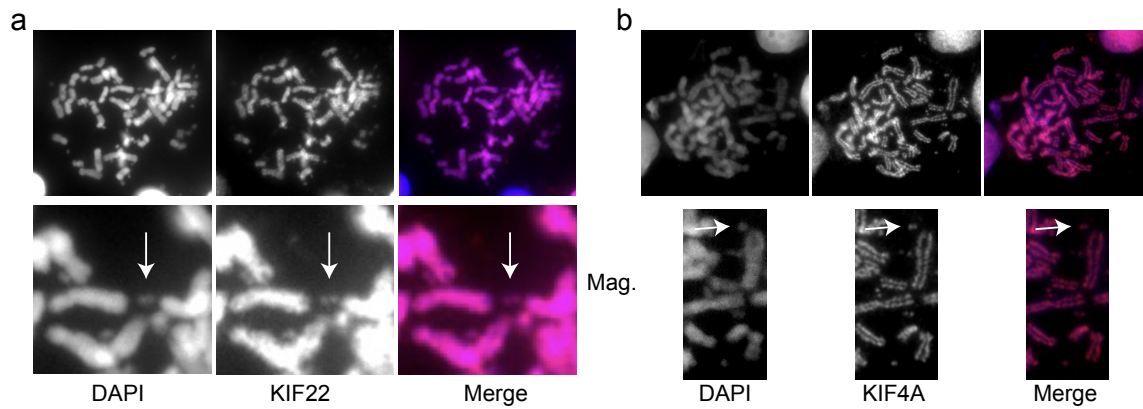
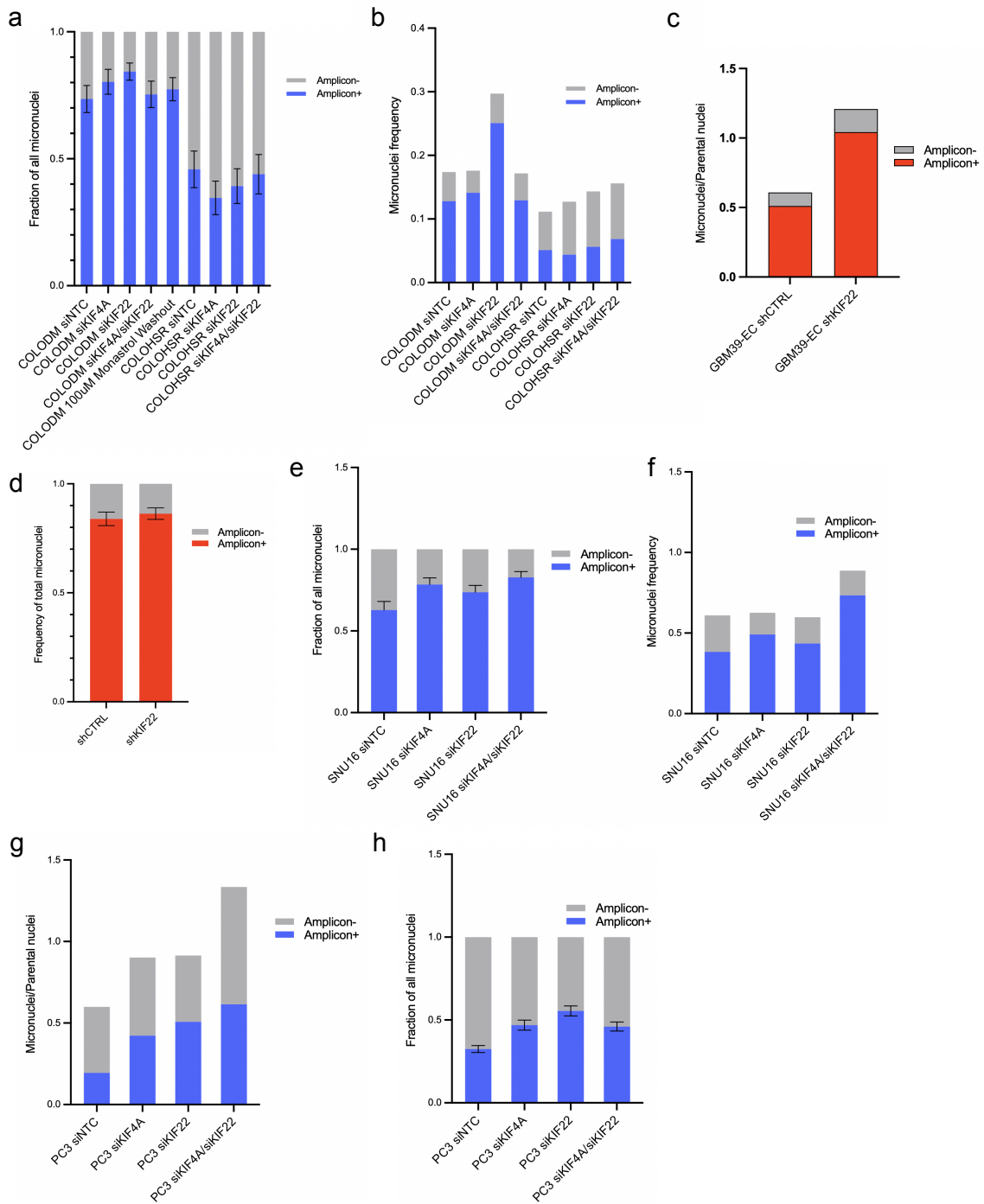


Figure 3.8 | Chromokinesins localize to ecDNA along with chromosome arms in metaphase.

a, Representative image of a COLO320DM metaphase spread with IF for KIF22. Second row is a subset of the first row at higher magnification to show detail of KIF22 staining on ecDNA. **b**, Representative image of a COLO320DM metaphase spread with IF for KIF4A. Second row is a subset of the first row at higher magnification to show detail of KIF4A staining on ecDNA.

Figure 3.9 | Genetic knockdown of KIF4A and KIF22 increase rates of ecDNA+ micronuclei across multiple cell line models.

a, Quantification of the fraction of all micronuclei that contain the amplified MYC gene or not under different knockdown conditions in COLO320DM and COLO320HSR cells. **b**, Quantification of the total frequency of micronuclei (micronuclei / parental nuclei), segregated by containing MYC or not, in different knockdown conditions in COLO320DM and COLO320HSR cells. **c**, Quantification of total micronuclei frequency in control and KIF22 shRNA condition in GBM39-EC. **d**, Quantification of the fraction of all micronuclei that contain the amplified EGFR gene in GBM39-EC under control or shKIF22 conditions. **e-f**, Quantification of micronuclei frequencies in SNU16 cells, similar to those presented in **a-b**. **g-h**, Similar to **e-f** in PC3 cells.



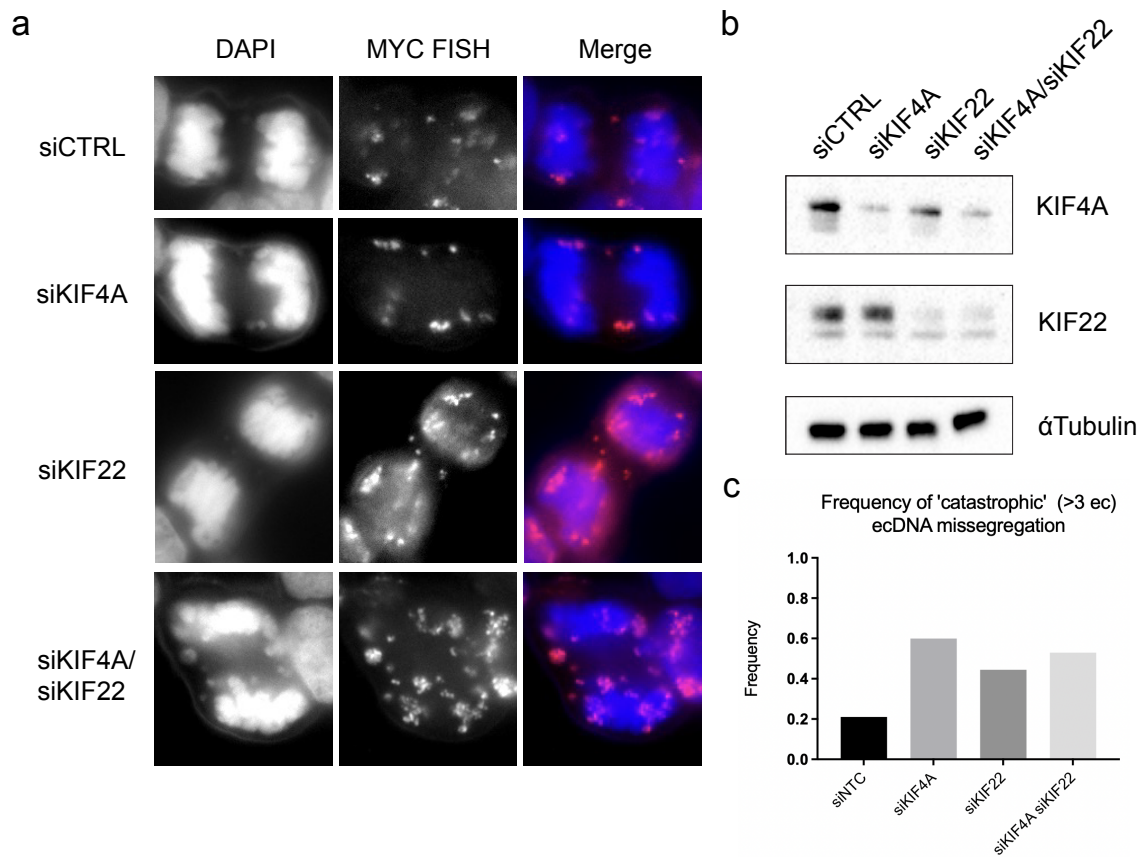
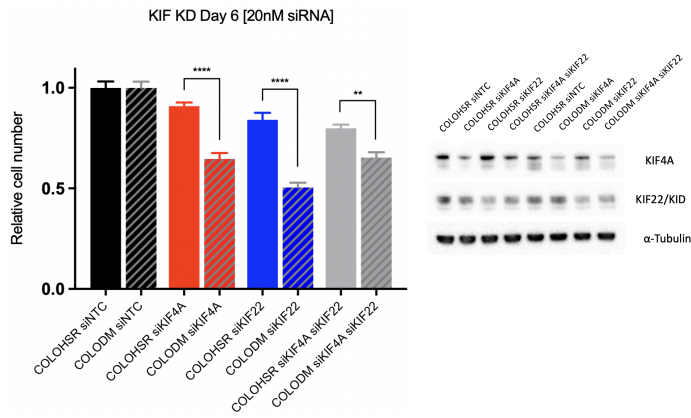
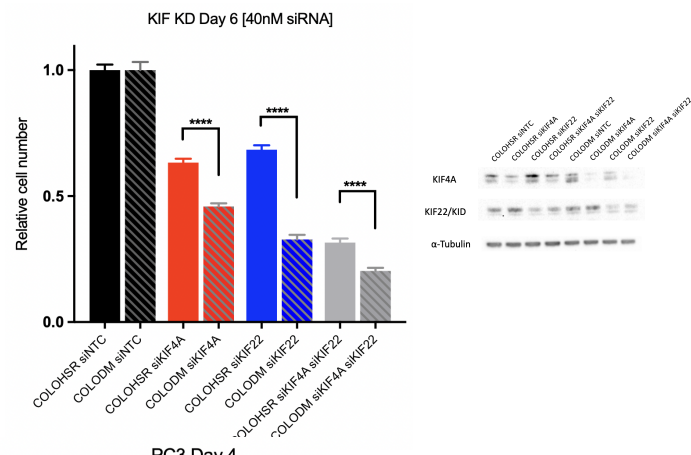
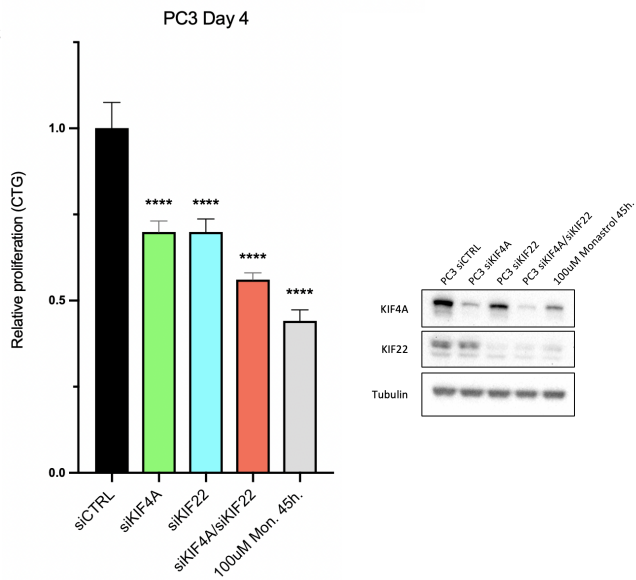


Figure 3.10 | Chromokinesins aid in proper segregation of ecDNA.

a, Representative mitoses from COLO320DM cells under indicated siRNA conditions. ecDNA are visualized by MYC FISH (shown in red). **b**, Western blot showing knockdown of KIF4A and KIF22 protein levels under siRNA knockdown. **c**, Quantification of 'catastrophic' ecDNA missegregation—defined as more than 3 ecDNA not attached or overlapping with chromosomal DNA.

Figure 3.11 | Chromokinesin knockdown reduces proliferation rates in ecDNA+ cell lines.

a, Cell numbers of COLO320DM and COLO320HSR cell lines relative to scrambled siCTRL conditions at day 6 after transfection of siRNA. Note significantly increased sensitivity to knockdown in COLO320DM cells compared to COLO320HSR cells. Western blot showing knockdown of protein levels on day 6. Likely that protein levels had begun to recover by this point. **b**, Repeat of the experiment described in **a** with increased siRNA concentration used to 40nM. **c**, Proliferation rates of PC3 cells measured by Cell Titer Glo 2.0 on day 4 after siRNA transfection, relative to scrambled siCTRL condition. Knockdown of protein levels shown in western blot (right).

a**b****c**

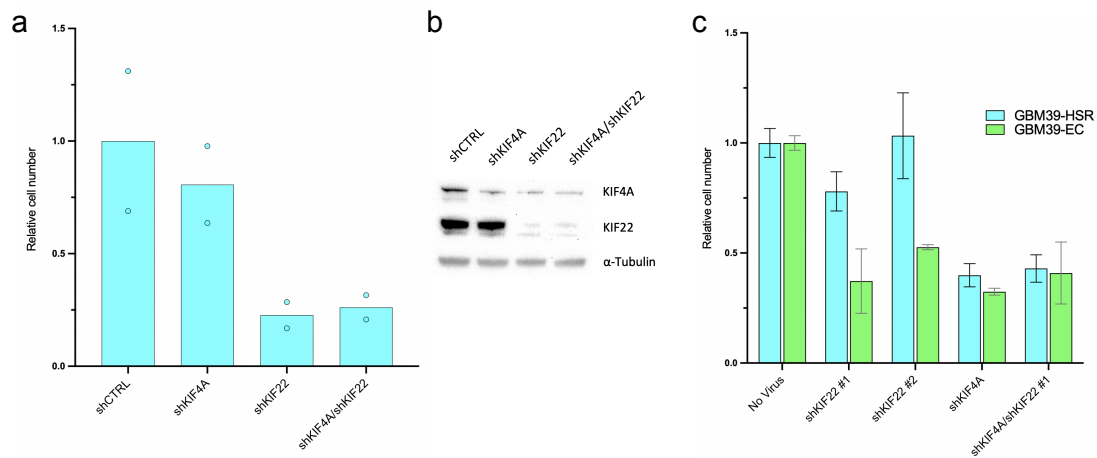


Figure 3.12 | Chromokinesin knockdown reduces proliferation in GBM39-EC relative to GBM39-HSR.

a, Relative cell number in GBM39-EC 5 days after shRNA lentiviral infection. Relative to shCTRL infection conditions. **b**, Western blot showing knockdown of KIF4A and KIF22 levels in GBM39-EC after lentiviral infection. **c**, Relative cell number 8 days after lentiviral infection in GBM39-EC and GBM39-HSR cell lines. Note increased sensitivity to knockdown in GBM39-EC cell line.

D. Materials and Methods

Cell Culture

Cell lines were purchased from ATCC. GBM39-HSR and GBM39-EC were derived from a GBM patient as previously described. PC3 cells were cultured in DMEM with 10% fetal bovine serum (FBS). COLO320-HSR and COLO320-DM were cultured in DMEM/F12 50%:50% with 10% FBS. SNU16 were grown in RPMI-1640 with 10% FBS. GBM39-HSR and GBM39-EC neurospheres were grown in DMEM/F12 with B27, Glutamax, heparin (5 $\mu\text{g/ml}$), EGF (20 ng/ml) and FGF (20 ng/ml). Cell numbers were counted with a TC20 automated cell counter (Bio-Rad).

Metaphase chromosome spreads

Cells were concentrated in metaphase by treatment with KaryoMAX colcemid (Gibco) at 100 ng/ml for between 3 hours and overnight (based on proliferation rate). Cells were washed once with PBS and a single cell suspension was incubated in 75 mM KCl for 15 min. at 37°C. Cells were then fixed with Carnoy's fixative (3:1 methanol : glacial acetic acid) and spun down. Cells were washed with fixative 3 additional times. Cells were then dropped onto humidified glass slides and aged overnight.

Fluorescence *in situ* hybridization (FISH)

Fixed samples on coverslips or slides were equilibrated in 2x SSC. They were dehydrated in ascending ethanol series of 70%, 85% and 100% for approximately 2 min. each. FISH probes were diluted in hybridization buffer (Empire Genomics) and added to

the sample with the addition of a coverslip or slide. Samples were denatured at 72°C for 2 minutes and then hybridized at 37°C overnight in a humid and dark chamber. Samples were then washed with 0.4x SSC followed by 2x SSC 0.1% Tween-20 and 2x SSC (2 min. each). DAPI (100 ng/ml) was applied to the samples for 10 minutes. Samples were washed again with 2x SSC Tween and 2x SSC. Samples were briefly washed in water and mounted with Prolong Gold and sealed with nail polish. FISH probes were purchased from Empire Genomics and diluted to manufacturer's recommendations.

Cytospin metaphase spread immunofluorescence

Cells were concentrated in metaphase by treatment with KaryoMAX colcemid (Gibco) at 100 ng/ml for between 3 hours and overnight (based on proliferation rate). Cells were washed once in cold PBS. Cells were resuspended in 1 ml cold 75mM KCl and incubated on ice for 15 minutes. Cells were adjusted to a concentration of 50,000 cells in 400 µl of KCl. Tween-20 was added to aid in spreading at 0.1% concentration. 400 µl cell suspension was added to cytospin funnels attached to glass slides. Cytospin was run at 800 rpm for 8 minutes. Cells on slides were then permeabilized with 0.5% Triton-X for 10 minutes at room temperature and then blocked in 5% BSA 0.05% Triton-X for 30 minutes at room temperature. Samples were then incubated with primary KIF22 (PA5-29490 ThermoFisher) and KIF4A (PA5-83243 ThermoFisher) antibodies overnight at 1:100 dilution in blocking buffer at 4 degrees Celsius.

Samples were washed 3 times in 0.05% Triton-X PBS (PBS-T) and incubated in secondary antibody 1:200 (anti-rabbit 568 Life Technologies) for 1 hour at room

temperature in the dark. Cells were wash 3 times in PBS-T and once in 0.1% PBS-T and once in PBS. Samples were then fixed in 4% paraformaldehyde (PFA) for 20 minutes at room temperature in the dark. Samples were washed and mounted with Prolong Gold containing DAPI and sealed with nail polish. Secondary only controls were performed to ensure specific signal.

Microscopy

Conventional fluorescence microscopy was performed using an Olympus BX43 microscope; images were acquired with a QI-Click cooled camera – or with a DeltaVision Elite imaging system (Applied Precision) and microscope (model IX-71; Olympus) controlled by SoftWoRx software (Applied Precision) with a CoolSNAP HQ2 camera (Photometrics).

Flow cytometry

Single cell suspensions were made, washed once in PBS and passed through a cell filter to ensure single cells. Cells were fixed in cold 70% EtOH for 30 minutes on ice and washed in PBS once. Cells were resuspended in DNA detection buffer: PBS, 2 µg/ml propidium iodide, 0.2 µg/ml RNase A. Cells were incubated at room temperature in the dark for 30 minutes. Flow cytometry was performed using a BD Fortessa X-20 machine and analysis and gating were performed using BD FACSDiva software. Approximately 20,000 events were recorded for each cell line.

TCGA mRNA expression data acquisition and analysis

All implementation was performed in R, using RStudio. Sample barcodes for tumors identified as either ecDNA⁺ or ecDNA⁻ were acquired from a prior publication. Gene expression data was downloaded from the Genomic Data Commons using the TCGAbiolinks package. Once acquired, gene expression data was used to generate normalized read counts using the DESeq2 package. Normalized read counts were fed into the Gene Set Enrichment Analysis program and analyzed using standard settings and Hallmarks gene sets. The ranked gene list from GSEA analysis was used to feed the top 1,000 genes preferentially expressed in ecDNA⁺ tumors into Gene Ontology (geneontology.org) to identify upregulated biological processes. Visualization of GSEA data was taken directly from GSEA output. Visualization of GO data was performed manually.

Dose response curves for nocodazole and Monastrol

Cells were plated at 10,000 cells per well in 96-well plates. Serial dilutions of the compounds were prepared, and each dose was equalized for total DMSO level. Cells were treated in biological duplicate for 4 days. Then, 50 μ l of Cell Titer Glo 2.0 reagent was added to each well (prior volume of 100 μ l). Reagent was incubated with cells for 10 minutes at room temperature, and the luminescence was read using a Tecan M1000 plate reader. Dose response curves were generated and plotted using GraphPad Prism with 1.0 set as the value for DMSO only control wells. IC₅₀ values were calculated by Prism.

siRNA transfections

siRNA transfections were performed following the guidelines of RNAiMAX transfection reagent manufacturer recommendations. Briefly, RNAiMAX was diluted in OPTIMEM media. siRNA was diluted to desired concentration in OPTIMEM. These two dilutions were incubated at room temperature for 5 minutes and then mixed together and incubated at room temperature for 15-20 minutes. For 6-well plates, 300 μ l of siRNA liposomes were added dropwise to cells with 2.5 ml total volume. Media was replaced the following day and cells progressed to desired experiment.

Lentiviral infections of shRNA

Plasmids containing shRNA were grown in bacteria and isolated using Endotoxin Free miniprep kit (Zymogen). Viral protein plasmids Gag/Pol, Tat, Rev and VSVG were combined at concentration of 400 ng/ μ l. 7.5 μ l of the viral mix was combined with approximately 6 μ g shRNA plasmid DNA and 1 ml of OPTIMEM. X-tremeGENE (Millipore Sigma) was added at 27 μ l and the mixture was added dropwise to HEK293T cells in 10 cm dishes. Media was replaced the following day.

Virus was collected on days 2 and 3 post transfection. Briefly, media was draw up into a syringe and passed through a 0.45 μ m filter. Titters were verified using Lenti-X GoStix (Takara).

Infection of GBM39 cells was carried out while cells were growing as neurospheres in suspension. Approximately 600 μ l of virus was added to 10 ml media in T25 flasks.

Media was replaced the following day and cells were progressed either onto coverslips for imaging or into flasks for proliferation measurements.

Western blots

Cells were collected via trypsinization and washed once in cold PBS. Samples were lysed in RIPA buffer with added protease and phosphatase inhibitors. Samples were incubated on ice for approximately 30 minutes, with periodic agitation during incubation. Lysates were centrifuged at max speed for 15 minutes at 4 degrees Celsius. Lysate supernatant was collected and transferred to fresh tubes.

Protein concentration was determined using BCA assay and BSA standard. 5 μ l lysates were incubated with 100 μ l BCA reagent at 37 degrees Celsius for 30 minutes. Absorbance was read at 562 nm using a Tecan M1000 plate reader. Having determined protein concentrations, samples were combined with 1x Laemmli buffer with added β -mercaptoethanol. Samples were heated at 99°C for 5-10 minutes. Samples were loaded onto NuPAGE 4-12% Bis-Tris gels and run at 125V for 1.5-2 hours.

Gel was washed in ddH₂O and added to transfer sandwich using Trans-Blot Turbo PVDF transfer packs (BioRad). Transfer was run on standard setting for 30 minutes using BioRad Trans-Blot Turbo transfer system. Membranes were then washed in PBST (Tween-20 0.1%) and blocked in 5% milk in PBST for 1 hour at room temperature. Membrane was incubated with primary antibodies (1:1000 for KIF4A and KIF22, 1:3000 for tubulin (2125 Cell Signaling) overnight at 4°C in blocking buffer. Membrane was then washed 3 times in PBST and incubated with secondary antibody for 1 hour at room temperature (1:1000

for KIF4A and KIF22, 1:3000 for tubulin). Membrane washed 3 times in PBST. Bands were detected using ECL substrate (Pierce ThermoFisher) and image using ChemiDoc (BioRad).

E. Acknowledgements

Chapter III contains co-authored/unpublished material of which the dissertation author was the primary investigator and author. Joshua T. Lange, Jens Luebeck, Vineet Bafna, Paul S. Mischel. Chapter III, Identifying genetic targets to disrupt ecDNA segregation and proliferation.

CHAPTER IV: CONCLUSIONS AND FUTURE DIRECTIONS

A. Summary of findings

In this dissertation, I have presented a body of work in which I have sought to push understanding in the field of ecDNA biology forward. This field can date its origins in the 1960s, when ecDNA were first described in patient tumors^{10,11}. While significant work was done on ecDNA prior to 2000^{15,16,19}, the focus on sequencing and genomic characterization of cancer saw ecDNA largely ignored⁶. However, recent work pioneered by our group and others has recently pushed this field back into the fore of cancer biology. This dissertation seeks to continue this progress and continue to improve our understanding of how ecDNA affects cell behavior at the point of division and how this further alters tumor behavior.

In Chapter II I present data that conclusively measures the random nature of ecDNA inheritance at cell division. While this pattern is not exactly random, likely due to incompletely dissolved ecDNA hubs, it can be approximated by a random binomial process. I further present evidence that this pattern of inheritance results in more heterogeneous populations, in cell lines and patient tumor samples, than would be expected if amplifications were localized to chromosomal loci. I also present evidence that this increased genetic diversity throughout the population decreases sensitivity to environmental and therapeutic challenges. We see effects of ecDNA on initial responses to these challenges as well as longer term resistance formation as the population is able to shift its genetic makeup to suit the new environment – this again is significantly less likely when alterations are fixed on chromosomes which generally assort properly. Finally, I presented data that demonstrates that even this increased level of complexity in terms of our understanding of how tumors with ecDNA behave may not be the full story. Studies of

cell lines with multiple species of ecDNA show a correlation in their inheritance patterns, while each retains random segregation when measured alone. This suggests that significantly more complex models of heterogeneity and evolution must be developed to consider ecDNA driven tumors with multiple ecDNA species. Taken together the data presented in Chapter II propose a clear mathematically supported model of how ecDNA promote tumor heterogeneity and resistance. These findings help to explain why ecDNA tumors cause poorer survival outcomes in patients.

In Chapter III I present a sequence of data which suggests an important role for increased expression of key mitotic regulators and machinery to decrease instances of ecDNA missegregation into micronuclei. Given the acentric nature of ecDNA, predictions and observations of abnormal mitoses have been made previously. However, our understanding of the specific mechanisms that ecDNA use, and thus can be disrupted to specifically target ecDNA, is lacking. I present genetic data demonstrating the role of chromokinesins KIF4A and KIF22 in promoting segregation of ecDNA. Depletion of these proteins increased micronucleation in an ecDNA-specific manner, and specifically disrupted the proliferation of ecDNA-containing cell lines. The data presented in Chapter III provide clear evidence that ecDNA represent a challenge for dividing cells that must be overcome, likely through the upregulation of mitotic proteins and chromokinesins specifically. While further data is needed in this area, the data presented herein suggest pharmacologic disruption of KIF4A and or KIF22 may represent a real therapeutic strategy, when used in combination with existing treatments, to increase toxicity to ecDNA-containing tumor cells. This strategy additionally is unlikely to present significant toxicity

to healthy dividing tissue since chromokinesins seem relatively dispensable in my experiments to cells without ecDNA.

B. Future areas of investigation

Significant progress in our understanding of the fundamental biology of ecDNA has been made in the past decade; however, there are important areas where our understanding is lacking and which are important for the development of improved therapeutic strategies for ecDNA cancers. In this section, I will outline the key areas, as I see them, in which research investments must be made to accelerate the development of understanding and therapeutic strategies toward ecDNA.

***In vivo* experiments and patient samples**

In this dissertation, I present limited data showing the heterogeneous and dynamic nature of ecDNA exists in human tumor settings. However, this data is quite limited and thus presents a limited picture of ecDNA biology *in vivo*. In order to address this, we must make use of *in vivo* mouse models to further our study of ecDNA. Unpublished data from other members of our group have suggested that ecDNA cell lines may behave quite differently when observed in cell culture conditions as compared to xenograft conditions. The fundamental biological findings of random inheritance, increased heterogeneity and resistance, altered gene expression patterns and the role of chromokinesins should be replicated using carefully controlled mouse model systems in order to test whether these findings hold in an *in vivo* context.

Similarly, I have presented data in this dissertation regarding the gene expression profiles of ecDNA⁺ and ecDNA⁻ tumors. These data present a high-level view of these tumors but require large numbers of patients to overcome the inherent noise associated with these data, especially considering the altered expression profiles of different tumor types. In order to push our understanding of ecDNA's impact on tumor behavior and outcomes, we need to invest in longitudinal studies of ecDNA⁺ and ecDNA⁻ tumors. Initially, this can be accomplished using retrospective studies of patients within a given tumor type for which we have primary tumor tissue and sequencing data to confirm ecDNA driven amplification. By comparing patients with and without ecDNA present in their tumor and understanding the outcome profiles for these patients, we can more definitively link ecDNA to various outcomes and nuances of tumor evolution, including presence and time to metastasis and time to relapse or resistance. These studies will need to be done in close collaboration with physicians in order to understand the nuances of different outcome profiles.

Interrogating mitotic proteins that may impact ecDNA segregation

I have presented data here that suggest an important role for KIF4A and KIF22 in supporting segregation of ecDNA to daughter cells. However, disruption of these proteins did not entirely prevent proliferation of ecDNA cells, nor did it result in missegregation of the majority of ecDNA. Thus, it is likely that these factors are working in concert with other mitotic actors to promote ecDNA segregation. Understanding these specific mechanisms, and how they interconnect, is important since disruption of ecDNA-specific mitotic processes is an attractive strategy for treating ecDNA driven tumors.

Recent studies have shed considerable light on how DNA behaves and interacts with proteins that alter DNA condensation and segmentation. Ki-67 has been shown to act as a biological surfactant which promotes the separation of individual mitotic chromosomes after nuclear envelop breakdown⁸⁹. This function enables safe progression into anaphase with chromosomes that are not intermixed. Given Ki-67's binding along the length of chromosome arms, I would hypothesize that ecDNA are lined with Ki-67 in mitosis as well. Ki-67 on ecDNA may actually promote missegregation and decrease the tethering that has been proposed to be important to ecDNA segregation.

Another protein that has recently been characterized to play an important role in mitotic DNA dynamics is barrier-to-autointegration factor (BAF). Research has shown that BAF promotes the cross-bridging of mitotic chromosome in order to form a dense network of mitotic DNA which enables proper segmentation of daughter cell nuclei⁹⁰. Disruption of BAF levels results in segmentation daughter cell DNA into multiple nuclei. I hypothesize that this may represent a mechanistic explanation for the tethering hypothesis that was described previously. BAF may be important for ensuring ecDNA are retained within the chromosomal DNA networks; this may represent the primary mechanism through which ecDNA segregate, with chromokinesins and other mechanical factors only utilized to correct failures in this system. Relatedly, VRK1 has been shown to regulate the timing of BAF localization to mitotic chromosomes⁹¹. Experiments testing the role of BAF in specifically altering ecDNA segregation dynamics are essential.

ecDNA and the immune system

The past decade has seen a significant increase in researchers' interest and understanding of the interplay between cancer and the immune system⁹². This has yielded significant and tangible improvements in the therapeutic potential to treat many different tumor types, with highly-mutagenized melanoma being the biggest stand out⁹³⁻⁹⁵. Recent work has suggested many different paths that may connect genome and chromosomal instability and the immune system^{50,96,97}. Given ecDNA is likely to represent both a consequence and a player in this area, it is essential to understand the links that may exist between ecDNA specifically and both innate and adaptive immune responses.

One link to the innate immune system may be found in ecDNA's frequent incorporation into micronuclei (Figure 3.4). Micronuclei are prone to triggering cell-intrinsic immune reactions when their nuclear envelope is broken. The mechanism for this is found in the cGAS-STING pathway, which interprets cytoplasmic DNA as a possible viral invasion which must be addressed⁹⁸⁻¹⁰⁰. Given the propensity for ecDNA to be segregated into micronuclei, understanding (especially using *in vivo* system with intact or humanized immune systems) ecDNA's role in triggering this signaling pathway is an important future area of research.

REFERENCES

- 1 Beroukhim, R., Mermel, C. H., Porter, D., Wei, G., Raychaudhuri, S., Donovan, J., Barretina, J., Boehm, J. S., Dobson, J., Urashima, M., Mc Henry, K. T., Pinchback, R. M., Ligon, A. H., Cho, Y. J., Haery, L., Greulich, H., Reich, M., Winckler, W., Lawrence, M. S., Weir, B. A., Tanaka, K. E., Chiang, D. Y., Bass, A. J., Loo, A., Hoffman, C., Prensner, J., Liefeld, T., Gao, Q., Yecies, D., Signoretti, S., Maher, E., Kaye, F. J., Sasaki, H., Tepper, J. E., Fletcher, J. A., Taberero, J., Baselga, J., Tsao, M. S., Demichelis, F., Rubin, M. A., Janne, P. A., Daly, M. J., Nucera, C., Levine, R. L., Ebert, B. L., Gabriel, S., Rustgi, A. K., Antonescu, C. R., Ladanyi, M., Letai, A., Garraway, L. A., Loda, M., Beer, D. G., True, L. D., Okamoto, A., Pomeroy, S. L., Singer, S., Golub, T. R., Lander, E. S., Getz, G., Sellers, W. R. & Meyerson, M. The landscape of somatic copy-number alteration across human cancers. *Nature* **463**, 899-905, doi:10.1038/nature08822 (2010).
- 2 Zack, T. I., Schumacher, S. E., Carter, S. L., Cherniack, A. D., Saksena, G., Tabak, B., Lawrence, M. S., Zhsng, C. Z., Wala, J., Mermel, C. H., Sougnez, C., Gabriel, S. B., Hernandez, B., Shen, H., Laird, P. W., Getz, G., Meyerson, M. & Beroukhim, R. Pan-cancer patterns of somatic copy number alteration. *Nat Genet* **45**, 1134-1140, doi:10.1038/ng.2760 (2013).
- 3 Felsberg, J., Hentschel, B., Kaulich, K., Gramatzki, D., Zacher, A., Malzkorn, B., Kamp, M., Sabel, M., Simon, M., Westphal, M., Schackert, G., Tonn, J. C., Pietsch, T., von Deimling, A., Loeffler, M., Reifenberger, G., Weller, M. & German Glioma, N. Epidermal Growth Factor Receptor Variant III (EGFRvIII) Positivity in EGFR-Amplified Glioblastomas: Prognostic Role and Comparison between Primary and Recurrent Tumors. *Clin Cancer Res* **23**, 6846-6855, doi:10.1158/1078-0432.CCR-17-0890 (2017).

- 4 Shukla, A., Nguyen, T. H. M., Moka, S. B., Ellis, J. J., Grady, J. P., Oey, H., Cristino, A. S., Khanna, K. K., Kroese, D. P., Krause, L., Dray, E., Fink, J. L. & Duijf, P. H. G. Chromosome arm aneuploidies shape tumour evolution and drug response. *Nat Commun* **11**, 449, doi:10.1038/s41467-020-14286-0 (2020).
- 5 Luebeck, J., Coruh, C., Dehkordi, S. R., Lange, J. T., Turner, K. M., Deshpande, V., Pai, D. A., Zhang, C., Rajkumar, U., Law, J. A., Mischel, P. S. & Bafna, V. AmpliconReconstructor integrates NGS and optical mapping to resolve the complex structures of focal amplifications. *Nat Commun* **11**, 4374, doi:10.1038/s41467-020-18099-z (2020).
- 6 Albertson, D. G. Gene amplification in cancer. *Trends Genet* **22**, 447-455, doi:10.1016/j.tig.2006.06.007 (2006).
- 7 Kaufman, R. J., Brown, P. C. & Schimke, R. T. Amplified dihydrofolate reductase genes in unstably methotrexate-resistant cells are associated with double minute chromosomes. *Proc Natl Acad Sci U S A* **76**, 5669-5673, doi:10.1073/pnas.76.11.5669 (1979).
- 8 Turner, K. M., Deshpande, V., Beyter, D., Koga, T., Rusert, J., Lee, C., Li, B., Arden, K., Ren, B., Nathanson, D. A., Kornblum, H. I., Taylor, M. D., Kaushal, S., Cavenee, W. K., Wechsler-Reya, R., Furnari, F. B., Vandenberg, S. R., Rao, P. N., Wahl, G. M., Bafna, V. & Mischel, P. S. Extrachromosomal oncogene amplification drives tumour evolution and genetic heterogeneity. *Nature* **543**, 122-125, doi:10.1038/nature21356 (2017).
- 9 Kim, H., Nguyen, N. P., Turner, K., Wu, S., Gujar, A. D., Luebeck, J., Liu, J., Deshpande, V., Rajkumar, U., Namburi, S., Amin, S. B., Yi, E., Menghi, F., Schulte, J. H., Henssen, A. G., Chang, H. Y., Beck, C. R., Mischel, P. S., Bafna, V. & Verhaak, R. G. W. Extrachromosomal DNA is associated with oncogene

- amplification and poor outcome across multiple cancers. *Nat Genet* **52**, 891-897, doi:10.1038/s41588-020-0678-2 (2020).
- 10 Cox, D., Yuncken, C. & Spriggs, A. I. Minute Chromatin Bodies in Malignant Tumours of Childhood. *Lancet* **1**, 55-58, doi:10.1016/s0140-6736(65)90131-5 (1965).
 - 11 Lubs, H. A., Jr. & Salmon, J. H. The Chromosomal Complement of Human Solid Tumors. Ii. Karyotypes of Glial Tumors. *J Neurosurg* **22**, 160-168, doi:10.3171/jns.1965.22.2.0160 (1965).
 - 12 Lubs, H. A., Jr., Salmon, J. H. & Flanigan, S. Studies of a glial tumor with multiple minute chromosomes. *Cancer* **19**, 591-599, doi:10.1002/1097-0142(196604)19:4<591::aid-cnrc2820190419>3.0.co;2-5 (1966).
 - 13 Wu, S., Turner, K. M., Nguyen, N., Raviram, R., Erb, M., Santini, J., Luebeck, J., Rajkumar, U., Diao, Y., Li, B., Zhang, W., Jameson, N., Corces, M. R., Granja, J. M., Chen, X., Coruh, C., Abnoui, A., Houston, J., Ye, Z., Hu, R., Yu, M., Kim, H., Law, J. A., Verhaak, R. G. W., Hu, M., Furnari, F. B., Chang, H. Y., Ren, B., Bafna, V. & Mischel, P. S. Circular ecDNA promotes accessible chromatin and high oncogene expression. *Nature* **575**, 699-703, doi:10.1038/s41586-019-1763-5 (2019).
 - 14 Garsed, D. W., Marshall, O. J., Corbin, V. D., Hsu, A., Di Stefano, L., Schroder, J., Li, J., Feng, Z. P., Kim, B. W., Kowarsky, M., Lansdell, B., Brookwell, R., Myklebost, O., Meza-Zepeda, L., Holloway, A. J., Pedoutour, F., Choo, K. H., Damore, M. A., Deans, A. J., Papenfuss, A. T. & Thomas, D. M. The architecture and evolution of cancer neochromosomes. *Cancer Cell* **26**, 653-667, doi:10.1016/j.ccell.2014.09.010 (2014).

- 15 Brown, P. C., Beverley, S. M. & Schimke, R. T. Relationship of amplified dihydrofolate reductase genes to double minute chromosomes in unstably resistant mouse fibroblast cell lines. *Mol Cell Biol* **1**, 1077-1083, doi:10.1128/mcb.1.12.1077-1083.1981 (1981).
- 16 Haber, D. A. & Schimke, R. T. Unstable amplification of an altered dihydrofolate reductase gene associated with double-minute chromosomes. *Cell* **26**, 355-362, doi:10.1016/0092-8674(81)90204-x (1981).
- 17 Kaufman, R. J., Brown, P. C. & Schimke, R. T. Loss and stabilization of amplified dihydrofolate reductase genes in mouse sarcoma S-180 cell lines. *Mol Cell Biol* **1**, 1084-1093, doi:10.1128/mcb.1.12.1084-1093.1981 (1981).
- 18 Kaufman, R. J. & Schimke, R. T. Amplification and loss of dihydrofolate reductase genes in a Chinese hamster ovary cell line. *Mol Cell Biol* **1**, 1069-1076, doi:10.1128/mcb.1.12.1069-1076.1981 (1981).
- 19 Kanda, T., Sullivan, K. F. & Wahl, G. M. Histone-GFP fusion protein enables sensitive analysis of chromosome dynamics in living mammalian cells. *Curr Biol* **8**, 377-385, doi:10.1016/s0960-9822(98)70156-3 (1998).
- 20 Deshpande, V., Luebeck, J., Nguyen, N. D., Bakhtiari, M., Turner, K. M., Schwab, R., Carter, H., Mischel, P. S. & Bafna, V. Exploring the landscape of focal amplifications in cancer using AmpliconArchitect. *Nat Commun* **10**, 392, doi:10.1038/s41467-018-08200-y (2019).
- 21 Chapman, O. S., Luebeck, J., Wani, S., Tiwari, A., Pagadala, M., Wang, S., Larson, J. D., Lange, J. T., Wong, I. T.-L., Dehkordi, S. R., Chandran, S., Adam, M., Lin, Y., Juarez, E., Robinson, J. T., Sridhar, S., Malicki, D. M., Coufal, N., Levy, M., Crawford, J. R., Pomeroy, S. L., Rich, J., Scheuermann, R. H., Carter, H., Dixon,

- J., Mischel, P. S., Fraenkel, E., Wechsler-Reya, R. J., Bafna, V., Mesirov, J. P. & Chavez, L. The landscape of extrachromosomal circular DNA in medulloblastoma. *bioRxiv*, 2021.2010.2018.464907, doi:10.1101/2021.10.18.464907 (2021).
- 22 Morton, A. R., Dogan-Artun, N., Faber, Z. J., MacLeod, G., Bartels, C. F., Piazza, M. S., Allan, K. C., Mack, S. C., Wang, X., Gimple, R. C., Wu, Q., Rubin, B. P., Shetty, S., Angers, S., Dirks, P. B., Sallari, R. C., Lupien, M., Rich, J. N. & Scacheri, P. C. Functional Enhancers Shape Extrachromosomal Oncogene Amplifications. *Cell* **179**, 1330-1341 e1313, doi:10.1016/j.cell.2019.10.039 (2019).
- 23 Zhu, Y., Gujar, A. D., Wong, C. H., Tjong, H., Ngan, C. Y., Gong, L., Chen, Y. A., Kim, H., Liu, J., Li, M., Mil-Homens, A., Maurya, R., Kuhlberg, C., Sun, F., Yi, E., deCarvalho, A. C., Ruan, Y., Verhaak, R. G. W. & Wei, C. L. Oncogenic extrachromosomal DNA functions as mobile enhancers to globally amplify chromosomal transcription. *Cancer Cell* **39**, 694-707 e697, doi:10.1016/j.ccell.2021.03.006 (2021).
- 24 Hung, K. L., Yost, K. E., Xie, L., Shi, Q., Helmsauer, K., Luebeck, J., Schopflin, R., Lange, J. T., Chamorro Gonzalez, R., Weiser, N. E., Chen, C., Valieva, M. E., Wong, I. T., Wu, S., Dehkordi, S. R., Duffy, C. V., Kraft, K., Tang, J., Belk, J. A., Rose, J. C., Corces, M. R., Granja, J. M., Li, R., Rajkumar, U., Friedlein, J., Bagchi, A., Satpathy, A. T., Tjian, R., Mundlos, S., Bafna, V., Henssen, A. G., Mischel, P. S., Liu, Z. & Chang, H. Y. ecDNA hubs drive cooperative intermolecular oncogene expression. *Nature* **600**, 731-736, doi:10.1038/s41586-021-04116-8 (2021).
- 25 Lundberg, G., Rosengren, A. H., Hakanson, U., Stewenius, H., Jin, Y., Stewenius, Y., Pahlman, S. & Gisselsson, D. Binomial mitotic segregation of MYCN-carrying double minutes in neuroblastoma illustrates the role of randomness in oncogene amplification. *PLoS One* **3**, e3099, doi:10.1371/journal.pone.0003099 (2008).

- 26 Shoshani, O., Brunner, S. F., Yaeger, R., Ly, P., Nechemia-Arbely, Y., Kim, D. H., Fang, R., Castillon, G. A., Yu, M., Li, J. S. Z., Sun, Y., Ellisman, M. H., Ren, B., Campbell, P. J. & Cleveland, D. W. Chromothripsis drives the evolution of gene amplification in cancer. *Nature* **591**, 137-141, doi:10.1038/s41586-020-03064-z (2021).
- 27 Silk, A. D., Zasadil, L. M., Holland, A. J., Vitre, B., Cleveland, D. W. & Weaver, B. A. Chromosome missegregation rate predicts whether aneuploidy will promote or suppress tumors. *Proc Natl Acad Sci U S A* **110**, E4134-4141, doi:10.1073/pnas.1317042110 (2013).
- 28 McClintock, B. The Stability of Broken Ends of Chromosomes in Zea Mays. *Genetics* **26**, 234-282, doi:10.1093/genetics/26.2.234 (1941).
- 29 Ly, P., Teitz, L. S., Kim, D. H., Shoshani, O., Skaletsky, H., Fachinetti, D., Page, D. C. & Cleveland, D. W. Selective Y centromere inactivation triggers chromosome shattering in micronuclei and repair by non-homologous end joining. *Nat Cell Biol* **19**, 68-75, doi:10.1038/ncb3450 (2017).
- 30 Moller, H. D., Lin, L., Xiang, X., Petersen, T. S., Huang, J., Yang, L., Kjeldsen, E., Jensen, U. B., Zhang, X., Liu, X., Xu, X., Wang, J., Yang, H., Church, G. M., Bolund, L., Regenber, B. & Luo, Y. CRISPR-C: circularization of genes and chromosome by CRISPR in human cells. *Nucleic Acids Res* **46**, e131, doi:10.1093/nar/gky767 (2018).
- 31 Burrell, R. A., McGranahan, N., Bartek, J. & Swanton, C. The causes and consequences of genetic heterogeneity in cancer evolution. *Nature* **501**, 338-345, doi:10.1038/nature12625 (2013).

- 32 Jamal-Hanjani, M., Quezada, S. A., Larkin, J. & Swanton, C. Translational implications of tumor heterogeneity. *Clin Cancer Res* **21**, 1258-1266, doi:10.1158/1078-0432.CCR-14-1429 (2015).
- 33 Murtuza, A., Bulbul, A., Shen, J. P., Keshavarzian, P., Woodward, B. D., Lopez-Diaz, F. J., Lippman, S. M. & Husain, H. Novel Third-Generation EGFR Tyrosine Kinase Inhibitors and Strategies to Overcome Therapeutic Resistance in Lung Cancer. *Cancer Res* **79**, 689-698, doi:10.1158/0008-5472.CAN-18-1281 (2019).
- 34 Ricordel, C., Friboulet, L., Facchinetti, F. & Soria, J. C. Molecular mechanisms of acquired resistance to third-generation EGFR-TKIs in EGFR T790M-mutant lung cancer. *Ann Oncol* **29**, i28-i37, doi:10.1093/annonc/mdx705 (2018).
- 35 Westover, D., Zugazagoitia, J., Cho, B. C., Lovly, C. M. & Paz-Ares, L. Mechanisms of acquired resistance to first- and second-generation EGFR tyrosine kinase inhibitors. *Ann Oncol* **29**, i10-i19, doi:10.1093/annonc/mdx703 (2018).
- 36 McGranahan, N. & Swanton, C. Clonal Heterogeneity and Tumor Evolution: Past, Present, and the Future. *Cell* **168**, 613-628, doi:10.1016/j.cell.2017.01.018 (2017).
- 37 consortium, T. R. R. TRACERx Renal: tracking renal cancer evolution through therapy. *Nat Rev Urol* **14**, 575-576, doi:10.1038/nrurrol.2017.112 (2017).
- 38 Mitchell, T. J., Turajlic, S., Rowan, A., Nicol, D., Farmery, J. H. R., O'Brien, T., Martincorena, I., Tarpey, P., Angelopoulos, N., Yates, L. R., Butler, A. P., Raine, K., Stewart, G. D., Challacombe, B., Fernando, A., Lopez, J. I., Hazell, S., Chandra, A., Chowdhury, S., Rudman, S., Soultati, A., Stamp, G., Fotiadis, N., Pickering, L., Au, L., Spain, L., Lynch, J., Stares, M., Teague, J., Maura, F., Wedge, D. C., Horswell, S., Chambers, T., Litchfield, K., Xu, H., Stewart, A., Elaidi, R., Oudard, S., McGranahan, N., Csabai, I., Gore, M., Futreal, P. A., Larkin, J., Lynch, A. G.,

- Szallasi, Z., Swanton, C., Campbell, P. J. & Consortium, T. R. R. Timing the Landmark Events in the Evolution of Clear Cell Renal Cell Cancer: TRACERx Renal. *Cell* **173**, 611-623 e617, doi:10.1016/j.cell.2018.02.020 (2018).
- 39 Negrao, M. V., Quek, K., Zhang, J. & Sepesi, B. TRACERx: Tracking tumor evolution to impact the course of lung cancer. *J Thorac Cardiovasc Surg* **155**, 1199-1202, doi:10.1016/j.jtcvs.2017.10.134 (2018).
- 40 Przewlaka, M. R. & Glover, D. M. The kinetochore and the centromere: a working long distance relationship. *Annu Rev Genet* **43**, 439-465, doi:10.1146/annurev-genet-102108-134310 (2009).
- 41 Kanda, T., Otter, M. & Wahl, G. M. Mitotic segregation of viral and cellular acentric extrachromosomal molecules by chromosome tethering. *J Cell Sci* **114**, 49-58 (2001).
- 42 Greaves, M. & Maley, C. C. Clonal evolution in cancer. *Nature* **481**, 306-313, doi:10.1038/nature10762 (2012).
- 43 Dagogo-Jack, I. & Shaw, A. T. Tumour heterogeneity and resistance to cancer therapies. *Nat Rev Clin Oncol* **15**, 81-94, doi:10.1038/nrclinonc.2017.166 (2018).
- 44 O'Connor, J. P., Rose, C. J., Waterton, J. C., Carano, R. A., Parker, G. J. & Jackson, A. Imaging intratumor heterogeneity: role in therapy response, resistance, and clinical outcome. *Clin Cancer Res* **21**, 249-257, doi:10.1158/1078-0432.CCR-14-0990 (2015).
- 45 Turner, N. C. & Reis-Filho, J. S. Genetic heterogeneity and cancer drug resistance. *Lancet Oncol* **13**, e178-185, doi:10.1016/S1470-2045(11)70335-7 (2012).

- 46 Andor, N., Maley, C. C. & Ji, H. P. Genomic Instability in Cancer: Teetering on the Limit of Tolerance. *Cancer Res* **77**, 2179-2185, doi:10.1158/0008-5472.CAN-16-1553 (2017).
- 47 Tubbs, A. & Nussenzweig, A. Endogenous DNA Damage as a Source of Genomic Instability in Cancer. *Cell* **168**, 644-656, doi:10.1016/j.cell.2017.01.002 (2017).
- 48 Bakhoun, S. F. & Cantley, L. C. The Multifaceted Role of Chromosomal Instability in Cancer and Its Microenvironment. *Cell* **174**, 1347-1360, doi:10.1016/j.cell.2018.08.027 (2018).
- 49 Bakhoun, S. F. & Compton, D. A. Chromosomal instability and cancer: a complex relationship with therapeutic potential. *J Clin Invest* **122**, 1138-1143, doi:10.1172/JCI59954 (2012).
- 50 Bakhoun, S. F., Ngo, B., Laughney, A. M., Cavallo, J. A., Murphy, C. J., Ly, P., Shah, P., Sriram, R. K., Watkins, T. B. K., Taunk, N. K., Duran, M., Pauli, C., Shaw, C., Chadalavada, K., Rajasekhar, V. K., Genovese, G., Venkatesan, S., Birkbak, N. J., McGranahan, N., Lundquist, M., LaPlant, Q., Healey, J. H., Elemento, O., Chung, C. H., Lee, N. Y., Imielenski, M., Nanjangud, G., Pe'er, D., Cleveland, D. W., Powell, S. N., Lammerding, J., Swanton, C. & Cantley, L. C. Chromosomal instability drives metastasis through a cytosolic DNA response. *Nature* **553**, 467-472, doi:10.1038/nature25432 (2018).
- 51 Gozgit, J. M., Wong, M. J., Moran, L., Wardwell, S., Mohemmad, Q. K., Narasimhan, N. I., Shakespeare, W. C., Wang, F., Clackson, T. & Rivera, V. M. Ponatinib (AP24534), a multitargeted pan-FGFR inhibitor with activity in multiple FGFR-amplified or mutated cancer models. *Mol Cancer Ther* **11**, 690-699, doi:10.1158/1535-7163.MCT-11-0450 (2012).

- 52 Buoen, L. C. & Brand, K. G. Double-minute chromosomes in plastic film-induced sarcomas in mice. *Naturwissenschaften* **55**, 135-136, doi:10.1007/BF00624255 (1968).
- 53 Batty, P. & Gerlich, D. W. Mitotic Chromosome Mechanics: How Cells Segregate Their Genome. *Trends Cell Biol* **29**, 717-726, doi:10.1016/j.tcb.2019.05.007 (2019).
- 54 Perea-Resa, C., Bury, L., Cheeseman, I. M. & Blower, M. D. Cohesin Removal Reprograms Gene Expression upon Mitotic Entry. *Mol Cell* **78**, 127-140 e127, doi:10.1016/j.molcel.2020.01.023 (2020).
- 55 Latt, S. A. Microfluorometric detection of deoxyribonucleic acid replication in human metaphase chromosomes. *Proc Natl Acad Sci U S A* **70**, 3395-3399, doi:10.1073/pnas.70.12.3395 (1973).
- 56 Severin, E. & Ohnemus, B. UV dose-dependent increase in the Hoechst fluorescence intensity of both normal and BrdU-DNA. *Histochemistry* **74**, 279-291, doi:10.1007/BF00495837 (1982).
- 57 Xie, L., Dong, P., Chen, X., Hsieh, T. S., Banala, S., De Marzio, M., English, B. P., Qi, Y., Jung, S. K., Kieffer-Kwon, K. R., Legant, W. R., Hansen, A. S., Schulmann, A., Casellas, R., Zhang, B., Betzig, E., Lavis, L. D., Chang, H. Y., Tjian, R. & Liu, Z. 3D ATAC-PALM: super-resolution imaging of the accessible genome. *Nat Methods* **17**, 430-436, doi:10.1038/s41592-020-0775-2 (2020).
- 58 Grimm, J. B., Tkachuk, A. N., Xie, L., Choi, H., Mohar, B., Falco, N., Schaefer, K., Patel, R., Zheng, Q., Liu, Z., Lippincott-Schwartz, J., Brown, T. A. & Lavis, L. D. A general method to optimize and functionalize red-shifted rhodamine dyes. *Nat Methods* **17**, 815-821, doi:10.1038/s41592-020-0909-6 (2020).

- 59 Rath, O. & Kozielski, F. Kinesins and cancer. *Nat Rev Cancer* **12**, 527-539, doi:10.1038/nrc3310 (2012).
- 60 Tischer, J. & Gergely, F. Anti-mitotic therapies in cancer. *J Cell Biol* **218**, 10-11, doi:10.1083/jcb.201808077 (2019).
- 61 Wong, Y. L., Anzola, J. V., Davis, R. L., Yoon, M., Motamedi, A., Kroll, A., Seo, C. P., Hsia, J. E., Kim, S. K., Mitchell, J. W., Mitchell, B. J., Desai, A., Gahman, T. C., Shiau, A. K. & Oegema, K. Cell biology. Reversible centriole depletion with an inhibitor of Polo-like kinase 4. *Science* **348**, 1155-1160, doi:10.1126/science.aaa5111 (2015).
- 62 Yan, V. C., Butterfield, H. E., Poral, A. H., Yan, M. J., Yang, K. L., Pham, C. D. & Muller, F. L. Why Great Mitotic Inhibitors Make Poor Cancer Drugs. *Trends Cancer* **6**, 924-941, doi:10.1016/j.trecan.2020.05.010 (2020).
- 63 Dominguez-Brauer, C., Thu, K. L., Mason, J. M., Blaser, H., Bray, M. R. & Mak, T. W. Targeting Mitosis in Cancer: Emerging Strategies. *Mol Cell* **60**, 524-536, doi:10.1016/j.molcel.2015.11.006 (2015).
- 64 Komlodi-Pasztor, E., Sackett, D. L. & Fojo, A. T. Inhibitors targeting mitosis: tales of how great drugs against a promising target were brought down by a flawed rationale. *Clin Cancer Res* **18**, 51-63, doi:10.1158/1078-0432.CCR-11-0999 (2012).
- 65 Almeida, A. C. & Maiato, H. Chromokinesins. *Curr Biol* **28**, R1131-R1135, doi:10.1016/j.cub.2018.07.017 (2018).
- 66 Funabiki, H. & Murray, A. W. The *Xenopus* chromokinesin Xkid is essential for metaphase chromosome alignment and must be degraded to allow anaphase

- chromosome movement. *Cell* **102**, 411-424, doi:10.1016/s0092-8674(00)00047-7 (2000).
- 67 Karg, T., Elting, M. W., Vicars, H., Dumont, S. & Sullivan, W. The chromokinesin Klp3a and microtubules facilitate acentric chromosome segregation. *J Cell Biol* **216**, 1597-1608, doi:10.1083/jcb.201604079 (2017).
- 68 Levesque, A. A. & Compton, D. A. The chromokinesin Kid is necessary for chromosome arm orientation and oscillation, but not congression, on mitotic spindles. *J Cell Biol* **154**, 1135-1146, doi:10.1083/jcb.200106093 (2001).
- 69 Mazumdar, M., Sundareshan, S. & Misteli, T. Human chromokinesin KIF4A functions in chromosome condensation and segregation. *J Cell Biol* **166**, 613-620, doi:10.1083/jcb.200401142 (2004).
- 70 Warecki, B. & Sullivan, W. Mechanisms driving acentric chromosome transmission. *Chromosome Res* **28**, 229-246, doi:10.1007/s10577-020-09636-z (2020).
- 71 Marquis, C., Fonseca, C. L., Queen, K. A., Wood, L., Vandal, S. E., Malaby, H. L. H., Clayton, J. E. & Stumpff, J. Chromosomally unstable tumor cells specifically require KIF18A for proliferation. *Nat Commun* **12**, 1213, doi:10.1038/s41467-021-21447-2 (2021).
- 72 Taniwaki, M., Takano, A., Ishikawa, N., Yasui, W., Inai, K., Nishimura, H., Tsuchiya, E., Kohno, N., Nakamura, Y. & Daigo, Y. Activation of KIF4A as a prognostic biomarker and therapeutic target for lung cancer. *Clin Cancer Res* **13**, 6624-6631, doi:10.1158/1078-0432.CCR-07-1328 (2007).

- 73 Ohsugi, M., Adachi, K., Horai, R., Kakuta, S., Sudo, K., Kotaki, H., Tokai-Nishizumi, N., Sagara, H., Iwakura, Y. & Yamamoto, T. Kid-mediated chromosome compaction ensures proper nuclear envelope formation. *Cell* **132**, 771-782, doi:10.1016/j.cell.2008.01.029 (2008).
- 74 Wandke, C., Barisic, M., Sigl, R., Rauch, V., Wolf, F., Amaro, A. C., Tan, C. H., Pereira, A. J., Kutay, U., Maiato, H., Meraldi, P. & Geley, S. Human chromokinesins promote chromosome congression and spindle microtubule dynamics during mitosis. *J Cell Biol* **198**, 847-863, doi:10.1083/jcb.201110060 (2012).
- 75 Soeda, S., Yamada-Nomoto, K. & Ohsugi, M. The microtubule-binding and coiled-coil domains of Kid are required to turn off the polar ejection force at anaphase. *J Cell Sci* **129**, 3609-3619, doi:10.1242/jcs.189969 (2016).
- 76 Hou, G., Dong, C., Dong, Z., Liu, G., Xu, H., Chen, L., Liu, L., Wang, H. & Zhou, W. Upregulate KIF4A Enhances Proliferation, Invasion of Hepatocellular Carcinoma and Indicates poor prognosis Across Human Cancer Types. *Sci Rep* **7**, 4148, doi:10.1038/s41598-017-04176-9 (2017).
- 77 Dong, Z., Zhu, C., Zhan, Q. & Jiang, W. Cdk phosphorylation licenses Kif4A chromosome localization required for early mitotic progression. *J Mol Cell Biol* **10**, 358-370, doi:10.1093/jmcb/mjy033 (2018).
- 78 Pike, R., Ortiz-Zapater, E., Lumicisi, B., Santis, G. & Parsons, M. KIF22 coordinates CAR and EGFR dynamics to promote cancer cell proliferation. *Sci Signal* **11**, doi:10.1126/scisignal.aaq1060 (2018).
- 79 Bruzzoni-Giovanelli, H., Fernandez, P., Veiga, L., Podgorniak, M. P., Powell, D. J., Candeias, M. M., Mourah, S., Calvo, F. & Marin, M. Distinct expression patterns

- of the E3 ligase SIAH-1 and its partner Kid/KIF22 in normal tissues and in the breast tumoral processes. *J Exp Clin Cancer Res* **29**, 10, doi:10.1186/1756-9966-29-10 (2010).
- 80 Love, M. I., Huber, W. & Anders, S. Moderated estimation of fold change and dispersion for RNA-seq data with DESeq2. *Genome Biol* **15**, 550, doi:10.1186/s13059-014-0550-8 (2014).
- 81 Subramanian, A., Tamayo, P., Mootha, V. K., Mukherjee, S., Ebert, B. L., Gillette, M. A., Paulovich, A., Pomeroy, S. L., Golub, T. R., Lander, E. S. & Mesirov, J. P. Gene set enrichment analysis: a knowledge-based approach for interpreting genome-wide expression profiles. *Proc Natl Acad Sci U S A* **102**, 15545-15550, doi:10.1073/pnas.0506580102 (2005).
- 82 Ashburner, M., Ball, C. A., Blake, J. A., Botstein, D., Butler, H., Cherry, J. M., Davis, A. P., Dolinski, K., Dwight, S. S., Eppig, J. T., Harris, M. A., Hill, D. P., Issel-Tarver, L., Kasarskis, A., Lewis, S., Matese, J. C., Richardson, J. E., Ringwald, M., Rubin, G. M. & Sherlock, G. Gene ontology: tool for the unification of biology. The Gene Ontology Consortium. *Nat Genet* **25**, 25-29, doi:10.1038/75556 (2000).
- 83 Gene Ontology, C. The Gene Ontology resource: enriching a GOLD mine. *Nucleic Acids Res* **49**, D325-D334, doi:10.1093/nar/gkaa1113 (2021).
- 84 Santaguida, S. & Amon, A. Short- and long-term effects of chromosome mis-segregation and aneuploidy. *Nat Rev Mol Cell Biol* **16**, 473-485, doi:10.1038/nrm4025 (2015).
- 85 Crasta, K., Ganem, N. J., Dagher, R., Lantermann, A. B., Ivanova, E. V., Pan, Y., Nezi, L., Protopopov, A., Chowdhury, D. & Pellman, D. DNA breaks and

- chromosome pulverization from errors in mitosis. *Nature* **482**, 53-58, doi:10.1038/nature10802 (2012).
- 86 Zhang, C. Z., Spektor, A., Cornils, H., Francis, J. M., Jackson, E. K., Liu, S., Meyerson, M. & Pellman, D. Chromothripsis from DNA damage in micronuclei. *Nature* **522**, 179-184, doi:10.1038/nature14493 (2015).
- 87 Levine, M. S. & Holland, A. J. The impact of mitotic errors on cell proliferation and tumorigenesis. *Genes Dev* **32**, 620-638, doi:10.1101/gad.314351.118 (2018).
- 88 Nielsen, C. F., Zhang, T., Barisic, M., Kalitsis, P. & Hudson, D. F. Topoisomerase IIalpha is essential for maintenance of mitotic chromosome structure. *Proc Natl Acad Sci U S A* **117**, 12131-12142, doi:10.1073/pnas.2001760117 (2020).
- 89 Cuylen, S., Blaukopf, C., Politi, A. Z., Muller-Reichert, T., Neumann, B., Poser, I., Ellenberg, J., Hyman, A. A. & Gerlich, D. W. Ki-67 acts as a biological surfactant to disperse mitotic chromosomes. *Nature* **535**, 308-312, doi:10.1038/nature18610 (2016).
- 90 Samwer, M., Schneider, M. W. G., Hoefler, R., Schmalhorst, P. S., Jude, J. G., Zuber, J. & Gerlich, D. W. DNA Cross-Bridging Shapes a Single Nucleus from a Set of Mitotic Chromosomes. *Cell* **170**, 956-972 e923, doi:10.1016/j.cell.2017.07.038 (2017).
- 91 Molitor, T. P. & Traktman, P. Depletion of the protein kinase VRK1 disrupts nuclear envelope morphology and leads to BAF retention on mitotic chromosomes. *Mol Biol Cell* **25**, 891-903, doi:10.1091/mbc.E13-10-0603 (2014).
- 92 Hanahan, D. & Weinberg, R. A. Hallmarks of cancer: the next generation. *Cell* **144**, 646-674, doi:10.1016/j.cell.2011.02.013 (2011).

- 93 Sharma, P., Wagner, K., Wolchok, J. D. & Allison, J. P. Novel cancer immunotherapy agents with survival benefit: recent successes and next steps. *Nat Rev Cancer* **11**, 805-812, doi:10.1038/nrc3153 (2011).
- 94 Zaidi, N. & Jaffee, E. M. Immunotherapy transforms cancer treatment. *J Clin Invest* **129**, 46-47, doi:10.1172/JCI126046 (2019).
- 95 Drake, C. G., Lipson, E. J. & Brahmer, J. R. Breathing new life into immunotherapy: review of melanoma, lung and kidney cancer. *Nat Rev Clin Oncol* **11**, 24-37, doi:10.1038/nrclinonc.2013.208 (2014).
- 96 Mackenzie, K. J., Carroll, P., Martin, C. A., Murina, O., Fluteau, A., Simpson, D. J., Olova, N., Sutcliffe, H., Rainger, J. K., Leitch, A., Osborn, R. T., Wheeler, A. P., Nowotny, M., Gilbert, N., Chandra, T., Reijns, M. A. M. & Jackson, A. P. cGAS surveillance of micronuclei links genome instability to innate immunity. *Nature* **548**, 461-465, doi:10.1038/nature23449 (2017).
- 97 Zhang, H., Christensen, C. L., Dries, R., Oser, M. G., Deng, J., Diskin, B., Li, F., Pan, Y., Zhang, X., Yin, Y., Papadopoulos, E., Pyon, V., Thakurdi, C., Kwiatkowski, N., Jani, K., Rabin, A. R., Castro, D. M., Chen, T., Silver, H., Huang, Q., Bulatovic, M., Dowling, C. M., Sundberg, B., Leggett, A., Ranieri, M., Han, H., Li, S., Yang, A., Labbe, K. E., Almonte, C., Sviderskiy, V. O., Quinn, M., Donaghue, J., Wang, E. S., Zhang, T., He, Z., Velcheti, V., Hammerman, P. S., Freeman, G. J., Bonneau, R., Kaelin, W. G., Jr., Sutherland, K. D., Kersbergen, A., Aguirre, A. J., Yuan, G. C., Rothenberg, E., Miller, G., Gray, N. S. & Wong, K. K. CDK7 Inhibition Potentiates Genome Instability Triggering Anti-tumor Immunity in Small Cell Lung Cancer. *Cancer Cell* **37**, 37-54 e39, doi:10.1016/j.ccell.2019.11.003 (2020).

- 98 Sun, L., Wu, J., Du, F., Chen, X. & Chen, Z. J. Cyclic GMP-AMP synthase is a cytosolic DNA sensor that activates the type I interferon pathway. *Science* **339**, 786-791, doi:10.1126/science.1232458 (2013).
- 99 Harding, S. M., Benci, J. L., Irianto, J., Discher, D. E., Minn, A. J. & Greenberg, R. A. Mitotic progression following DNA damage enables pattern recognition within micronuclei. *Nature* **548**, 466-470, doi:10.1038/nature23470 (2017).
- 100 Krupina, K., Goginashvili, A. & Cleveland, D. W. Causes and consequences of micronuclei. *Curr Opin Cell Biol* **70**, 91-99, doi:10.1016/j.ceb.2021.01.004 (2021).